Summer 2021

The Development of a Tractable System to Assess *Caulobacter*-Plant Interactions

Louis Berrios

The Development of a Tractable System to Assess *Caulobacter*-Plant Interactions

by

Louis Berrios

Bachelor of Science
Francis Marion University, 2017

Submitted in Partial Fulfillment of the Requirements

For the Degree of Doctor of Philosophy in

Biological Sciences

College of Arts and Sciences

University of South Carolina

2021

Accepted by:

Berten Ely, Major Professor

Zhengqing Fu, Committee Member

Beth Krizek, Committee Member

Thomas Makris, Committee Member

Johannes Stratmann, Committee Member

Tracey L. Weldon, Interim Vice Provost and Dean of the Graduate School

DEDICATION

For Bubbie: thank you for a wonderful 10 years. You will undoubtedly be missed every second of every day and will forever remain in my heart.

ACKNOWLEDGEMENTS

To the people who continue to provide me with pure joy and love and all the intangibles mere words cannot explain—Sarah, Mom, Dad, and Grandma—thank you for your constant support. I love you each to no end. To my dissertation committee, thank you for your input and support throughout this process. And a special thanks to my mentor, Bert Ely, for providing me with the creative and intellectual independence and support that I needed to develop the *Caulobacter-Arabidopsis* system in his lab.

ABSTRACT

Bacteria play an integral role in regulating plant growth and development. However, many of the mechanisms encompassing bacteria-plant interactions are poorly understood and thus require detailed assessments (see CHAPTER 1). To this end, I coupled bacterial (*Caulobacter* sp.) and plant model organisms (*Arabidopsis*) to determine 1) the degree to which select bacteria can enhance the growth and development of plants, and 2) what functions these bacteria possess that enable them to aid plant development. Employing bacterial isolation techniques, monoculture inoculum-based plant growth assays, biochemical assays, comparative genomics, functional genetics, and real-time quantitative PCR (RT-qPCR), I determined that 1) *Caulobacter-Arabidopsis* interactions vary from mutualistic to parasitic; 2) common biosynthates are not required for many beneficial *Caulobacter-Arabidopsis* interactions; 3) redox-related genes and bacterial cell curvature facilitate *Caulobacter-Arabidopsis* interactions, and 4) bacterial concentration and bacterial induced pH reductions contribute to *Caulobacter*-mediated seed germination inhibition.

Collecting and processing soil and root samples from South Carolina and Florida, I uncovered two novel *Caulobacter* strains that can enhance the biomass of *Arabidopsis*. To contextualize these findings, I tested the ability of previously obtained stock cultures of *Caulobacter* strains (collected from both aquatic and soil environments) to also enhance plant growth. As a result, I determined that 1) plant

growth enhancement is not a conserved feature in the *Caulobacter* genus, and 2) isolation source did not correlate with plant-growth-promoting (PGP) factors (i.e., not all soil-derived strains enhanced plant growth and not all aquatic-derived strains failed to enhance plant growth). Using established biochemical tests as proxies for plant-growth-promotion factors, I determined that (among the 11 *Caulobacter* strains that I assayed) *Caulobacter* strains do not use these common PGP factors to enhance plant growth. Employing a comparative genomics approach, I determined that each of the PGP *Caulobacter* strains that I assayed harbors a unique set of genes (*cyo* operon) with predicted functions in betalain biosynthesis—a ROS scavenging metabolite—in its genome. Since ROS molecules are critical for plant growth and development, I hypothesized that these genes may be involved in the ability of PGP *Caulobacter* strains to enhance the growth and development of *Arabidopsis* (see CHAPTER 2).

To determine whether the *cyo* operon genes are necessary for *Caulobacter*-mediated plant growth enhancement, I disabled the function of one of the subunits (*cyoB*) using homologous recombination in two different PGP *Caulobacter* species and assessed the potential of the resultant mutant strains to enhance plant growth relative to their parental strain. As a result, I determined that a functional *cyo* operon facilitates *Caulobacter*-mediated growth enhancement of *Arabidopsis* since the mutant strains were unable to enhance plant growth relative to their parental strains. Interestingly, using RT-qPCR, I determined that one PGP *Caulobacter* strain expresses the *cyoB* gene (and additional genes with predicted betalain biosynthesis functions; see CHAPTER 3) significantly more than other

strains and subsequently hinders the germination rate of *Arabidopsis* seeds. I also constructed a flux balance analysis (FBA) to gauge the relative metabolic activity between *Caulobacter* strains since a large portion (~80%) of variation in seed germination inhibition was explained by the culturing media type (media used for bacterial-seed plating assays). To this end, the FBA and subsequent pH measurements suggested that increased H^+ ion excretion likely contributes to *Caulobacter*-mediated seed germination inhibition, although abundant bacterial growth also contributes to the observed inhibition. Moreover, I hypothesized that bacterial cell shape would facilitate plant growth since previous reports have shown that *Caulobacter* cell shape impacts niche habitancy, and I showed that *Caulobacter* cell curvature is required for this bacterium to enhance the growth of *Arabidopsis*. Therefore, I established a genetic framework to investigate the mechanisms that undergird *Caulobacter-Arabidopsis* interactions. Taken together, I fused two reliable genetic models (*Caulobacter* and *Arabidopsis*) to generate a working model for bacteria-plant interactions. Leveraging the high-quality genomic database for *Caulobacter* strains, I discovered genetic factors that facilitate the ability of select Caulobacter strains to enhance the growth of *Arabidopsis* plants.

PREFACE

CHAPTER 1 details an overview of plant-microbe interactions to contextualize the content in CHAPTER 2 and 3 with respect to agricultural and ecosystem sustainability. The contents of CHAPTER 1 have been packaged into a review/hypothesis article, which is currently under review. CHAPTER 2 communicates the findings of published work that details the varied interactions between *Caulobacter* strains and *Arabidopsis* plants. CHAPTER 3 details published findings that elucidate genetic factors involved in interactions between select *Caulobacter* species and *Arabidopsis* plants. Each chapter includes either content from manuscripts in review (i.e., CHAPTER 1) or published manuscripts in their entirety (i.e., CHAPTER 2 and 3). Citation formats conform to the publisher's specifications.

TABLE OF CONTENTS

LIST OF FIGURES

LIST OF ABBREVIATIONS

BRD……..….Basal rosette diameter

IH…….…...Inflorescence height

MMN……..…Microbe-microbe network

PFs…….Protein families

PGP……..….Plant growth-promoting bacteria

PMN…….……..Plant-microbe network

PW……..Plant weight

SQ……..Silique quantity

WGS…….…...Whole-genome sequence

CHAPTER 1

THE SOCIAL NETWORK OF PLANT MICROBIOMES: A NEGLECTED TOPIC OF CRUCIAL IMPORTANCE FOR AGRICULTURAL AND ECOSYSTEM SUSTAINABILITY[1]

[1]Berrios L (2021) The Social Network of Plant Microbiomes: A Neglected Topic of Crucial Importance for Agricultural and Ecosystem Sustainability. *BioEssays* (under review)

Abstract

For centuries, the human-plant relationship has been borne out of human necessity and circumstance. Neglect on our part was failing to recognize that the plant-microbe relationship has been developing for millions of years, and it is only recently that we have begun to understand that the health of a plant is inextricably linked to the health of its associated microbial community members. Historically, however, plant heath has not been assessed as a factor of its microbiota's health. As a result, many current strategies seeking to promote plant health can counter the reparations required for holistically fortifying both above and belowground organisms in relation to ecosystem sustainability. In this perspective review essay, I discuss the importance of an integrative approach to uncovering the complex dynamics among plant associated microbes to the end of realizing agricultural and ecosystem sustainability. Moreover, I posit the meritocratic compartmentalization hypothesis (MCH) to frame subsequent investigations of community-centered plant-microbe dynamics.

1 Introduction

The Holocene Epoch has encompassed its fair share of natural and anthropogenic interactions. Southwest Asia experienced its burgeoning of wheat, barley, lentil, pea, chickpea, broadbean, flax, and olive ~12,000 years ago [1]. Processes such as flooding and wildfire are suggested to have generated a patchy landscape in the Amazon [2], which presumably spurred the subsequent agricultural ingenuity of its indigenous people, and the inhabitants of North America began supporting squash, sunflower, sumpweed, and pitseed goosefoot roughly 6,000 years ago [1].

Indeed, both the Old and New Worlds have shaped their inhabitants, and the inhabitants have also shaped the landscapes (for better and worse) in these ecosystems.

The onset of crop management remains one of the key catalysts that led to the reconfiguration of human culture as we have come to know it today. From early Native American settlers practicing companion cropping [3]—where discrete crops are planted in proximity to one another to boost each other's fitness—to Martinus Beijerinck's discovery of plant symbiotic bacteria (Rhizobium) at the end of the 19th century, the human conceptualization of micro- and macro-scale organismal interactions has been around for centuries. Even Aristotle some 2400 years ago connected the interplay between soil dwelling organisms and their host plants. However, harnessing a long-standing recognition for the at-times-harmonious interspecies interactions still failed to foster balanced aims toward ecosystem management and agricultural sustainability in past decades. In short, recent generations have ordered a pre-made cocktail of hot-n-ready solutions that neglected to balance current needs on the scale of future projections.

Nonetheless, green initiatives that discourage excessive fertilizer use and thwart ecosystem disruption have recently been developed [4-8] and efforts to enhance crop maintenance for current and future generations have been initiated [9,10]. Companies such as biovanteTM have created products (e.g., BioCoreTM, BioRedTM, Invade 5GTM) that have exploited beneficial soil microbes to condition soils and promote plant growth, and these efforts have proven to be effective [7]. Similarly, other commercially available soil amendments (i.e., SynComs) such as

VESTA have been shown to restructure existing plant associated microbes and resultantly enhance plant and soil health; however, the mechanisms that underpin these network-based microbial interactions remain relatively unexplored [11]. Thus, efforts to understand how plant microbe networks (PMNs) collectively shape plant development will hone societal shifts toward reducing (and fine-tuning) chemical inputs and capturing the power within the soil.

In this perspective review essay, I will reframe research on plant-microbe interactions in terms of plant microbe networks (PMNs) with an emphasis on symbiotic plant microbes to highlight the requirement for interdisciplinary and translational efforts regarding microbial ecology and agricultural sustainability. Moreover, I posit the meritocratic compartmentalization hypothesis (MCH) to structure subsequent plant-microbe investigations in relation to microbial ecology and agricultural sustainability.

1.1 Prosocial Actions Above and Below Ground

Nurturing positive interactions between plants and their associated microbes (i.e., supplying plants and soils with adequate inputs that generate minimal waste and support plant-microbe homeostasis) can benefit ecosystems and economies on a global scale. Climate change—an omnipotent driver of ecosystem restructuring—will inevitably reshape our global ecosystems. However, from nutrient cycling to warding off imminent climate-driven threats (e.g., drought, desertification, elevated CO_2), plant-associated microbes can bolster plant fitness under both stressful and optimal plant growth conditions [12-20]. For example, a total of ~16 billion tonnes of CO_2 equivalents per year were generated from global food system emissions

between 2012 and 2017 [21]. And, even if national pledges to the Paris climate agreement are upheld, an anticipated 2.5°C temperature increase would still likely occur by the end of the century, which would dramatically alter the flora and fauna that regulate our ecosystems. But, if estimates suggesting the power of implementing plant associated microbes to buffer such climate-driven effects are realized [22,23], a revitalization in global ecosystem functioning will also be realized. As such, ecosystem and economic functionalities are inextricably linked given that climate dictates seasonality and seasonality dictates the outcomes of forgeable lands. Therefore, efforts must be expedited to catalogue microbial taxa that can effectively benefit their plant host(s) across varying abiotic and biotic conditions (i.e., context dependencies). In doing so, microbial species can be applied strategically (i.e., in a network-based fashion) to generate climate-ready ecosystems, enhance crop production, and subsequently buffer economies.

1.2 Reductionism in the Face of Realism

Perhaps the most challenging aspect of studying plant-microbe interactions in natural systems hearkens back to their innate complexity. Estimates suggest that a single gram of soil can house billions of microbial cells (e.g., archaea, bacteria, fungi, protists, viruses) [24], and upwards of 50,000 unique strains may be present [25]. Plant roots have been shown to selectively restrict access to select microbial strains in and around their root system, thus generating a biological system in flux and varying in interspecies intimacy [26]. Moreover, strain composition varies as a function of not only biotic interactions but also abiotic factors (e.g., seasonality, soil pH, ecosystem disturbance), which suggests that specific paradigmatic presets

determine microbial functions and their impact on plant fitness. Although these estimates provide insightful information, their derivation comes from sequence-based (e.g., amplicon sequencing and metagenomics) technologies that only provide insights regarding relative/absolute abundance of microbial species and their potential function (i.e., genetic composition) [27-30]. Thus, the timing of microbial interactions in relation to plant development, the modes-of-action of microbial partners and their efficacy, and the molecular networks that initiate and maintain connections within these biological systems are largely unknown. As such, two general tradeoffs persist within experimental design approaches: size and realism. For instance, large metagenomic sequencing projects can estimate microbial functions (e.g., antibiotic resistance, phytohormone production, siderophore excretion) and abundances (i.e., OTUs and ASVs), but they often obfuscate causal links among microbial partners (i.e., only one or two types of microbial organism may be investigated) and their host plant. Similarly, confining investigations to the interactions between single strains and a single host plant creates a largely artificial environment but nonetheless possesses the power to illustrate how select microbial strains can interact with select host plants. Despite each general approach maintaining its own innate benefits and limitations, neither approach alone contextually progresses plant-microbe research much further than did the efforts of Beijerinck in the 19th century.

1.3 Multiplexing Omics-Based Strategies

Efforts to enhance the technological deficits that can hinder accurate representations of plant-microbe interactions have provided glimpses of the

detailed mechanisms that are employed by PMNs. For example, the use of DNA stable-isotope labeling and fluorescent microscopy techniques have delineated the carbon flow patterns and spatial arrangements between plants and microbes [31-35]. Here, relatively natural environmental conditions can be preserved while gaining insight into how plants sequester beneficial microbes across space and time. However, these techniques often fail to capture the resolution required to detail mechanistic microbe-microbe interactions. The implementation of RT-qPCR and proteomics (e.g., LC-MS) have in turn been employed to detail specific mechanistic interactions regarding select microbe-host pairings. For instance, relatively recent research has shown that mixtures of bacteria in the genus Bacillus upregulate nitrate and ammonium gene expression in Arabidopsis thaliana [36], albeit artificial experimental conditions limit the applicability of the derived results. Similarly, others have recently employed proteomics to uncover plant nitrogen regulation as a factor of microbial colonization [37]. Moreover, metabolomics-based approaches are regularly being used to determine microbe-microbe and plant-microbe interactions, but sampling times are often limited in scope. Likewise, microfluidics can be used to frame interspecies interactions at microscales [38,39], which is required to understand the presumably unintuitive interactions that take place underground. Although these systems offer a relatively unparalleled level of precision [40], they often greatly reduce the complexity that persists in plant microbiomes. Thus, integrating gene-protein-metabolite networks for all members of the biological system across several developmental stages and under conditions that mimic natural environmental fluxes, i.e., diverse microbial composition (e.g.,

archaea, bacteria, fungi, protists, viruses), diverse macroscopic members (e.g., neighboring plants, insects, earthworms), and fluctuating abiotic factors (e.g., rainfall, humidity, sunlight, soil pH) would enhance our understanding of how plants develop with their associated microbes across space and time.

1.4 Leveraging Omics to Realize Holistic Functions

A systems approach that links multiple technical methods indeed appears to offer a robust understanding of the complexity within plant microbiomes. Computational approaches have enabled network-based integrations of large-scale data, and addition-deletion experiments (ADE)—where a single organism is removed from a synthetic microbial consortium—can offer insight into how microbial partners adjust to the presence or absence of another in relation to plant development. Coupling ADE experiments with genetic manipulations of microbial species can also add an additional layer of nuance since a single microbial organism may employ several distinct mechanisms to influence plant growth. The use of genetically mutant plants can also provide insight into which plant signaling pathways are sufficient and necessary for plant-microbe interactions to ensue. Therefore, both the effects of presumptive molecular functions and the physical presence of selected organisms can be overlain to parse primary and additional plant influencing factors. For example, a single bacterial genus (*Variovorax*) was shown to maintain root growth in a complex plant microbiome [14]. Linking gene function to metabolite production, they found that *Variovorax* could fine-tune plant hormone (auxin) fluxes and degrade microbial-associated molecular patterns to reduce the negative effects that a 185-microbial member consortium had on root

growth and that auxin regulation was sufficient and necessary for the action of this *Variovorax* species. Moreover, these interactions were assessed across a landscape of differing abiotic factors (i.e., salinity, temperature, phosphate concentration, and pH), which provides the key to unlock general rules that govern plant-microbe interactions. Nonetheless, despite these pioneering advancements, mycorrhizal associations (integral plant microbe interactions) were not investigated in their primary plant model system (Arabidopsis, which does not engage in mycorrhizal symbioses) or secondary (tomato seedlings). Given that an estimated 90% of vascular plants form symbiotic associations [41-43] mycorrhizae can contribute up to nearly 80% of a plant's nitrogen and phosphorus sources [44,45], a translational hurdle (e.g., to forest ecosystems and agricultural crops) may remain ahead.

The post-genomic era has nevertheless reinvigorated the field of microbial ecology, and applications to ecosystem management and agricultural practices have resultantly catapulted our understanding of interspecies interactions. The efficacy of integrating knowledge regarding plant-microbe interactions into useful platforms that buffer ecosystem disturbance and enhance crop production, however, remains challenging.

2 Framing the Dynamics of Plant Microbiomes as 'Networks'

Each member of the holobiont (plant + microbial members) must maintain their own degree of homeostasis in the larger context of their counterparts to survive and reproduce. To this end, carbon, nitrogen, phosphorus, micronutrients, and water function as 'bartering resources' to propel the dynamics of plant microbial

networks (PMNs). Moreover, depending on relative microbial turnover rates (i.e., growth rate differences between taxa and death to microbes based on nutrient limitation or predation), fluctuations in microbial-derived consumables likely occur on both local and systemic spatiotemporal scales. In addition, seeds in natural or variable settings (e.g., crop fields and terrestrial ecosystems) do not develop as 'blank slates', given their vertically transmitted microbiota and the diversity of soil microbes that surround them [46,47]. Therefore, PMNs initially form as a result of circumstance, and PMN optimization results in part by interspecies interactions and plant development (i.e., spatiotemporal fluctuations of root exudates). Given this semi-predetermined environmental heterogeneity, the start-up PMN (SuPMN) must provide a habitable environment for the seedling to effectively develop, while subsequent root-root signaling primes the soil conditions and in turn shapes the proximal (endosphere and rhizosphere) and distal (bulk soil) microbial members within the holobiont. An implication of this notion is that the soil dwelling microbes capable of survival and reproduction without the addition of root exudates will likely be high-concentration members of the SuPMN. In addition, the microbes that can outcompete others for the plant bartering resources (but are not dependent on them) will likely be present throughout the entire course of plant development (**Figure 1.1**). Together, concerted shifts in PMN assemblages rely on nutrient distributions in relation to interspecies interactions as a function of abiotic contextual factors.

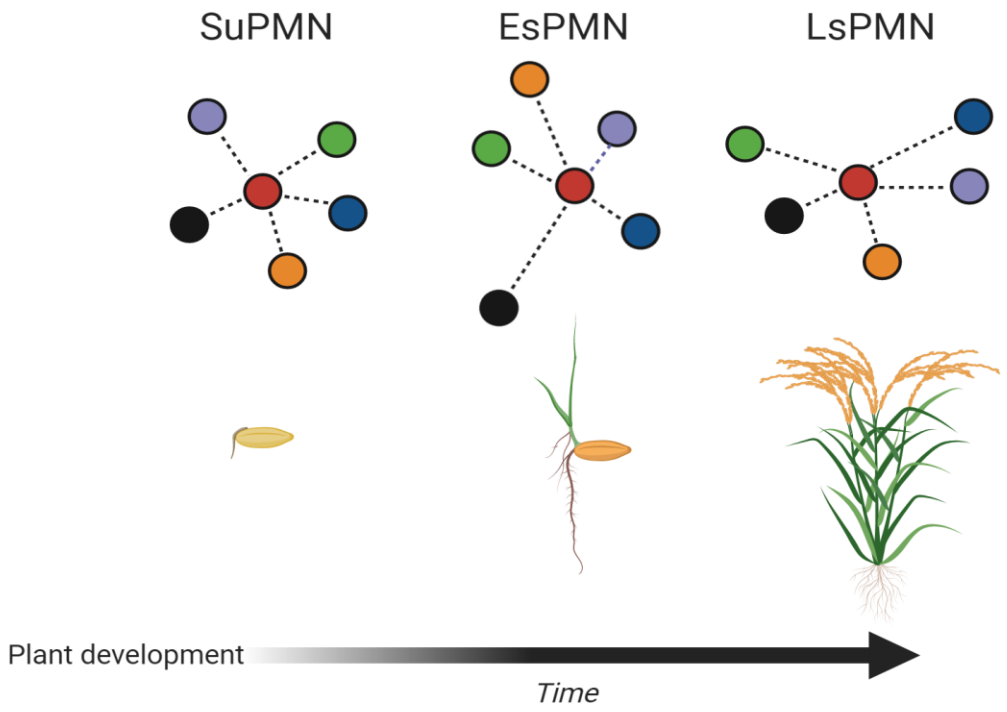

Figure 1.1. Plant microbe network (PMN) dynamics. Circles represent distinct microbial taxa, and dotted lines capture interactions and relative intensities (shorter distance = greater intensity) between taxa. PMNs are represented as in flux as a function of plant development with the start-up PMN (SuPMN) subsequently shaping into the early-stage PMN (EsPMN) and the late-stage PMN (LsPMN).

2.1 Time and Probability: The Cyclical Nature of PMNs

Presumably, microbial members that harbor considerable genomic versatility (i.e., can utilize diverse substrates for energy production and can survive in diverse abiotic conditions) would be better fit as continued members in a PMN than those that are restricted to narrow niches. For instance, PMN members that harbor the enzymatic machinery to efficiently consume plant exudates at rates that neither outpace the plant's net nutrient production nor expedite the growth of pathogenic organisms, while reciprocally bolstering plant growth (e.g., hormonal regulation or

nutrient acquisition) theoretically possess the greatest ‘value points’ within the PMN. As such, for early-stage PMN (EsPMN) and late-stage PMN (LsPMN) members to maintain their membership, they must either 1) provide a fitness benefit to the surrounding organisms (i.e., microbes or plant) or 2) limit the growth of pathogenic organisms to the degree of enhancing plant fitness. Therefore, the two classical shapes that PMNs can assume for the systemic betterment of the plant are either direct benefits (e.g., increase nutrient availability, regulate phytohormone production) or indirect benefits (e.g., suppress the uprise of pathogenic agents). However, a microbial member could presumably benefit the fitness of a plant pathogen (e.g., provide nutrients or diminish the fitness of a pathogen’s pathogen). In this case, these ‘pathogen helpers’ would swap their PMN membership (either temporarily or throughout the remainder of the plant’s development) for membership into a microbe-microbe network (MMN) with the aim of reducing the plant’s fitness for immediate gains provided by switching to a microbe-microbe network.

The oscillation between PMN-centered and MMN-centered gameplay is likely highly dependent on the oscillations between nutrient availability and the enzymatic capacity of the microbial members. Plants shift between net carbon storage and net carbon utilization strategies as a function of photosynthetic rate [48]. As a result, concomitant shifts in microbial abundance and composition follow these nutrient flows [49,50]. Therefore, universal rules for PMNs and MMNs likely persist, but specific gameplay rules will always pervade given the relative heterogeneous biodiversity across landscapes driven by contextual dependencies.

For instance, a group of saprotrophic microbes (thrive on decaying organic matter) with little advantages competing within their PMN during the start-up stage would likely thrive during periods of plant senescence (**Figure 1.2**). Thus, if saprotrophs are abundant during the SuPMN and can effectively persist near root tips (rhizosphere), then their enzymatic capabilities would provide them with a relative fitness advantage over neighboring microbes (in LsPMNs) that harbor inferior enzymatic machinery to degrade decaying organic matter. In contrast, their presence and activity would theoretically be decreased if A) their primary substrates for energy and biomass attainment are limited or B) neighboring individuals encroach on their ability to thrive in a given niche and neither abiotic nor biotic factors are sufficient enough to counteract nutrient limitations.

Similar models could indeed be generated to represent the flux of additional macro- and micronutrients in relation to plant development and PMN composition. And, with the expanding literature dedicated to communicating relative soil characteristics and microbial abundance/composition, these ends will likely be realized. The primary issue, however, as mentioned above is that although general rules can be applied to nearly every PMN and MMN, specific rules that govern interspecies interactions will likely lag behind the required technological leaps (e.g., real-time monitoring of spatiotemporal gene-protein-metabolite and microbial distributions). Nonetheless, the general rules governing plant-microbe and microbe-microbe interactions will largely explain their relative contributions to plant growth and development.

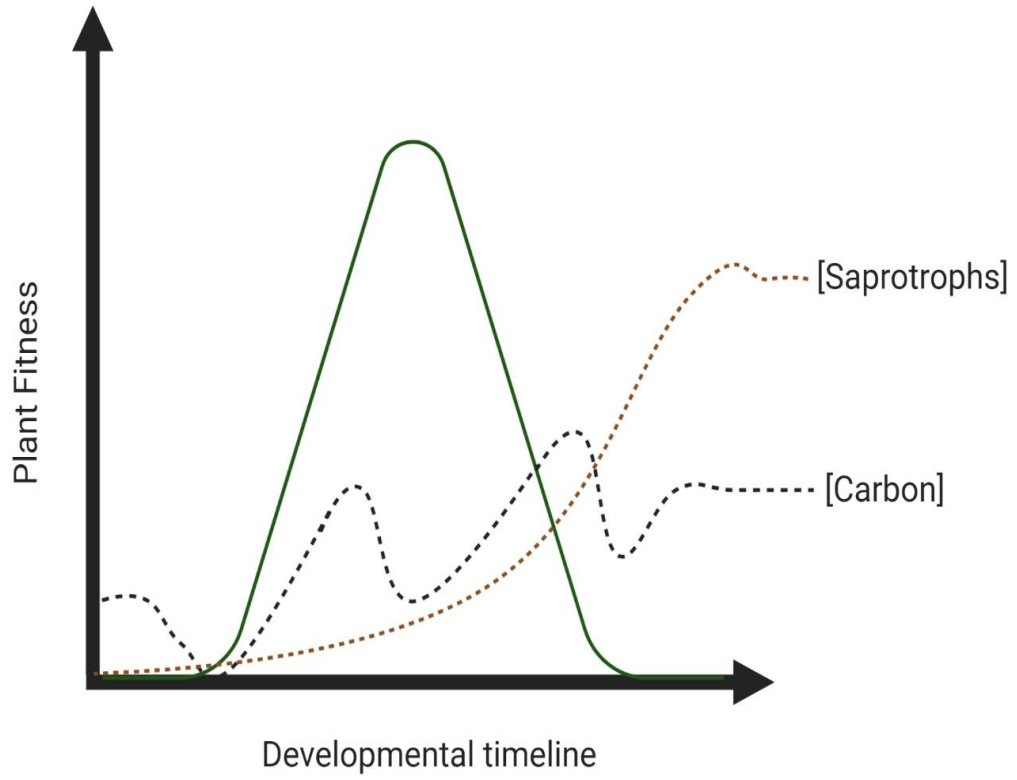

Figure 1.2. Simplified model of a single functional group dynamic in PMNs. The concentration of carbon peaks during active photosynthesis, whereas troughs indicate periods of carbon utilization. Decaying plant material becomes abundant as plant fitness decreases (i.e., completion of senescence), and saprotrophic organisms give rise given their proclivity for decaying plant material as a primary substrate.

2.2 Gameplay in a Meritocratic Microbial Milieu

Membership within PMNs likely follows a meritocratic hierarchical distribution, and functional characteristics as a factor of the environment determine biogeographical distribution. Lone exceptions to these rules likely involve transient microbes that have happened upon their niche but are unable to dwell there effectively. Thus, some general rules of PMN assemblages can be estimated if sufficient input

information for a given system are available. For example, the efficacy of ectomycorrhizal (EM) fungal associations is interdependent on plant host fitness. EM plants invest ~30% of their carbon budget into the soil [51], and EM fungi use this carbon as a source of energy while supplying nitrogen (N), phosphorus (P), and water in return. Due to their intimate association with plant roots, EM fungi (i.e., mycorrhizas) function as an 'extended root system' that not only acts as a highway for underground organisms but can also connect the root systems of plant species. Thus, analyzing the rhizospheric PMN community outward toward the bulk soil, one would expect to see a gradient of microbes fractionated by 1) their ability to reach the root system (or maintain their position if part of a SuPMN) and/or 2) the efficiency of their collective enzymatic activity (e.g., hydrolytic potential) to use the N and P resources provided by the EM fungi (**Figure 1.3**) with less of their genomic architecture dedicated to carbon cycling (unless capable of fixing atmospheric CO_2). EM fungi 'highways' would then resemble the backbone of many PMNs across the developmental period of the plant, which would render testable predictions regarding the composition and spatiotemporal distributions of other members in the PMN.

In addition, PMN metabolic reconstructions can also be employed to generate a theoretical map of how PMNs structure themselves across space and time. Coupling site soil characteristics (e.g., texture, relative moisture, C:N ratio, and P concentration) with metagenomic data, metabolite cycling within a flexible system (i.e., PMN assemblages across time) can be predicted to enhance existing

models. As a result, net substrate utilization and production can be estimated to predict the shape of the PMN (**Figure 1.4**).

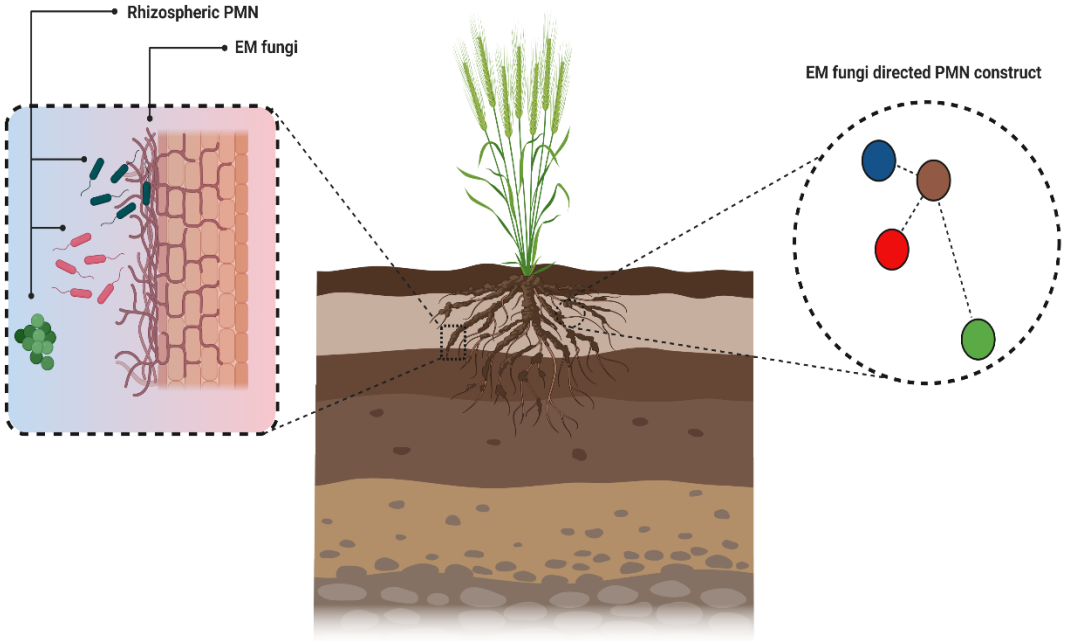

Figure 1.3. EM fungi restricted gradient of PMN members. Host-microbe interdependency and capability theoretically frames the spatiotemporal distributions of PMN members.

In theory, once the initial metabolite concentrations and general species interactions of a PMN are known, metabolic reconstructions and enzymatic kinetic dynamics could be fine-tuned to resolve the metabolite flux input-output distributions of the PMN and better understand the factors that dictate PMN assemblages. Unfortunately, the implementation of such pairwise models such as Lotka-Volterra (i.e., prey-predator) first-order differential equations fail to capture the complexity of the presumed 50,000 unique members within tight spatial scales (~1 g of soil) of a PMN. However, viewing microbial populations as networks that

are portioned by primary gameplay strategy and substrate proclivity may allow for partial predictability of PMN assemblages across space and time. As such, general principles that govern the community assemblages of PMNs could be ascertained, which would likely frame specific PMN interactions in realistic contexts.

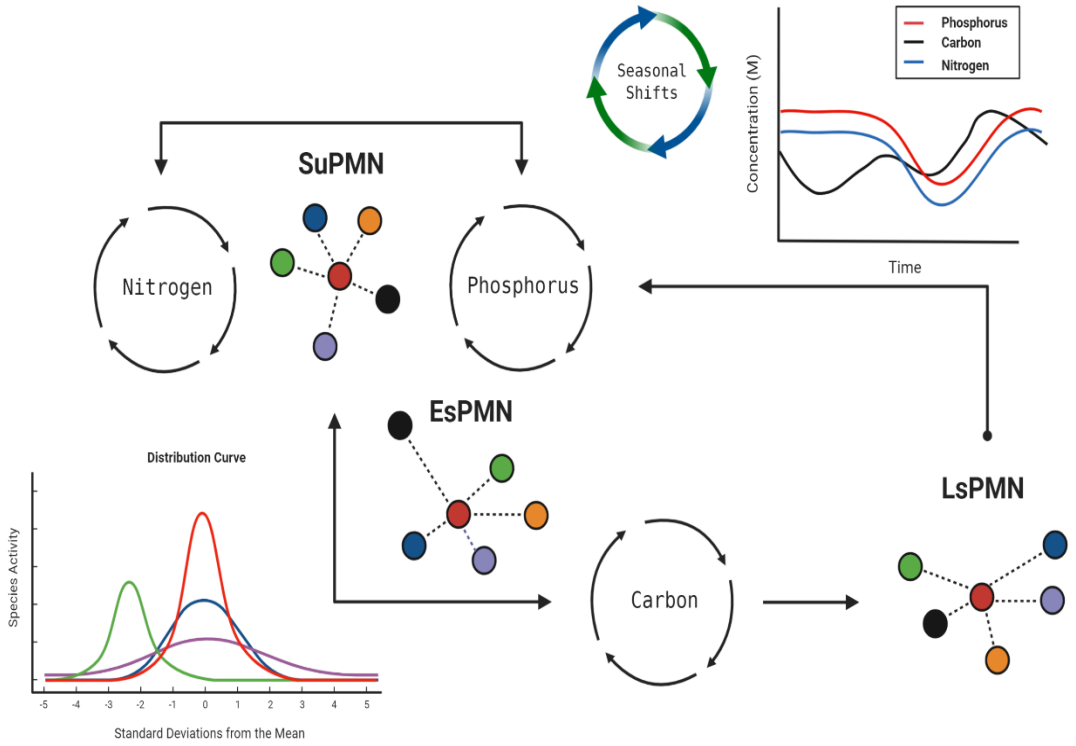

Figure 1.4. Hypothetical schema for assessing the shape of PMNs. Both metabolite composition and microbial member composition can be estimated within the PMN given sufficient input data, e.g., species composition, substrate proclivity, microbe-microbe gameplay strategies, soil composition, and host plant developmental cycle.

2.3 Function, Value, and Anti-Egalitarianism in PMNs

It is well-established that select microbial members can either enhance, decrease, or render no observable impact to the fitness of their plant host [12,52,53]. The ‘either’ here should, however, be viewed through a context dependent lens. For example, the mode-of-action efficacy of microbial bio-stimulants/bio-inhibitors (e.g., plant growth promoting microbes and plant pathogens) shifts as a function of ecosystem interactions (i.e., biotic and abiotic interactions). As recently demonstrated [14], removing a single member from a 185-member microbial consortium can dramatically alter the fitness of host plants. Thus, metabolic input values for a given microbial member (e.g., auxin production) can be used as rough estimates to predict PMN and MMN fitness, but value points that reflect total PMN and MMN architectures are required to generate estimates of their relative impacts on plant growth and development (i.e., net positive, neutral, negative).

Inherent to the constant metabolite fluxes within PMNs is the generation of ‘reusable’ and ‘consumable’ resources that partition subsequent substrates from deleterious or non-consumable by- and end-products. Uninterrupted cycling of select molecules (e.g., cellulose, nitrates, phosphates) may persist in a given PMN cycle, but spatially confined hotspots may bias the distribution of PMN members. In contrast, transient molecule oscillations may give rise to ‘underdog’ PMN members, who persist at low concentrations under ‘normal’ or ‘static’ conditions but proliferate and thrive when a substrate becomes available that only they can efficiently consume. Moreover, chemical pools that are generated in PMNs likely interact to produce novel downstream chemicals [54]. As such, the value placed

on a single PMN member depends on its ability to functionally benefit the balance of the entire PMN, and this impact could presumably be concentrated to a single moment with respect to space and time or continuously across varying levels of PMN assembly (i.e., SuPMN, EsPMN, LsPMN). Together, the complexity within PMNs necessitates the integration of several scientific disciplines and model configurations that include gene-protein-metabolite networks as a function of metabolite partitioning and repurposing will likely represent the spatiotemporal dynamics of PMNs with a high degree of realism.

Both PMN and MMN assemblages are inextricably anti-egalitarian. The sociality of these interspecies interactions is predicated on life history, genomic versatility, gameplay strategies, and ecological circumstance—all of which can be summed under the umbrella of adaptability. Therefore, factoring in contextual gradients, symbiotic PMN members must provide fitness benefits to either the host plant or community microbes, which secures its position throughout PMN development. If, however, the PMN balance is disrupted to a point beyond where effective buffering can be maintained by symbiotic PMN members, then select symbiotic PMN members (depending on their adaptability) would be outcompeted by pathogenic microbes, and plant fitness will incur a decrease (**Figure 1.5**). Therefore, niche exclusion (e.g., competition for proximity to the root system) would be predicated on the elasticity of the symbiotic PMN architecture and thus its ability to thwart off the encroachment of pathogenic members. In turn, competition for this niche compartment would continue throughout the development of the plant, and gameplay strategies would continue in flux to the

end of securing niche occupancy and robust resources. Given that the interdependence between symbiotic PMN members and plants follows a proximity-based pattern (i.e., closer to the root system = greater chance of eliciting a strong interspecies response), the link between root exudates and enzymatic potential should undergird the gradient of species distributions in and around plant roots.

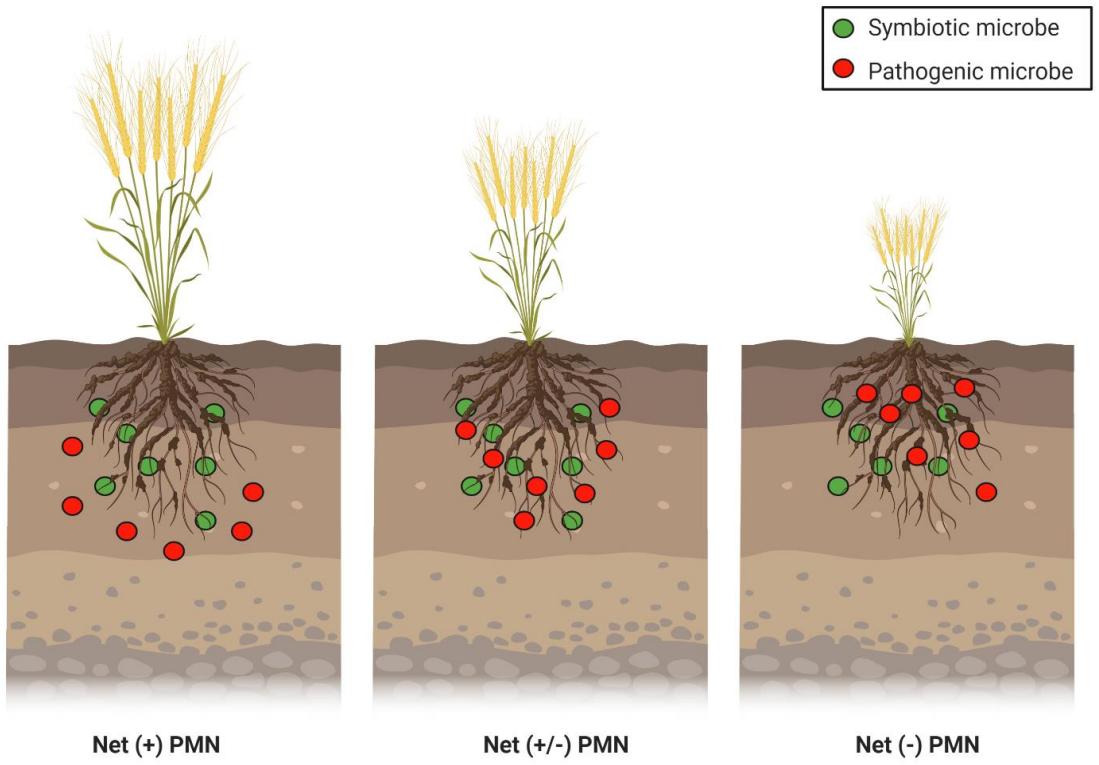

Figure 1.5. Simplified PMN assemblage outcomes. Functional predeterminants and nutrient availability dictate nutrient and species distributions. Cooperative and competitive gameplay strategies likely propel in concert. However, overall PMN fitness (positive, neutral, and negative) could hypothetically be ascertained by assessing the stratification of symbiotic and pathogenic microbes in relation to root structures.

3 Testing the Meritocratic Compartmentalization Hypothesis

Addressing the meritocratic compartmentalization hypothesis (MCH) could be achieved in both natural and artificial settings—both of which offering unique advantages and disadvantages. For example, in natural systems (i.e., terrestrial ecosystems or agricultural fields) soil and root cores could be extracted using a hypodermic or coring approach that would limit the amount of community disruption. Fractions of the sample would be assayed using high-performance liquid chromatography (HPLC) for chemical/metabolite analyses, and additional soil fractions (same sample) would be subjected to DNA sequencing and RNA transcriptomics to assess the relative diversity and abundance of the microbial organisms in the sample(s). Moreover, stable-isotope labeling can be employed to distinguish metabolically active microbes from those that are metabolically inactive. Investigating natural systems in such a way will elucidate microbial and chemical distributions in relation to plant roots, their relative abundances, and the relative activity of microbial populations at the given timepoint. Although many of the above strategies are regularly adopted for plant-microbe interaction investigations [27,55-59] the novelty of framing these investigations in the MCH rests in the sampling strategies and the presumed relative connectivity between root systems and microbial members. Thus, increased sample sizes (endosphere, rhizosphere, and bulk soil) from a single site should be collected, and a detailed account of the environmental conditions (e.g., tree health and developmental stage, humidity, relative rainfall, fog index, sampling time) should be explicitly stated in scientific communications. Taken together, when possible, multiple

strategic methods should be aggregated to mitigate discrepancies inherent to single-approach schemas.

Regarding artificial experimental settings (e.g., environmental chamber and greenhouse), the above methodology can also be applied. However, a mechanistic (e.g., cause and effect) approach can be employed. For example, synthetic microbial communities (SynComs) can be generated to test the genetic prerequisites for select metabolic functions that contribute to the spatiotemporal distributions of PMN members and those that elicit a net positive or net negative interaction with their plant host. Similarly, fluorescently labeled organisms can be introduced into the system to determine motility and colonization potential within a complex or highly reduced PMN. Given the relatively controlled conditions, the spatiotemporal dynamics of PMNs can also be determined as a function of time without the intrusion of additional variables (e.g., parasitism, sporadic rainfall, variable humidity). Moreover, perturbations to the artificial system (e.g., nutrient fluxes, lighting modifications, watering variability) can singly or concertedly be introduced to tease out consequential results. For example, shifts to PMNs as a result of climate related factors (e.g., elevated temperature, drought, flood) hold promise for assessing the changes in PMN assemblages in relation to plant dysbiosis. Importantly, transgenerational factors can be assessed by probing the PMN architecture in response to emigrant plant species and/or continued growth support, and single-line experiments (i.e., using seeds derived from an inoculated plant) can be set-up to a) determine the conservation of the seed microbiota and b) model the development of PMNs (SuPMN, EsPMN, LsPMN) across

generational shifts. Essentially, artificial experimental systems that closely mimic natural system will provide the most realistic representation of how PMNs assembly across space and time.

Given sufficient input information regarding the PMN (e.g., microbial composition, plant developmental stage, relative interspecies interaction potential), the MCH can be directly tested. For instance, if EM fungi are present, then restricted bacterial coexistence should be present and predicated on their enzymatic capability to metabolize primary macronutrients (C, N, P) or those secreted by the root-mycorrhiza complex while maintaining homeostasis for the proximal PMN. Moreover, flux balance analyses can be rendered to model metabolite fluxes and interspecies interactions within a PMN, and laser-assisted electrospray ionization could validate the spatiotemporal dynamics of metabolite and microbial member fluxes within PMNs. Therefore, relative point values for a given PMN or PMN member can be generated as function of both the abiotic and biotic factors that undergird the biological system (**Figure 1.6**) to hone modeling predictive power and integrate incremental factors of complexity. Taken together, assessments geared toward unveiling the inputs required to drive PMN interactions and the interactions therein that ensue as a result of both atypical and typical environmental fluctuations, and framing plant-microbe interactions in the context of the MCH should elucidate general principles that govern microbe-microbe and plant-microbe interactions.

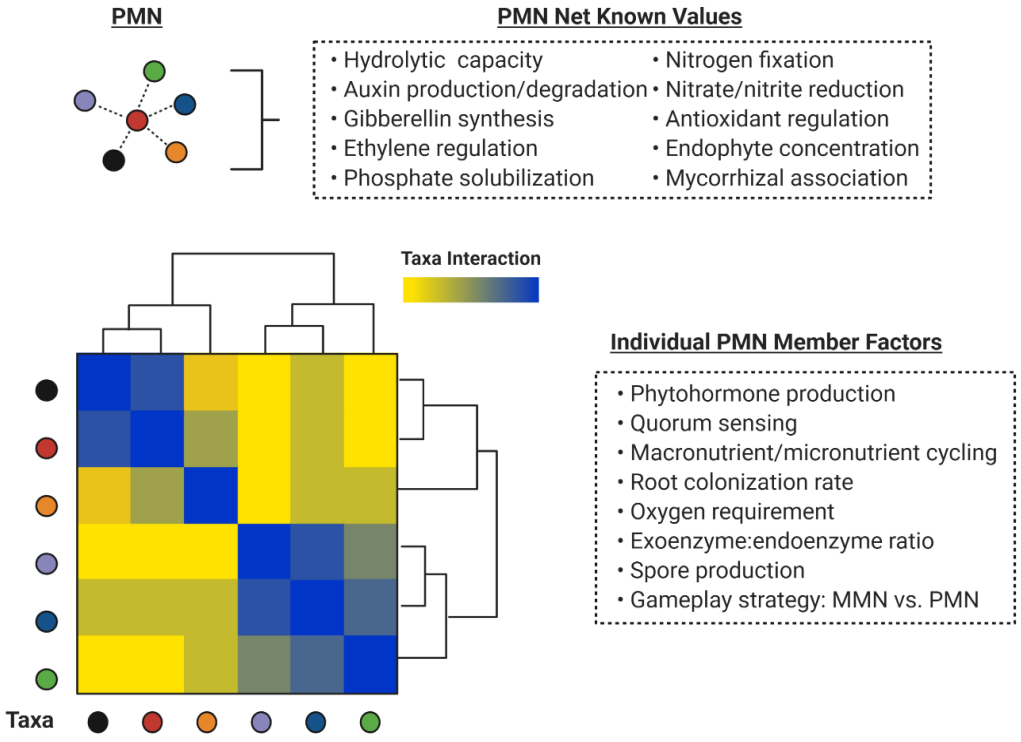

Figure 1.6. Value-based assessment of PMN members in network and out-of-network. Input values for a given PMN member (e.g., phytohormone production) should be assessed in relation to other PMN members to effectively model the outcome (i.e., net positive, neutral, negative) of plant-microbe interactions. The efficacy of individual PMN member factors will be dependent on neighboring microbial members. Therefore, input values should be viewed holistically once individual values have been obtained.

Conclusions and Future Perspectives

Research on plant-microbe interactions requires a holistic approach to successfully integrate findings derived from restricted experimental setups into complex environments (e.g., terrestrial ecosystems and croplands). No single organism is an island: organisms function optimally when their predispositions are balanced by their environment. As such, although tradeoffs persist between artificial and natural system setups, a concentrated goal among researchers must

be to strive for enhancing our understanding of the detailed mechanisms that govern PMN dynamics.

Both technological advancements and conceptual reframing will expedite efforts to unlock key signatures of PMNs. From multipronged experimental schemas (e.g., transcriptomics, isotope profiling, metabolomics) to computationally modeling interspecies interactions, effectively progressing the field of plant-microbe interactions will require methodological standardizations and/or detailed communications that address inherent methodological shortcomings. Thus, cohesive collaborations in pursuit of implementing rigorous reporting and standardized practices will progress the development of PMN database curations that lend reproducible and illuminating findings.

The environmental effects of climate change are expected to surge between 2027 and 2042 [60], and drastic shifts in PMN compositions and abundances will likely be disrupted beyond reparation in some cases. However, investigative forethought and coordinated collaboration can better our chances of securing the power of PMNs to buffer climate-driven environmental fluxes. Given that the health of plants is inextricably linked to the health of their associated microbes, there is an urgent need to capture the spatiotemporal dynamics among microbes and their host to better buffer the imminent dysfunctions that will plague terrestrial ecosystems and agricultural lands in the upcoming decades.

4 References

1) Larson G, Piperno DR, Allaby RG, Purugganan MD, Andersson L, Arroyo-Kalin M, Barton L, Vigueira CC, Denham T, Dobney K, Doust AN. Current perspectives and the future of domestication studies. Proceedings of the National Academy of Sciences. 2014 Apr 29;111(17):6139-46.

2) Silva LC, Corrêa RS, Wright JL, Bomfim B, Hendricks L, Gavin DG, Muniz AW, Martins GC, Motta AC, Barbosa JZ, Young SD. A new hypothesis for the origin of Amazonian Dark Earths. Nature Communications. 2021 Jan;12(1):1-1.

3) Staller JE, Tykot RH, Benz BF. The science behind the Three Sisters mound system: An agronomic assessment of an indigenous agricultural system in the northeast. Histories of Maize: Multidisiplinary approaches to the prehistory, linguistics, biogeography, domestication, and evolution of Maize.

4) Chen P, Du Q, Liu X, Zhou L, Hussain S, Lei LU, Song C, Wang X, Liu W, Yang F, Shu K. Effects of reduced nitrogen inputs on crop yield and nitrogen use efficiency in a long-term maize-soybean relay strip intercropping system. PloS one. 2017 Sep 14;12(9):e0184503.

5) Liu J, Ouyang X, Shen J, Li Y, Sun W, Jiang W, Wu J. Nitrogen and phosphorus runoff losses were influenced by chemical fertilization but not by pesticide application in a double rice-cropping system in the subtropical hilly region of China. Science of The Total Environment. 2020 May 1;715:136852.

6) Shah F, Wu W. Soil and crop management strategies to ensure higher crop productivity within sustainable environments. Sustainability. 2019 Jan;11(5):1485.

7) Swift R, Denton MD, Melino VJ. Plant probiotics for nutrient acquisition by agriculturally important grasses: A comprehensive review of the science and the application. Annual Plant Reviews online. 2018 Feb 15:537-84.

8) Zhang L, Yan C, Guo Q, Zhang J, Ruiz-Menjivar J. The impact of agricultural chemical inputs on environment: global evidence from informetrics analysis and visualization. International Journal of low-Carbon technologies. 2018 Dec;13(4):338-52.

9) Pereira L, Wynberg R, Reis Y. Agroecology: The future of sustainable farming?. Environment: Science and Policy for Sustainable Development. 2018 Jul 4;60(4):4-17.

10) Reimer A, Doll JE, Basso B, Marquart-Pyatt ST, Robertson GP, Stuart D, Zhao J. Moving toward sustainable farming systems: Insights from private and public sector dialogues on nitrogen management. Journal of Soil and Water Conservation. 2017 Jan 1;72(1):5A-9A.

11) Deng S, Wipf HM, Pierroz G, Raab TK, Khanna R, Coleman-Derr D. A plant growth-promoting microbial soil amendment dynamically alters the strawberry root bacterial microbiome. Scientific reports. 2019 Nov 27;9(1):1-5.

12) Berrios L, Ely B. Plant growth enhancement is not a conserved feature in the Caulobacter genus. Plant and Soil. 2020 Mar 2:1-5.

13) Chouyia FE, Romano I, Fechtali T, Fagnano M, Fiorentino N, Visconti D, Idbella M, Ventorino V, Pepe O. P-Solubilizing Streptomyces roseocinereus MS1B15 with multiple plant growth-promoting traits enhance barley development

and regulate rhizosphere microbial population. Frontiers in Plant Science. 2020;11.

14) Finkel OM, Salas-González I, Castrillo G, Conway JM, Law TF, Teixeira PJ, Wilson ED, Fitzpatrick CR, Jones CD, Dangl JL. A single bacterial genus maintains root growth in a complex microbiome. Nature. 2020 Nov;587(7832):103-8.

15) Guo J, Lv X, Jia H, Hua L, Ren X, Muhammad H, Wei T, Ding Y. Effects of EDTA and plant growth-promoting rhizobacteria on plant growth and heavy metal uptake of hyperaccumulator Sedum alfredii Hance. Journal of Environmental Sciences. 2020 Feb 1;88:361-9.

16) Li X, Zhang Q, Ma J, Yang Y, Wang Y, Fu C. Flooding Irrigation Weakens the Molecular Ecological Network Complexity of Soil Microbes during the Process of Dryland-to-Paddy Conversion. International Journal of Environmental Research and Public Health. 2020 Jan;17(2):561.

17) Luo D, Langendries S, Mendez SG, De Ryck J, Liu D, Beirinckx S, Willems A, Russinova E, Debode J, Goormachtig S. Plant growth promotion driven by a novel Caulobacter strain. Molecular Plant-Microbe Interactions. 2019 Sep 14;32(9):1162-74.

18) Torres-Martinez L, Sanchez-Julia M, Kimbrough E, Hendrix TC, Hendrix M, Day RH, Krauss KW, Van Bael SA. Influence of soil microbiota on Taxodium distichum seedling performance during extreme flooding events. Plant Ecology. 2020 Sep;221(9):773-93.

19) Xie L, Lehvävirta S, Timonen S, Kasurinen J, Niemikapee J, Valkonen JP. Species-specific synergistic effects of two plant growth—promoting microbes on green roof plant biomass and photosynthetic efficiency. PloS one. 2018 Dec 31;13(12):e0209432.

20) Zhang M, Yang L, Hao R, Bai X, Wang Y, Yu X. Drought-tolerant plant growth-promoting rhizobacteria isolated from jujube (Ziziphus jujuba) and their potential to enhance drought tolerance. Plant and Soil. 2020 Jul;452(1):423-40.

21) Gütschow J, Jeffery ML, Gieseke R, Günther A. The PRIMAP-hist national historical emissions time series (1850-2017). V. 2.1.

22) Naamala J, Smith DL. Relevance of plant growth promoting microorganisms and their derived compounds, in the face of climate change. Agronomy. 2020 Aug;10(8):1179.

23) Piotrowski K, Romanowska-Duda Z. Positive impact of bio-stimulators on growth and physiological activity of willow in climate change conditions. International agrophysics. 2018;32(2).

24) Torsvik V, Goksøyr J, Daae FL. High diversity in DNA of soil bacteria. Applied and environmental microbiology. 1990 Mar 1;56(3):782-7.

25) Roesch LF, Fulthorpe RR, Riva A, Casella G, Hadwin AK, Kent AD, Daroub SH, Camargo FA, Farmerie WG, Triplett EW. Pyrosequencing enumerates and contrasts soil microbial diversity. The ISME journal. 2007 Aug;1(4):283-90.

26) Durán P, Thiergart T, Garrido-Oter R, Agler M, Kemen E, Schulze-Lefert P, Hacquard S. Microbial interkingdom interactions in roots promote Arabidopsis survival. Cell. 2018 Nov 1;175(4):973-83.

27) Levy A, Conway JM, Dangl JL, Woyke T. Elucidating bacterial gene functions in the plant microbiome. Cell host & microbe. 2018 Oct 10;24(4):475-85.

28) Prabha R, Singh DP, Gupta S, Gupta VK, El-Enshasy HA, Verma MK. Rhizosphere Metagenomics of Paspalum scrobiculatum L.(Kodo Millet) Reveals Rhizobiome Multifunctionalities. Microorganisms. 2019 Dec;7(12):608.

29) Wu L, Wang J, Wu H, Chen J, Xiao Z, Qin X, Zhang Z, Lin W. Comparative metagenomic analysis of rhizosphere microbial community composition and functional potentials under Rehmannia glutinosa consecutive monoculture. International journal of molecular sciences. 2018 Aug;19(8):2394.

30) Yurgel SN, Douglas GM, Langille MG. Metagenomic functional shifts to plant induced environmental changes. Frontiers in microbiology. 2019;10:1682.

31) Dörr J, Hurek T, Reinhold-Hurek B. Type IV pili are involved in plant–microbe and fungus–microbe interactions. Molecular microbiology. 1998 Oct;30(1):7-17.

32) Jones DL, Nguyen C, Finlay RD. Carbon flow in the rhizosphere: carbon trading at the soil–root interface. Plant and soil. 2009 Aug 1;321(1-2):5-33.

33) Pang Q, Zhang T, Wang Y, Kong W, Guan Q, Yan X, Chen S. Metabolomics of early stage plant cell–microbe interaction using stable isotope labeling. Frontiers in plant science. 2018 Jun 5;9:760.

34) Rasche F, Lueders T, Schloter M, Schaefer S, Buegger F, Gattinger A, Hood-Nowotny RC, Sessitsch A. DNA-based stable isotope probing enables the identification of active bacterial endophytes in potatoes. New Phytologist. 2009 Mar;181(4):802-7.

35) Starr EP, Shi S, Blazewicz SJ, Probst AJ, Herman DJ, Firestone MK, Banfield JF. Stable isotope informed genome-resolved metagenomics reveals that Saccharibacteria utilize microbially-processed plant-derived carbon. Microbiome. 2018 Dec;6(1):122.

36) Calvo P, Zebelo S, McNear D, Kloepper J, Fadamiro H. Plant growth-promoting rhizobacteria induce changes in Arabidopsis thaliana gene expression of nitrate and ammonium uptake genes. Journal of Plant Interactions. 2019 Jan 1;14(1):224-31.

37) Jacoby RP, Succurro A, Kopriva S. Nitrogen substrate utilization in three rhizosphere bacterial strains investigated using proteomics. Frontiers in Microbiology. 2020 Apr 28;11:784.

38) Aufrecht JA, Timm CM, Bible A, Morrell-Falvey JL, Pelletier DA, Doktycz MJ, Retterer ST. Quantifying the spatiotemporal dynamics of plant root colonization by beneficial bacteria in a microfluidic habitat. Advanced Biosystems. 2018 Jun;2(6):1800048.

39) Massalha H, Korenblum E, Malitsky S, Shapiro OH, Aharoni A. Live imaging of root–bacteria interactions in a microfluidics setup. Proceedings of the National Academy of Sciences. 2017 Apr 25;114(17):4549-54.

40) Aleklett K, Kiers ET, Ohlsson P, Shimizu TS, Caldas VE, Hammer EC. Build your own soil: exploring microfluidics to create microbial habitat structures. The ISME journal. 2018 Feb;12(2):312-9.

41) Brundrett MC. Mycorrhizal associations and other means of nutrition of vascular plants: understanding the global diversity of host plants by resolving conflicting information and developing reliable means of diagnosis. Plant and Soil. 2009 Jul 1;320(1-2):37-77.

42) Brundrett M. Mycorrhizas in natural ecosystems. InAdvances in ecological research 1991 Jan 1 (Vol. 21, pp. 171-313). Academic Press.

43) Read DJ. Mycorrhizas in ecosystems. Experientia. 1991 Apr 1;47(4):376-91.

44) Van Der Heijden MG, Martin FM, Selosse MA, Sanders IR. Mycorrhizal ecology and evolution: the past, the present, and the future. New phytologist. 2015 Mar;205(4):1406-23.

45) Van Der Heijden MG. Underground networking. Science. 2016 Apr 15;352(6283):290-1.

46) Kuźniar A, Włodarczyk K, Grządziel J, Woźniak M, Furtak K, Gałązka A, Dziadczyk E, Skórzyńska-Polit E, Wolińska A. New insight into the composition of wheat seed microbiota. International journal of molecular sciences. 2020 Jan;21(13):4634.

47) Zhou X, Wang JT, Zhang ZF, Li W, Chen W, Cai L. Microbiota in the rhizosphere and seed of rice from China, with reference to their transmission and biogeography. Frontiers in Microbiology. 2020 Jul 10;11:995.

48) Leake JR, Ostle NJ, Rangel-Castro JI, Johnson D. Carbon fluxes from plants through soil organisms determined by field 13CO2 pulse-labelling in an upland grassland. Applied Soil Ecology. 2006 Sep 1;33(2):152-75.

49) Kohli M, Henning JA, Borer ET, Kinkel L, Seabloom EW. Foliar fungi and plant diversity drive ecosystem carbon fluxes in experimental prairies. Ecology Letters. 2020 Jun 25.

50) Martínez Cano I, Shevliakova E, Malyshev S, Wright SJ, Detto M, Pacala SW, Muller-Landau HC. Allometric constraints and competition enable the simulation of size structure and carbon fluxes in a dynamic vegetation model of tropical forests (LM3PPA-TV). Global Change Biology. 2020 Aug;26(8):4478-94.

51) Whipps JM. Microbial interactions and biocontrol in the rhizosphere. Journal of experimental Botany. 2001 Mar 1;52(suppl_1):487-511.

52) Bulgarelli D, Rott M, Schlaeppi K, van Themaat EV, Ahmadinejad N, Assenza F, Rauf P, Huettel B, Reinhardt R, Schmelzer E, Peplies J. Revealing structure and assembly cues for Arabidopsis root-inhabiting bacterial microbiota. Nature. 2012 Aug;488(7409):91-5.

53) Kępczyńska E, Karczyński P. Medicago truncatula root developmental changes by growth-promoting microbes isolated from Fabaceae, growing on

organic farms, involve cell cycle changes and WOX5 gene expression. Planta. 2020 Jan 1;251(1):25.

54) van Dam NM, Bouwmeester HJ. Metabolomics in the rhizosphere: tapping into belowground chemical communication. Trends in plant science. 2016 Mar 1;21(3):256-65.

55) Chialva M, Ghignone S, Novero M, Hozzein WN, Lanfranco L, Bonfante P. Tomato RNA-seq Data Mining Reveals the Taxonomic and Functional Diversity of Root-Associated Microbiota. Microorganisms. 2020 Jan;8(1):38.

56) Fudyma JD, Lyon J, AminiTabrizi R, Gieschen H, Chu RK, Hoyt DW, Kyle JE, Toyoda J, Tolic N, Heyman HM, Hess NJ. Untargeted metabolomic profiling of Sphagnum fallax reveals novel antimicrobial metabolites. Plant direct. 2019 Nov;3(11):e00179.

57) Ortiz Y, Restrepo C, Vilanova-Cuevas B, Santiago-Valentin E, Tringe SG, Godoy-Vitorino F. Geology and climate influence rhizobiome composition of the phenotypically diverse tropical tree Tabebuia heterophylla. PloS one. 2020 Apr 7;15(4):e0231083.

58) Seybold H, Demetrowitsch TJ, Hassani MA, Szymczak S, Reim E, Haueisen J, Lübbers L, Rühlemann M, Franke A, Schwarz K, Stukenbrock EH. A fungal pathogen induces systemic susceptibility and systemic shifts in wheat metabolome and microbiome composition. Nature communications. 2020 Apr 20;11(1):1-2.

59) Yuan ZS, Liu F, Liu ZY, Huang QL, Zhang GF, Pan H. Structural variability and differentiation of niches in the rhizosphere and endosphere bacterial microbiome of moso bamboo (Phyllostachys edulis). Scientific Reports.;11(1):1-9.

60) Hébert R, Lovejoy S, Tremblay B. An observation-based scaling model for climate sensitivity estimates and global projections to 2100. Climate Dynamics. 2020 Dec 18:1-25.

CHAPTER 2

PLANT GROWTH ENHANCEMENT IS NOT A CONSERVED FEATURE IN THE *CAULOBACTER* GENUS[2]

[2]Berrios L, Ely B (2020) Plant growth enhancement is not a conserved feature in the *Caulobacter* genus. *Plant and Soil* 449, 81-95.

Abstract

Aims

Species within the *Caulobacter* genus have been termed ‘hub species’ in the plant microbiome. To understand these interactions, we assessed the interactions between several *Caulobacter* strains and a common host plant.

Methods

We identified a set of 11 *Caulobacter* strains that range in genetic diversity and tested them for their ability to increase the growth of *Arabidopsis thaliana.* In addition, biochemical assays were employed to determine if these *Caulobacter* strains produce common plant growth promoting (PGP) biosynthates. To identify potential PGP-related genes, genomic analyses were performed to compare the genomes of PGP *Caulobacter* strains to those of non-PGP *Caulobacter* strains.

Results

For the PGP *Caulobacter* strains, we observed that common PGP biosynthates did not contribute to the observed *Caulobacter*-mediated plant growth stimulation. Genomic analyses suggested that the genomes of PGP strains maintain similar metabolic pathways compared to those of non-PGP strains, and that common genes related to PGP factors do not explain the PGP mechanisms for the *Caulobacter* strains we analyzed.

Conclusions

Plant growth enhancement is not a conserved feature in the *Caulobacter* genus, and some *Caulobacter* strains even inhibit plant growth. Moreover, common PGP factors do not fully explain *Caulobacter*-mediated plant growth enhancement.

Introduction

Plant health is heavily influenced by bacterial associations (Bulgarelli et al. 2013). To date, many bacterial genera have been categorized as plant growth promoting bacteria (PGPB), and various biochemical mechanisms employed by select genera have been described (Agrawal et al. 2018; Backer et al. 2018; Chaiharn and Lumyong 2011; Etesami et al. 2015; Glick 2005; Glick 2014; Gurdeep and Reddy 2015; Zhang et al. 2019). Although strides have been taken to elucidate these causal mechanisms, additional studies are required to establish the genetic underpinnings that distinguish PGP strains from commensals. Given the growing interest in applying PGPB to increase agricultural output (Bhattacharyya and Jha 2012; Cole et al. 2017), a more thorough examination of the genetic factors separating PGPB from commensals will contribute to this goal.

Beginning in the mid-1930's, the genus *Caulobacter* has been described as comprising Gram-negative, unicellular bacteria (Henrici and Johnson 1935) that display a marked ability to outlive many bacterial organoheterotrophs in nutrient-deficient aquatic environments. These depictions cemented the identification of *Caulobacter* as aquatic and oligotrophic bacteria (Poindexter 1964). As a result, an abundance of research leading up to the turn of the 21st century has focused primarily on understanding how their dimorphic lifestyle and their holdfast-mediated adhesion facilitate their adaptation to nutrient-limited, aquatic environments (Jenal et al. 1995; Laub et al. 2007). However, recent reports have suggested that *Caulobacter* species may play a functional role in the plant-microbiome (de Jesus Suarez-Moo et al. 2019; Luo et al. 2019; Naveed et al. 2014;

Verma et al. 2018; Yang et al. 2019), and *Caulobacter* species have been termed a hub species due to their integral interactions with plants (Agler et al. 2016). Descriptions of these interactions often give the impression that *Caulobacter* species enhance plant growth by the production of indole-3-acetic acid (IAA), solubilizing phosphate, synthesizing siderophores, 1-aminocyclopropane-1-carboxylate (ACC) deaminase activity, or by modulating plant-host metabolic pathways (Naveed et al. 2014; Verma et al. 2018; Yang et al. 2019), but each of these reports only assessed a single *Caulobacter* strain and did not determine whether the presumed PGP factors are actually responsible for enhancing plant growth. In fact, *Caulobacter* sp. RHG1 was shown to increase the growth and development of *Arabidopsis thaliana* plants and colonize the roots and leaves independently of IAA, ACC deaminase activity, phosphate solubilization, siderophore biosynthesis, and nitrite reduction (Luo et al. 2019). Thus, *Caulobacter* strains may employ PGP factors that are different from what previous researchers have proposed.

To date, no reports have communicated the variety of interactions *Caulobacter* strains maintain with plants. Since the genetics of *Caulobacter* are well-established (Ely 1991; Laub et al. 2000), and we have previously assembled high-quality whole-genome sequences (WGS) for a variety of *Caulobacter* strains (Ash et al. 2014; Berrios and Ely 2018; Ely et al. 2019; Patel et al. 2015; Scott and Ely 2015), we screened 11 *Caulobacter* strains ranging in genomic relatedness for their ability to enhance the growth of *A. thaliana* and for the presence of common PGP biochemical activities to identify the diversity of PGP characteristics among

Caulobacter strains. In addition, we analyzed the WGS of select *Caulobacter* strains to investigate potential PGP-related genes. To this end, our data 1) demonstrate the strain-specific nature of *Caulobacter*-plant interactions, 2) indicate that conventional PGP-biochemical activity is not a prerequisite for *Caulobacter*-mediated plant enhancement, and 3) demonstrate that PGP *Caulobacter* possess unique protein families linked to bacteria-plant interactions.

Materials and Methods

Plant growth experiments

A. thaliana (Ler-O*)* seeds were sterilized using Cl_2 gas as previously described (Lindsey et al. 2017). An aliquot of 50 seeds per condition was placed in a sterile microfuge tube for each condition. Bacterial suspensions were grown overnight, adjusted to an OD_{600nm} = 1.0, pelleted, and suspended in 1 ml of sterile tap H_2O. A total of 500 µl of a given bacterial suspension was pipetted into its corresponding microfuge tube. Bacteria-seed mixtures were incubated at room temperature for 30 min, while seeds incubated with sterile tap H_2O functioned as a negative control. The mixtures were then spread onto Murashige and Skoog (MS) plates (Murashige and Skoog 1962), and seeds were stratified for four days at 4°C. Subsequently, plates were placed in an environmental chamber at a constant 23°C with a 16/8 light/dark photoperiod and a light intensity of ~150 µM/m2/s. After seven days, germination rates (total number of seeds germinated divided by total number of seeds plated multiplied by 100) were calculated, and seedlings along with any remaining ungerminated seeds were transplanted to plastic trays harboring sterilized soil. Trays were then covered with plastic domes (to control humidity)

and were placed in the environmental chamber. Domes were removed after a one-week period, and the plants were bottom-watered once per week for the first three weeks and then twice per week until complete senescence. Plants were thinned to one per plot after the first week, which resulted in 24 *A. thaliana* plants per condition. Germination rate (%), rosette diameter (mm), inflorescence height (mm), silique quantity, fresh plant weight (g), and root length (cm) data were collected and analyzed using statistical analyses in the R (3.6.0) package ggplot2 (Wickman 2016) and PAST (Hammer et al. 2001).

Bacterial strain isolations

The rhizosphere strain *Caulobacter* sp. CBR1 was isolated as previously described (Berrios and Ely 2019). The endophytic strains HB2a and HB4b were isolated from plant roots collected along the banks of the Hillsborough River in Thonotosassa, Florida (28°08’50.1”N 82°14’19.5”W) in October 2017. Plant roots were stored at 4°C for three days prior to bacterial isolations. Roots were rinsed with sterile deionized water (diH_2O) to remove all remnant dirt and debris. Afterwards, roots were soaked in a 50% bleach solution for five min, followed by one soak with 2 M HCl and one soak with 70% ethanol for three min each. Roots were then rinsed with sterile diH_2O for five min and subsequently soaked in sterile, diH_2O for three min. Roots were rinsed with sterile tap water, and aliquots of the rinse were aseptically spread on peptone yeast extract (PYE) plates to confirm that no bacteria remained on the root surface. Following the washing period, the roots were placed in a surface sterilized mortar, and a sterilized pestle was used to grind the roots. The ground roots were transferred to a sterilized test tube containing 10

ml of autoclaved tap water, and the mixture was vortexed for 30 s. A 100 µl aliquot of this mixture was spread onto a PYE plate containing 20 mg/l of ampicillin (AMP), since most Caulobacter strains are ampicillin resistant (Poindexter 1964). Colonies that resembled *Caulobacter* colonies were streaked onto PYE+AMP plates and were incubated overnight at 30°C. Single colonies were selected from plates appearing to possess pure cultures and were suspended in 3 ml of PYE. After overnight incubation at 30°C, bacterial cultures were analyzed with a light microscope to assess cellular shape and motility. Pure cultures that possessed presumed *Caulobacter* cells were used for DNA isolation, 16S rDNA gene amplification, and Sanger sequencing.

Bacterial strains from the plant growth assays were re-isolated as follows: 1 g of soil (after plant excision) was aseptically transferred to a sterile centrifuge tube, and 1 ml of sterile, tap water was added. The mixture was vortexed for 30 s, and then 100 µl of the supernatant was spread on a PYE plate. Isolated colonies were selected, suspended in PYE broth and grown overnight at 30°C. The resulting cultures were used for DNA isolation as described below.

DNA isolation and 16S rDNA gene sequencing

Bacterial DNA was isolated using a Sigma GenElute Bacterial Genomic DNA kit according to the manufacturer's instructions. The 16S rDNA gene was amplified by PCR under standard conditions using 5'-GGTTACCTTGTTACGACTT-3' and 5'-GTGCCAGCMGCCGCGGTAA-3' as forward and reverse primers, respectively. The nucleotide sequence of the amplified ~ 900 bp product was determined by Sanger sequencing, and the resulting 16S rDNA sequence was compared to other

bacterial 16S rDNA sequences using BLASTn (Altschul et al. 1997) to verify the recovery of the appropriate *Caulobacter* strain.

Whole-genome sequencing and bioinformatic analyses

The whole-genome sequence (WGS) of bacterial DNA was determined at the Delaware Bioinformatics Institute using a PacBio RSII single-molecule sequencer. The resulting sequence reads (read depth > 50X) were assembled into a single WGS contig using HGAP 3 in SMRT Portal through Amazon Machine Image (AMI) EC2 using the smrtanalysis-2.3.0-ami-20fb4848 image with the default *de novo* parameters. The consensus sequence was then annotated using the Rapid Annotation using Subsystem Technology (RAST) and the NCBI GenBank Prokaryotic Genome Annotation Pipeline (PGAP) (Aziz et al. 2008; Tatusova et al. 2016). A complete list of all strains used in the experiments and their corresponding GenBank accession numbers (if available) can be found in **Table A.1**.

Homology based analyses were performed using BLASTn and BLASTp for nucleotide and amino acid sequence comparisons, respectively. WGS comparisons and phylogenetic constructions were performed using the chromosome comparison module in the Bionumerics 7.6 platform. Protein family databases were created and analyzed in the PATRIC 3.5.41 depository platform (Wattam et al. 2016), and the principal component analysis (PCA) was performed using the R (3.6.0) packages ggplot2 (Wickman 2016) and ggfortify (Tang et al. 2016). Rendered graphics were polished in Adobe Illustrator CS6. Phylogenetic

analyses were computed using MEGA X (Felenstein et al. 1985; Kumar et al. 2018; Tamura and Nei 1993)

IAA quantification

IAA production was quantified as previously described (Patten and Glick 2002). Briefly, bacterial cultures were propagated overnight in 3 ml of PYE supplemented with 1 mg/ml of L-tryptophan. After incubation, bacterial concentrations were adjusted to an OD_{600nm} = 1.0. For each bacterial sample, a 1 ml aliquot of bacterial culture was centrifuged for 20 min at 10,000 x g, and the resulting supernatant was mixed with 2 ml of Salkowski's reagent (150 ml of 18 M H_2SO_4, 250 ml of diH_2O, 7.5 ml of 0.5 M $FeCl_3$) (Gordon and Weber 1951). Mixtures remained in a dark room at room temperature for 30 min before the absorbance at 535 nm was measured and compared to a standard curve. To confirm the IAA concentrations, samples were analyzed using a Waters Premier XE triple-quadruple mass-spectrometer with a Waters Aquity UPLC system. Each sample was prepared as previously described (Lin et al. 2015). The injection volume for each sample was 0.75 µl, and the flow rate was 0.2 ml/min. Mobile phase A consisted of 0.1% formic acid in H_2O, and mobile phase B consisted of 0.1% formic acid in acetonitrile. IAA concentrations were determined with the aid of an external standard curve ranging from 1 µg/ml to 10,000 µg/ml of IAA. Each bacterial sample was analyzed in triplicate, and the numerical values are expressed as mean concentrations with error bars representing ranges. Uninoculated PYE + 1 mg/ml L-tryptophan functioned as a negative control in each experiment. Statistical analyses were performed in GraphPad Prism 8.0.

Phosphate solubilization

Phosphate solubilizing activity was determined using the malachite green colorimetric assay. Briefly, bacteria were cultured overnight in PYE broth, and the cultures were adjusted to an OD_{600nm} = 1.0 after incubation. Bacterial cultures were then centrifuged for 10 min at 10,000 x g, and the resulting pellets were suspended in 1 ml of sterile, tap H_2O. For each bacterial sample, the resulting suspension was mixed in a 50 ml sterilized, polyethylene centrifuged tube with 25 ml of NBRIP broth (National Botanical Research Institute's Phosphate) supplemented with 10 g/l $Ca_3(PO_4)_2$ as an insoluble form of phosphate. Uninoculated NBRIP broth was used as a negative control. Samples were incubated on a rotary shaker (180 rpm) at 30°C for seven days. After incubation, each sample was centrifuged at 10,000 x g for 25 min. For each sample, a 3 ml aliquot of the resulting supernatant was transferred to a sterile test tube and was autoclaved thereafter. All sample supernatants were autoclaved for a 20 min sterilization period and were filtered through a 0.45 µm Millipore filter. Each sample supernatant was mixed at a 4:1 ratio with the malachite green complex as previously described (Baykov et al. 1988), and the OD_{630nm} was recorded for each sample. Phosphate concentrations were determined with the aid of a KH_2PO_4 standard curve. Each bacterial sample was assayed in triplicate.

Siderophore production

Siderophore production was analyzed qualitatively using the O-CAS method as previously described (Pérez-Miranda et al. 2007). Briefly, single bacterial colonies were streaked on PYE plates and incubated at 30°C for two days. A 4 ml aliquot

of the CAS overlay (Chrome azurol S (CAS) 60.5 mg, hexadecyltrimethyl ammonium bromide (HDTMA) 72.9 mg, piperazine-1,4-bis(2-ethanesulfonic acid) (PIPES) 30.24 g, 1mM $FeCl_3 \cdot 6H_2O$ in 10 mM HCl 10 ml, 0.9% agarose (w/v) per liter) was poured on top of each bacterial streak plate and was incubated overnight at 30°C. After incubation, the plates were analyzed based on a color change from blue to purple (catechol) or blue to yellow/orange (hydroxymates) in the medium surrounding the bacterial streaks. Each bacterial sample was tested in triplicate, and uninoculated PYE plates overlaid with the CAS reagent served as a negative control. *Pseudomonas* sp. HB2a functioned as a positive control.

ACC deaminase activity

ACC deaminase activity was assayed by measuring the amount of α-ketobutyrate produced as a result of the cleavage of ACC by the enzyme ACC deaminase (Penrose and Glick 2003). Briefly, overnight bacterial cultures were adjusted to an OD_{600nm} = 1.0 in minimal media supplemented with ACC as the sole nitrogen source. Bacterial cultures were centrifuged at 16,000 x g for 10 min, and the bacterial pellets were suspended in 1 ml of 0.1 M Tris-HCl (pH 7.6). Bacterial suspensions were recentrifuged at 16,000 x g for 10 min, and the pelleted bacteria were resuspended in 600 µl 0.1 M Tris-HCl (pH 8.5). Thirty microliters of toluene was added to each cell suspension, which was followed by a 30 s vortex period. Then, for each cell suspension, 200 µl from the suspension was mixed with 20 µl of 0.5 M ACC and incubated for 15 min at 30°C. After incubation, each suspension was mixed with 1 ml of 0.56 M HCl and was immediately centrifuged at 16,000 x g at room temperature for five min. For each suspension, 1 ml of the supernatant

was mixed with 500 µl of 0.56 M HCl. Afterwards, 1 ml of 0.2% 2,4-dinitrophenylhydrazine in 2 M HCl was added to the mixture, vortexed for 10 s and incubated at 30°C for 30 min. Two milliliters of 2 M NaOH was added to each mixture, and the absorbance for each sample was measured at 540 nm. Each bacterial strain was sampled in triplicate and compared to a standard curve of α-ketobutyrate ranging between 0.1 µM and 1.0 µM. Cell suspensions without ACC were used as negative controls, and cell suspensions with $(NH_4)SO_4$ (0.2% w/v) were used as positive controls. Each sample was tested in triplicate, and values are represented as mean concentrations with error bars indicating concentration ranges.

Results

Plant growth enhancement is not a shared feature among *Caulobacter* strains

Considering the relative abundance of *Caulobacter* reported in *A. thaliana* microbiome studies (Lundberg et al. 2012) coupled with reports indicating that *Caulobacter* strains appear to be hub species (Agler et al. 2016), we decided to explore the extent of species- and strain-specific interactions between *Caulobacter* and *A. thaliana*. To accomplish this goal, a set of *Caulobacter* strains ranging in genetic diversity (**Figure B.1 and Table A.1**) were individually assessed for their ability to impact the growth (weight) and development of *A. thaliana* plants. Of the 11 *Caulobacter* strains assessed, six (CB1, CB13, CB15, CBR1, *C. segnis* TK0059, and HB4b) increased the weight of *A. thaliana* (+); three strains (AP07, CB2, and CB4) decreased the weight of *A. thaliana* plants (-), and two strains (K31

and FWC20) produced no observable effect (+/-) on *A. thaliana* plant weight (**Figure 2.1a**). The reproducibility of the plant growth assay was verified for strain CBR1 using 3-fold larger sample sizes (**Figure 2.1b**) coupled with a replicated assessment on the effect selected bacterial had on plant weight (PW). When additional *A. thaliana* anatomical structures were assessed individually, we observed similar trends for each *Caulobacter* group (+, -, or +/-) regarding inflorescence height (IH) and basal rosette diameter (BRD) parameters. However, the silique quantity (SQ) parameter was highly variable among most of the strains, even among *Caulobacter* (+) group members (**Figure 2.1c**). Interestingly, *Caulobacter* sp. HB4b was the only strain that significantly increased the SQ of *A. thaliana*. Together, these results indicate that individual *Caulobacter* strains have diverse interactions with *A. thaliana*.

Since root growth is associated with plant growth, we hypothesized that *Caulobacter* (+) strains would alter root architecture by increasing overall primary root length compared to both control/*Caulobacter* (+/-) and *Caulobacter* (-) conditions. Surprisingly, we observed the formation of significantly more lateral roots and a larger primary root in the *Caulobacter* (+) group relative to the other groups (**Figure 2.1d**). Moreover, we also observed a severe decrease in lateral root formation for the *Caulobacter* (-) group, which suggests that the strains in the *Caulobacter* (-) group decrease the availability of nutrients for plant uptake. To verify that this effect was primarily driven by the inoculated bacterial strain, we analyzed representative soil samples and showed that we could re-isolate the original bacterial strains from each experimental condition. However, each soil

sample analyzed also contained relatively low (CFU g^{-1} ml^{-1} = 10^2) quantities of the bacterium *Sphingopyxis* sp*.* (**Table A.2**) that was not intentionally introduced. Although our gnotobiotic conditions included two bacterial strains instead of one, the control conditions retained the *Sphingopyxis* sp. At the same levels, indicating that it was a constant factor for all the plants. Moreover, only the intended bacteria were re-isolated from the soil in the initial experiment with CBR1 (**Figure 2.1b**), which suggested that the low levels of the *Sphingopyxis* sp. Had no impact on the growth experiment. We also observed intra- and inter-condition variation in bacterial abundance (**Table A.2**), so we decided to examine whether bacterial concentration correlated with PW. We hypothesized that higher concentrations of *Caulobacter* (+) bacteria would positively correlate with PW, and higher concentrations of *Caulobacter* (-) bacteria would negatively correlate with PW. In contrast, we hypothesized *Caulobacter* (+/-) and control group bacterial abundance would not correlate with PW. Although we had obtained only a few data points for each strain in the initial analysis, our preliminary analyses suggested strong correlations between bacterial concentration and PW in both the *Caulobacter* (+) and *Caulobacter* (-) groups, whereas the *Caulobacter* (+/-) group and the control condition showed little variation in bacterial concentration (**Figure 2.2**). To test this conclusion, the experiment was replicated to generate a larger dataset, and the resulting data corroborated the correlations computed in the initial analysis (**Figure B.3 and Table A.3**). Collectively, these results demonstrate the ability of select *Caulobacter* strains to modulate root architecture as recently

observed by Luo et al. (2019) and suggest that the interactions between *Caulobacter* strains and *A. thaliana* are concentration-dependent.

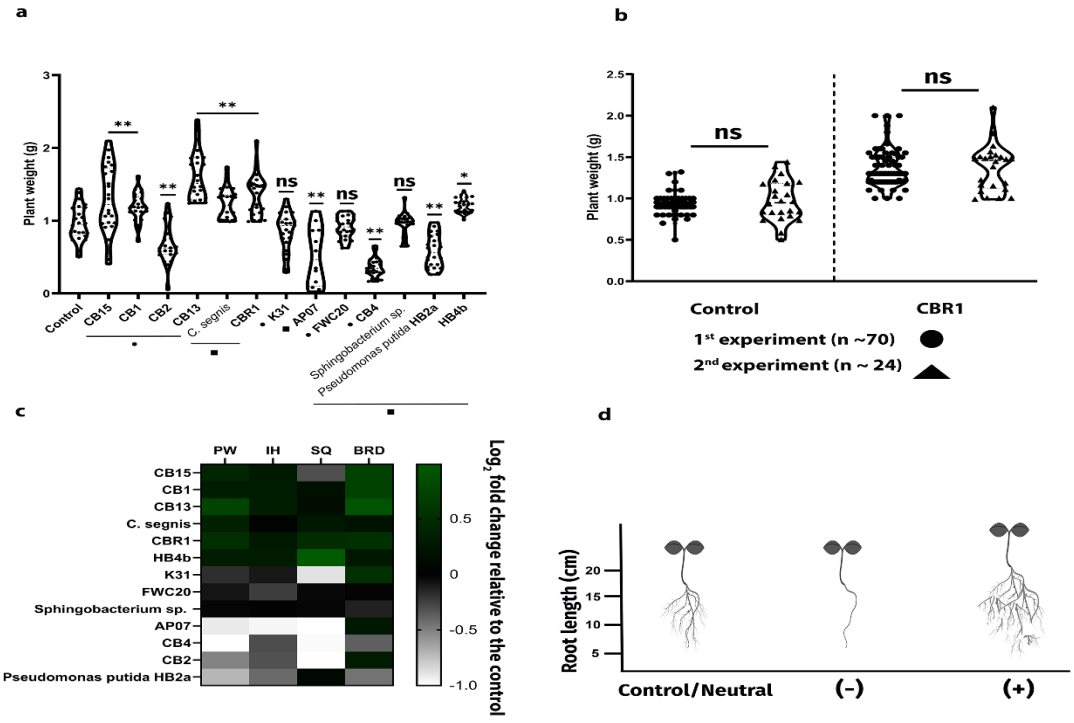

Figure 2.1 Impact of *Caulobacter* strains on the growth of *A. thaliana* plants **a)** Violin plot depicting the impact of a given bacterial strain on *A. thaliana* plant weight (PW) in grams (g). Samples (n) per condition (n=24). A one-way ANOVA was performed in R, and p-values were adjusted by the Benjamini-Hochberg method using the ggplot2 package. * ≤ 0.05; ** ≤ 0.001; ns = not significant relative to control plant weight (average). Circles below strain names indicate that those strains were isolated from aquatic sources, and squares below strain names indicate that those strains were isolated from soil environments. A *Sphingomonas* bacterium and a *Pseudomonas* sp. HB2a were used as neutral and negative controls, respectively. An extended data set (n=12) from a replicated experiment that depicts the PW for each condition can be found in **Figure B.2**. **b)** Violin plot illustrating the reproducibility of the plant growth assay. Statistical analyses were calculated as described for b. **c)** Heatmap illustrating the average $\log_2$ fold change of the specified *A. thaliana* growth parameters relative to the control (no added bacteria). PW (plant weight); IH (inflorescence height); SQ (silique quantity); BRD (basal rosette diameter). **D)** Binarized image of representative *A. thaliana* seedlings regarding *Caulobacter* +, -, and +/- and control groups.

Caulobacter (+) strains do not utilize presumed PGP factors to enhance *A. thaliana* growth

To identify potential PGP mechanisms employed by *Caulobacter* (+) strains, we assayed each strain for IAA biosynthesis, ACC deaminase activity, siderophore biosynthesis and phosphate solubilization, since these assays are continually used as screening methods for PGPB (Taurian et al. 2010; Yan et al. 2018). Interestingly, we found that only two of the *Caulobacter* (+) strains (*C. segnis* TK0059 and *Caulobacter* sp. HB4b) produced detectable levels of IAA based on data derived from the Salkowski colorimetric assay (data not shown) and verified with LC-MS (**Figure 2.3a**). However, these strains produced the lowest IAA levels among the IAA-producing *Caulobacter* analyzed. Of the three *Caulobacter* (-) strains, two (AP07 and CB4) produced relatively high amounts of IAA, and both *Caulobacter* (+/-) strains produced moderate amounts of IAA. In addition, despite reports indicating that IAA production is linked to increased germination rates and plant growth (Etesami et al. 2015; Naveed et al. 2014; Saleemi et al. 2017), our data indicate that neither germination rates (**Figure 2.3b**) nor plant weight increased in the presence of IAA-producing *Caulobacter*. In fact, most of the strains that produced IAA decreased germination (**Figure 2.3b**) rates and either had no effect on plant weight or negatively impacted plant weight (**Figure 2.3c**). Thus, perhaps the higher level of IAA produced by AP07 and CB4 is linked to inhibiting plant growth, not enhancing plant growth. Aside from the variable IAA production, we observed that each of the analyzed *Caulobacter* strains exhibited similar ACC deaminase activity (**Figure 2.3d**), while none of the strains were able

to produce siderophores or solubilize phosphate. Since each of these *Caulobacter* strains produced similar amounts of ACC deaminase, it is likely that this enzyme is not solely responsible for the beneficial effects observed in the *Caulobacter* (+) group. Taken together, our data indicate that 1) neither IAA production nor ACC deaminase activity is likely responsible for *Caulobacter*-mediated plant growth enhancement; 2) siderophore biosynthesis and phosphate solubilization do not contribute to plant growth enhancement in the strains we analyzed; and 3) common screening methods employed to select for PGP candidates could lead to the oversight of beneficially applicable PGP *Caulobacter* strains.

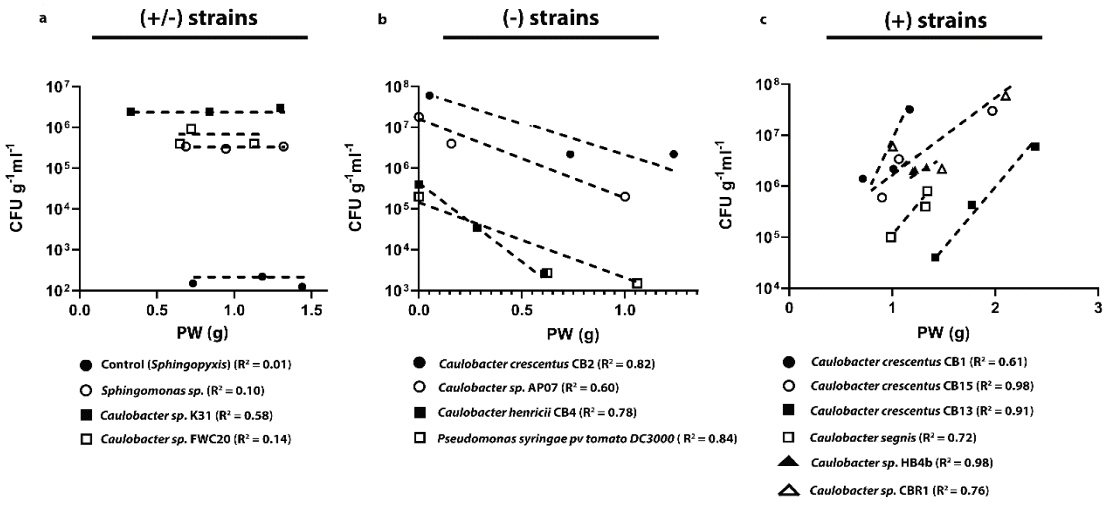

Figure 2.2 Pearson correlation analyses comparing the weight of *A. thaliana* to quantity of associated bacteria a) Depicts the bacterial concentration-independent relationship between (+/-) strains and *A. thaliana* plant weight. **B)** Illustrates the overall negative correlation between *A. thaliana* plant weight and (-) strain concentration. **C)** Represents the positive correlation between *A. thaliana* plant weight and (+) strain concentration. A shorter correlation line for the HB4b condition is present due to the limited range of PW that resulted in the HB4b condition (**Figure 2.1a**). A complete list of each sample correlation can be found in **Table A.2**. Correlation analyses were performed with data prior to log scale adjustment.

Metabolic synteny persists between PGP *Caulobacter* strains and genes related to common PGP factors are limited in *Caulobacter* genomes

Since IAA production and ACC deaminase activity did not appear to be associated with plant growth, we analyzed the genomes of representative +, -, and +/- *Caulobacter* groups (CB1, CB13, CB15, *C. segnis* TK0059, CB2, CB4, AP07, and K31) to identify potential genetic underpinnings involved in *Caulobacter*-mediated plant growth enhancement. Genome analyses revealed that genes related to common PGP factors (Lemanceau et al. 2017; Najimi et al. 2008) such as abscisic acid biosynthesis (isopentenyl-pyrophosphate isomerase), cytokinin biosynthesis (isopentenyl transferase), gibberellin synthesis (gibberellin 20-oxidase), phosphate solubilization (pyrroloquinoline quinone), nitrogen fixation (*nif*A), or siderophore biosynthesis (2,3-dihydroxybenzoate-AMP ligases and isochorismatases) were not present in any of the *Caulobacter* genomes we analyzed. Furthermore, genes involved in tryptophan-dependent IAA production (tryptophan monooxygenase and indole pyruvate decarboxylase) were found only in the genomes of IAA-producing *Caulobacter* strains. To gain additional insight into the genomic underpinnings of *Caulobacter*-mediated plant growth enhancement, the predicted genes for each genome were grouped into one of seven categories related to general metabolic pathways, and overall gene abundance for each general pathway was used as the parameter for the initial comparative analysis (**Figure 2.4a**). Consistent with previous findings that detail the genomic features of bacterial adaptation to plants (de Souza et al. 2019; Levy et al. 2017), our comparison revealed that *Caulobacter* (+) strains CB1, CB13,

CB15, and *C. segnis* TK0059 maintained similar plant-related gene numbers in their genomes. To better highlight metabolic trends, genes involved in ~130 metabolic pathways were parsed individually and binned according to predicted functions. Representative strains from each *Caulobacter* group were subjected to an ordination by PCA, and the PCA results revealed distinct strain clustering based on the type of interaction with *A. thaliana* plants (+/-, +, -). A more in-depth analysis demonstrated that *Caulobacter* (+) strain genomes coded for more genes related to propanoate and butanoate metabolism. In addition, the genomes of *Caulobacter* (+) strains harbored more genes related to glycerolipid metabolism, while the genomes of *Caulobacter* (-) strains either had lower (>2-fold) or considerably higher (>7-fold) numbers of genes related to this pathway. Genes involved in tryptophan metabolism were depleted in the genomes of *Caulobacter* (+) compared to genomes of *Caulobacter* (-, +/-) strains, which reflects tryptophan-dependent IAA biosynthesis and complements a recent report that details a similar trend in the genomes of various bacterial genera (de Souza et al. 2019). Moreover, two genes, one coding for a peptidase S41 and one coding for a putative TonB-dependent receptor were exclusive to *Caulobacter* (+) genomes. Further, no differences were observed between the *Caulobacter* genomes analyzed that suggested a PGP function derived from the biosynthesis of presumed PGP factors such as brassinosteriods, flavonoids, terpenoids, or zeatin (Luo et al. 2019; Mierziak et al. 2014; Schäfer et al. 2015; Yazaki et al. 2017). Likewise, no variation in secretion systems or potential effector proteins was observed. Despite WGS analyses indicating closer nucleotide homology between CB2 and CB1 than

between CB2 and CB4 (**Figure 2.4b**), CB2 clustered with CB4 when analyzed based on shared predicted proteins contributing to metabolic pathways (**Figure 2.4c**). Further genome mining and BLASTp analyses indicated that the *Caulobacter* (+) strains harbor two operons predicted to code for proteins functioning in the complete conversion of betalmic acid to gomphrenin-I (BGC), which is a subclass of betalain that has been shown to possess high reactive oxygen species-scavenging activity compared to other betalains (Cai et al. 2003). In contrast, the genomes of the *Caulobacter* (-) strains harbor only one BGC

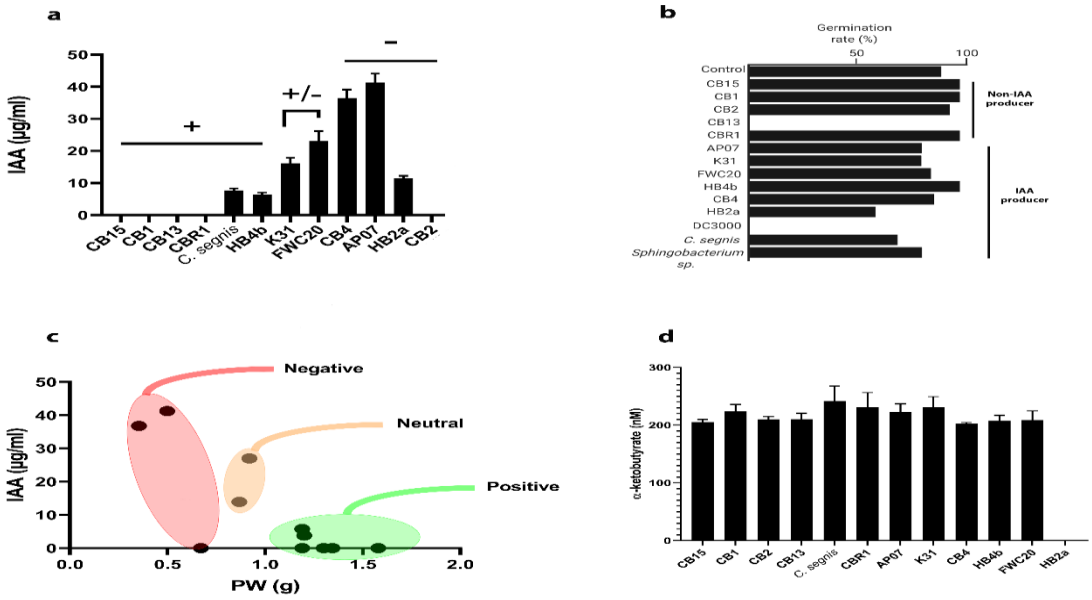

Figure 2.3 *Caulobacter* phytohormone production a) IAA concentrations detected using LC-MS. Each sample was analyzed in triplicate, and error bars represent concentration ranges. **B)** Germination rates for each condition (n = 90 seeds per condition) relative to IAA production. DC3000 corresponds to the plant pathogen *P. syringae* pv. Tomato DC3000, which was used as a negative control. **C)** IAA production relative to PW. Positive, neutral, and negative nomenclature pertains to impact on plant growth. **D)** Relative ACC deaminase activity expressed as total amount of α-ketobutyrate produced. Each sample was analyzed in triplicate. Error bars represent concentration ranges.

operon (**Figure 2.4d**). Similarly, a genome analysis of *Caulobacter* (+/-) strain K31 demonstrated that the K31 genome (chromosomal and plasmid DNA) also only harbors one BGC operon. Thus, this additional BGC operon could additively contribute to affect the PGP differences observed between the *Caulobacter* (+) and the *Caulobacter* (-, +/-) strains.

To better understand the potential contribution of the additional BGC operon regarding plant growth enhancement, we exploited the nucleotide synteny between CB1 (+) and CB2 (-) (~98% identity of shared sequence regions) (Ely et al. 2019) and sought to identify the underlying genetic causes responsible for the effect differences observed between the two strains relative to plant growth. Our analyses revealed that CB1 and CB2 share 2,829 distinct protein families (PFs) with a total of 274 and 311 unique PFs, respectively (**Table A.4**). Of the 274 PFs unique to the CB1 proteome, 72% are annotated as hypothetical proteins. Similarly, 89% of the 311 PFs unique to the CB2 proteome are annotated as hypothetical proteins. Of the remaining 28% (77 PFs) unique to the CB1 proteome, 50 PFs are predicted to function in cellular regulation; 5 PFs are annotated as transposases; 8 PFs are involved in nitrate/nitrite processing; 7 PFs protect against reactive oxygen species, and the remaining 7 PFs participate in peptidase/protease secretion. As mentioned above, the genome of CB1 contained a duplicated operon functioning in the production of gomphrenin-I, a betalain with high reactive oxygen species-scavenging activity, whereas the genome of CB2 only harbored one of these operons. Thus, the genomic synteny and functional disparity regarding *A. thaliana* interactions between CB1 and CB2 suggested that

CB1 and other *Caulobacter* (+) strains may be enhancing plant growth by modulating reactive-oxygen levels, since the remaining predicted protein discrepancies between the genomes of CB1 and CB2 offered little insight into the genetic mechanisms involved in plant growth enhancement. Considering that betalain production has been linked to plant health (Polturak et al. 2018), and that two copies of this BGC operon are present only in the genomes of *Caulobacter* (+) strains, it is possible that the difference between positive and negative *Caulobacter-A. thaliana* interactions depends on the functional role of this additional BGC operon.

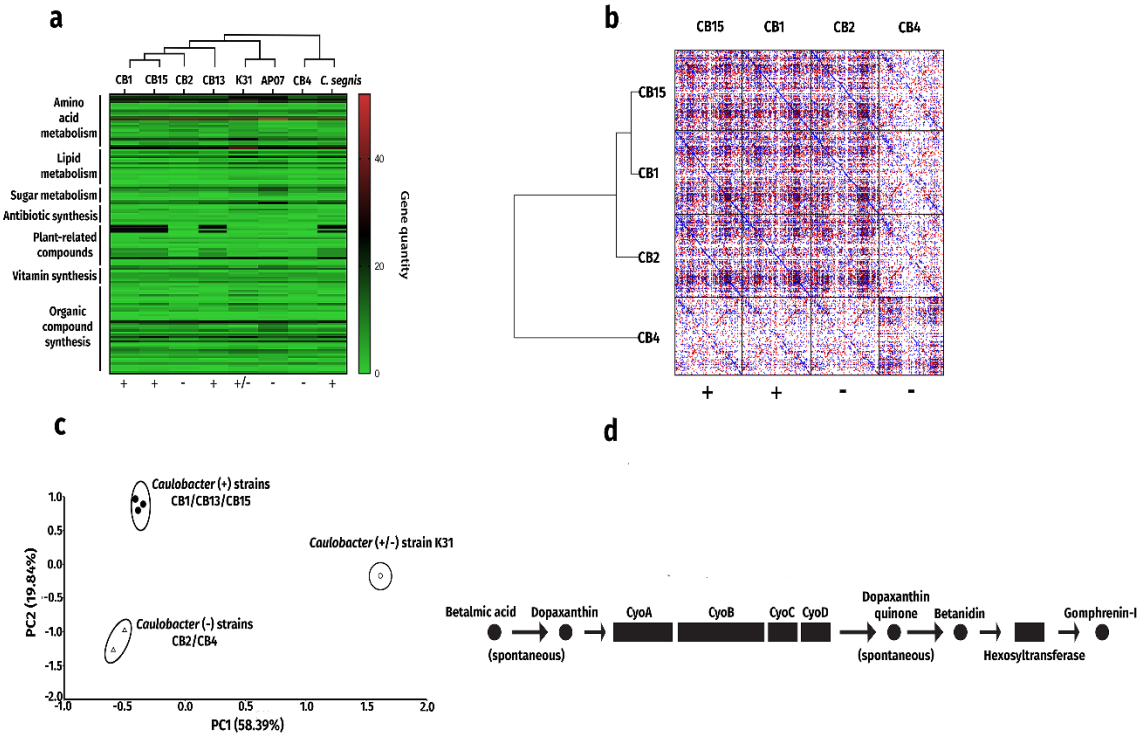

Figure 2.4 Genomic analyses of representative *Caulobacter* strains a) Heatmap illustrating predicted protein quantity regarding metabolic functions in *Caulobacter* (+, - , and +/-) groups. **B)** Dot plot depicting the WGS nucleotide synteny and dissimilarity between select strains. **C)** PCA of representative *Caulobacter* strains. **D)** Biosynthetic pathway schematic depicting the conversion of betalmic acid to gomphrenin-I with necessary genes (boxes) and substrates/intermediates/end-products (circles) illustrated.

Next, we sought to determine the frequency of genes related to common PGP factors by analyzing available *Caulobacter* genome sequences in the PATRIC database. To this end, we analyzed 61 available *Caulobacter* genomes (WGS or completed sequence) for the presence of genes related to the biosynthesis of abscisic acid (isopentenyl-pyrophosphate isomerase), cytokinins (isopentyl transferase), gibberellins (gibberellin 20-oxidase), siderophores (2,3-dihydroxybenzoate-AMP ligases and isochorismatases), phosphate solubilization (pyrroloquinoline quinone), and nitrogen fixation (*nifA*). We did not locate any genes predicted to code for the common proteins associated with these PGP factors, except for a predicted pyrroloquinoline quinone protein that was in 10 of the analyzed *Caulobacter* genomes and could be involved in phosphate solubilization (**Table A.5**). Interestingly, eight of the 10 strains that harbor this gene in their genome were isolated from the rhizosphere. The remaining two strains were isolated from sewage sludge or mine tailings. Further, seven of these strains (each isolated from either maize roots/rhizosphere or coralloid roots) formed a distinct phylogenetic branch when 107 essential genes (housekeeping and ribosomal proteins) were analyzed among 39 unique *Caulobacter* strains (Luo et al. 2019). The eighth was *Caulobacter mirabilis* FWC38, which was distantly related to the other 38 *Caulobacter* strains. The remaining two strains (*C. flavus* CGMCC1 15093 and *C. vibrioides* T5M6) were not included in this analysis. To determine if the pyrroloquinoline quinone gene facilitates phosphate solubilization, we obtained *C. mirabilis* FWC38 and demonstrated that it did not solubilize phosphate when we assayed it for phosphate solubilization. Thus, the

pyrroloquinoline quinone gene present in the genomes of the remaining seven *Caulobacter* strains is likely not involved in calcium phosphate solubilization. Moreover, we also sought to determine the relative frequency of the duplicated BGC operon in genomes of available *Caulobacter* strains. To this end, we determined that 23 of the available 61 *Caulobacter* genomes harbor this duplicated operon (**Table A.6**). Taken together, these data demonstrate that 1) genes related to many common PGP factors are not present in the genomes of most *Caulobacter* strains; 2) the pyrroloquinoline quinone gene exclusive to select *Caulobacter* genomes does not confer the ability to solubilize calcium phosphate, and 3) the majority of publicly-available sequenced *Caulobacter* genomes do not harbor a duplicated BGC operon.

Discussion

We identified strain-specific interactions between various *Caulobacter* strains and *A. thaliana*, demonstrating positive, negative, and neutral bacteria-host relationships. Thus, *Caulobacter* plant interactions are strain-specific. Results from our germination rate assays demonstrated that *Caulobacter* (+) strains, on average, increase germination rates (~one day faster than control conditions and a greater percentage of germinated seeds) independently of IAA production. Our plant growth assay results demonstrated that *Caulobacter* (+) strains stimulate *A. thaliana* root growth, while *Caulobacter* (-) strains inhibit root growth. The increase of lateral root formation in the *Caulobacter* (+) groups relative to control conditions was also observed for the *Caulobacter* PGP strain RHG1 (Luo et al. 2019) and suggests that the *Caulobacter* (+) strains that we analyzed may colonize *A.*

thaliana roots like *Caulobacter* sp. RHG1 colonizes *A. thaliana* roots (primarily at the root tip and lateral root emergence region). Moreover, our results suggested that *Caulobacter (*+ and -) bacterial concentrations may be associated with the intensity of impact on *A. thaliana* (**Figure 2.2; Figure B.3; Table A.3**). However, overall bacterial concentrations were considerably variable between the initial and extended re-isolation experiments (**Table A.2 and A.3**), which may be a result of an elongated incubation period: samples in the extended data group were analyzed one week after those analyzed in the initial re-isolation experiment. Nonetheless, it will be interesting to investigate whether *Caulobacter* root-colonization is a conserved feature, or if root-colonization is specific to PGP *Caulobacter*. Further, it will be interesting to determine where and how the endophytic strain *Caulobacter* sp. HB4b colonizes plant structures, since it was the only strain to significantly increase SQ relative to the control plants.

Although most studies of PGP *Caulobacter* have focused on bacteria isolated from the rhizosphere, we demonstrated that strains isolated from aquatic sources can either increase (CB1, CB13, and CB15) or decrease (CB2 and CB4) the growth and development of *A. thaliana*. Similarly, we demonstrated that *Caulobacter* strains isolated from the rhizosphere can either increase (*C. segnis* TK0059) or decrease (AP07) the growth and development of *A. thaliana*. Further, we demonstrated that laboratory strains of *Caulobacter* can be effective PGP strains, indicating that these PGP traits are not lost rapidly during laboratory culture.

Since previous reports have indicated that the biosynthesis of IAA, ACC deaminase, siderophores and phosphate solubilization are potential mechanisms involved in *Caulobacter*-mediated plant growth enhancement (Janssen et al. 2015; Naveed et al. 2014; Yang et al. 2019), we tested our strains for these PGP factors. In contrast to our expectations, *Caulobacter* strains AP07 and CB4 produced higher levels of IAA (> 40 µg/ml) and had a negative impact on plant growth, while four of the six *Caulobacter* (+) strains did not produce detectable levels of IAA (**Figure 2.3a**). Therefore, IAA production is not required for *C. crescentus*-mediated plant growth enhancement. However, it would be interesting to investigate whether AP07 and CB4 would inhibit *A. thaliana* growth if their IAA synthesis genes were knocked-out. We also demonstrated that each of the analyzed *Caulobacter* strains had similar levels of ACC deaminase activity despite their varied impact on plant growth and that none of the *Caulobacter* strains we analyzed produced a siderophore or solubilized phosphate. Thus, these *C. crescentus* strains do not enhance plant growth by producing IAA, siderophores or solubilizing phosphate, and ACC deaminase is not a determining factor for their plant growth promoting activity. Together, these results contextualize a recent report that details the dispensability of common PGP factors regarding the bacterial colonization of plants (de Souza et al. 2019) and demonstrates that common PGP factors do not completely explain *Caulobacter*-mediated plant growth enhancement.

Consistent with the results from our biochemical assays, we demonstrated that the IAA-producing *Caulobacter* strains each possess genes necessary to

produce IAA via a tryptophan-dependent pathway, since removing the tryptophan substrate disabled the ability of each IAA-producing strain to produce IAA (data not shown). Similarly, each *Caulobacter* strain assayed for ACC deaminase activity harbors a gene coding for an ACC deaminase protein. We also confirmed that none of the *Caulobacter* strains possess siderophore biosynthetic genes, which agreed with our failure to observe positive results in the siderophore production assay. Although Naveed et al. (2014) demonstrated that *Caulobacter* sp. FA13 can produce siderophores, our results, which were derived using the same siderophore detection assay, demonstrated that siderophore production is not a common feature of *Caulobacter* strains. In contrast, our phosphate solubilization data are consistent with the observations of Naveed et al. (2014) and Luo et al. (2019), since none of the *Caulobacter* strains we assayed solubilized phosphate, and no genes related to phosphate solubilization were discovered in the *Caulobacter* genomes we analyzed (**Figure 2.4a**). However, an additional genomic comparison using the PATRIC database revealed that 10 of the available 61 *Caulobacter* strain genomes harbor a gene predicted to code for a pyrroloquinoline quinone that is involved in phosphate solubilization. But, when we assayed one of these 10 strains (*C. mirabilis* FWC38) for phosphate solubilization, we did not observe any solubilized phosphate. Therefore, many commonly reported PGP factors do not explain *Caulobacter*-mediated plant growth enhancement, and the pyrroloquinoline quinone gene in the genomes of select *Caulobacter* species is most likely not conferring the ability to solubilize calcium phosphate.

Similar to the recent genome analysis of *Caulobacter* sp. RGH1 (Luo et al. 2019), we did not find any genes involved in either nitrogen fixation or the biosynthesis of abscisic acid or gibberellins in the genome of any *Caulobacter* strain we analyzed, which suggests that these PGP factors are not common among *Caulobacter* strains. Although we did not find previously reported genes related to cytokinin biosynthesis (Lemanceau et al. 2017), we did identify genes related to the biosynthesis of the cytokinin zeatin, but no gene abundance differences or alterations in active sites of the predicted proteins were observed when we analyzed the genomes of representative *Caulobacter* strains (+, -, +/-). Therefore, cytokinins can probably be excluded as primary PGP factors. Moreover, our WGS analysis of ~130 metabolic pathways present in the *Caulobacter* genomes we assessed illustrated predicted protein-coding trends specific to *Caulobacter* groups (+, -, +/-), which generally agreed with previous experiments that delineated genomic trends among ~ 1200 plant-associated bacteria (Levy et al. 2017). However, our genomic analyses accounted for bacteria-plant interactions (+, -, +/-) and thus enabled us to determine that an increased number of genes related to carbohydrate metabolism did not reflect PGP ability, since *Caulobacter* sp. AP07 (-) and *C. segnis* TK0059 (+) each had increased numbers of carbohydrate-related genes in their genomes relative to the other strains (**Figure 2.4a**). This phenomenon may, however, be associated with isolation source (both strains were isolated from the soil) in addition to relative genome size (~ 1Mbp greater than aquatic-derived strains), which agrees with the results communicated by Levy et al. (2017) and a previous report detailing that the genomes of soil-

derived *Caulobacter* strains are larger than those of aquatic-derived *Caulobacter* strains (Wilhelm 2018). In contrast, the genome of each *Caulobacter* (+) strain harbored fewer genes related to tryptophan metabolism and more genes related to butanoate and propanoate metabolism compared to the genomes of the *Caulobacter* (- and +/-) strains, suggesting that these pathways could be associated with beneficial bacterial-plant interactions as suggested previously by de Souza et al. (2019) and Khan et al. (2019). Similarly, we discovered a duplicated BGC operon exclusively in *Caulobacter* (+) strain genomes, which suggests that one mechanism that these strains use to enhance plant growth could be the regulation of reactive oxygen-species. An extended analysis of 61 *Caulobacter* strain genomes revealed that this duplicated BGC operon is present in only one-third of the genomes (**Table A.6**) and no isolation source bias was detected: roughly half of the strains were isolated from aquatic environments, while the other half were isolated from soil/rhizosphere environments.

In summary, our plant growth experiment analyses showed that different *Caulobacter* strains affected *A. thaliana* plants in different ways, and our biochemical assays and genomic comparisons demonstrated that many presumed PGP biochemical factors are not essential for *Caulobacter*-mediated plant growth enhancement.

Acknowledgements

We thank Bill Cotham for his assistance with data collection regarding HPLC results and thank Maegan Albert, Sarah Brand and Quill Thomas for their help with processing plants. We also thank Sarah Brand for her expertise regarding graphic design. Additionally, we thank John Nomellini, John Smit, and Sean Crosson for providing us with *C. mirabilis* FWC38.

References

1) Abraham WR, Strömpl C, Meyer H, Lindholst S, Moore ER, Christ R, Vancanneyt M et al. (1999) Phylogeny and polyphasic taxonomy of *Caulobacter* species. Proposal of *Maricaulis* gen. nov. with *Maricaulis maris* (Poindexter) comb. Nov. as the type species, and emended description of the genera *Brevundimonas* and *Caulobacter*. Int J Systematic and Evol Microbiol. 49:1053-1073. https://doi.org/10.1099/00207713-49-3-1053
2) Agler MT, Ruhe J, Kroll S, Morhenn C, Kim ST, Weigel D, Kemen EM (2016) Microbial hub taxa link host and abiotic factors to plant microbiome variation. PloS Biol 14:e1002352. https://doi.org/10.1371/journal.pbio.1002352
3) Agrawal T, Zaidi NW, Singh US (2018) Host Specific Plant Growth Promoting Activity of IAA Producing and Phosphate Solubilizing Fluorescent *Pseudomonas*. Int J Curr Microbiol App Sci 7:3511-3532. https://doi.org/10.20546/ijcmas.2018.702.418

Altschul S, Madden TL, Schäffer AA, Zhang J, Zhang Z, Miller W, Lipman DJ (1997) Gapped BLAST and PSI-BLAST: a new generation of protein

database search programs. Nucl Ac Res 25:3389-3402. https://doi.org/10.1093/nar/25.17.3389

4) Ash K, Brown T, Watford T, Scott LE, Stephens C and Ely B (2014) A comparison of the *Caulobacter* NA1000 and K31 genomes reveals extensive genome rearrangements and differences in metabolic potential. Open Biol 4:140128. https://doi.org/10.1098/rsob.140128

5) Aziz RK, Bartels D, Best AA, DeJongh M, Disz T, Edwards RA, Formsma K et al (2008) The RAST Server: rapid annotations using subsystems technology. BMC Genomics 9:75. https://doi:10.1186/1471-2164-9-75

6) Backer R, Rokem J, Ilangumaran G, Lamont J, Praslickova D, Ricci E, Subramanian S et al (2018) Plant growth-promoting rhizobacteria: context, mechanisms of action, and roadmap to commercialization of biostimulants for sustainable agriculture. Front in Plant Sci 9:1473. https://doi.org/10.3389/fpls.2018.01473

7) Baykov AA, Evtushenko OA, Avaeva SM (1988) A malachite green procedure for orthophosphate determination and its use in alkaline phosphatase-based enzyme immunoassay. Anal Biochem 171:266-270. https://doi.org/10.1016/0003-2697(88)90484-8

8) Berrios L, Ely B (2018) Achieving accurate sequence and annotation data for *Caulobacter vibrioides* CB13. Curr Microbiol 75:1642-1648. https://doi.org/10.1007/s00284-018-1572-3

9) Berrios L, Ely B (2019) The Isolation and Characterization of Kronos, a Novel *Caulobacter* Rhizosphere Phage that is Similar to Lambdoid Phages. Curr Microbiol 76:558-565. https://doi.org/10.1007/s00284-019-01677-w

10) Bhattacharyya PN, Jha DK (2012) Plant growth-promoting rhizobacteria (PGPR): emergence in agriculture. World J of Microbiol and Biotechnol 28:1327-1350. https://doi.org/10.1007%2Fs11274-011-0979-9

11) Brown SD, Utturkar SM, Klingeman DM, Johnson CM, Martin SL, Land ML, Lu TY et al. (2012) Twenty-one genome sequences from *Pseudomonas* species and 19 genome sequences from diverse bacteria isolated from the rhizosphere and endosphere of *Populus deltoides*. *J Bacteriol* 194:5991-5993. https://doi.org/10.1128/JB.01243-12

12) Buell CR, Joardar V, Lindeberg M, Selengut J, Paulsen IT, Gwinn ML, Dodson RJ et al. (2003) The complete genome sequence of the *Arabidopsis* and tomato pathogen *Pseudomonas syringae* pv. Tomato DC3000. Proc Natl Acad Sci USA 100:10181-10186. https://doi.org/10.1073/pnas.1731982100

13) Bulgarelli D, Schlaeppi K, Spaepen S, Van Themaat EV, Schulze-Lefert P (2013) Structure and functions of the bacterial microbiota of plants. Annual Review of Plant Biol 64:807-838. https://doi.org/10.1146/annurev-arplant-050312-120106

14) Cai Y, Sun M, Corke H (2003) Antioxidant activity of betalains from plants of the Amaranthaceae. Journal of Agricultural and Food Chem 51:2288-2294. https://doi.org/10.1021/jf030045u

15) Chaiharn M, Lumyong S (2011) Screening and optimization of indole-3-acetic acid production and phosphate solubilization from rhizobacteria aimed at improving plant growth. Curr Microbiol 62:173-181. https://doi.org/10.1007%2Fs00284-010-9674-6

16) Cole BJ, Feltcher ME, Waters RJ, Wetmore KM, Mucyn TS, Ryan EM, Wang G et al (2017) Genome-wide identification of bacterial plant colonization genes. PloS Biol 15:e2002860. https://doi.org/10.1371/journal.pbio.2002860

17) de Jesus Suarez-Moo P, Vovides AP, Griffith MP, Barona-Gomez F, Cibrian-Jaramillo A (2019) Unlocking a high bacterial diversity in the coralloid root microbiome from the cycad genus *Dioon*. PloS One 14:e0211271. https://doi.org/10.1371/journal.pone.0211271

18) de Souza RSC, Armanhi JS, Damasceno ND, Imperial J, Arruda P (2019) Genome sequences of a plant beneficial synthetic bacterial community reveal genetic features for successful plant colonization. Frontiers in Microbiol 10:1779. https://doi.org/10.3389/fmicb.2019.01779

19) Ely B (1991) Genetics of *Caulobacter crescentus*. In: Methods in Enzymology (Vol. 204, pp. 372-384). Academic Press. https://doi.org/10.1016/0076-6879(91)04019

20) Ely B, Wilson K, Ross K, Ingram D, Lewter T, Herring J, Duncan D et al (2019) Genome comparisons of wild isolates of *Caulobacter crescentus*

reveal rates of inversion and horizontal gene transfer. Curr Microbiol 76:159-167. https://doi.org/10.1007/s00284-018-1606-x

21) Etesami H, Alikhani HA, Hosseini HM (2015) Indole-3-acetic acid (IAA) production trait, a useful screening to select endophytic and rhizosphere competent bacteria for rice growth promoting agents. MethodsX 2:72-78. https://doi.org/10.1016/j.mex.2015.02.008
22) Felsenstein J. (1985) Confidence limits on phylogenies: An approach using the bootstrap. Evol 39:783-791
23) Glick BR (2005) Modulation of plant ethylene levels by the bacterial enzyme ACC deaminase. FEMS Microbiol Lett 251:1-7. https://doi.org/10.1016/j.femsle.2005.07.030
24) Glick BR (2014) Bacteria with ACC deaminase can promote plant growth and help to feed the world. Microbiol Res 169:30-39. https://doi.org/10.1016/j.micres.2013.09.009
25) Gordon SA, Weber RP (1951) Colormetric estimation of indoleacetic acid. Plant Physiol 26:192–195. https://doi.org/10.1104/pp.26.1.192
26) Gurdeep KA, Reddy MS (2015) Effects of phosphate-solubilizing bacteria, rock phosphate and chemical fertilizers on maize-wheat cropping cycle and economics. Pedosphere 25:428-437. https://doi.org/10.1016/S1002-0160(15)30010-2
27) Hammer Ø, Harper DA, Ryan PD (2001) PAST: Paleontological statistics software package for education and data analysis. Palaeontologia electronica 4:9

28) Henrici AT, Johnson DE (1935) Studies of freshwater bacteria: II. Stalked bacteria, a new order of schizomycetes. J Bacteriol 30:61-93

29) Janssen J, Weyens N, Croes S, Beckers B, Meiresonne L, Van Peteghem P, Carleer R et al (2015) Phytoremediation of metal contaminated soil using willow: exploiting plant-associated bacteria to improve biomass production and metal uptake. Int J of Phytorem 17:1123-1136. https:// doi.org/10.1080/15226514.2015.1045129

30) Jenal U, Stephens C, Shapiro L (1995) Regulation of asymmetry and polarity during the *Caulobacter* cell cycle. Adv Enzymol Relat Areas Mol Biol 71:1–39

31) Khan N, Bano A, Babar MA (2019) Metabolic and physiological changes induced by plant growth regulators and plant growth promoting rhizobacteria and their impact on drought tolerance in *Cicer arietinum L*. PloS One 14:e0213040. https://doi.org/10.1371/journal.pone.0213040

32) Kumar S, Stecher G, Li M, Knyaz C, Tamura K (2018). MEGA X: Molecular Evolutionary Genetics Analysis across computing platforms. Mol Biol and Evol 35:1547-1549

33) Laub MT, McAdams HH, Feldblyum T, Fraser CM, Shapiro L (2000) Global analysis of the genetic network controlling a bacterial cell cycle. Sci 290:2144-2148. https://doi.org/10.1126/science.290.5499.2144

34) Laub MT, Shapiro L, McAdams HH (2007) Systems biology of *Caulobacter*. Annu Rev Genet 41:429-441

35) Lemanceau P, Blouin M, Muller D, Moënne-Loccoz Y (2017) Let the core microbiota be functional. Trends in Plant Sci 22:583-595. https://doi.org/10.1016/j.tplants.2017.04.008

36) Levy A, Salas Gonzalez I, Mittelviefhaus M, Clingenpeel S, Paredes SH, Miao J, Wang K et al (2017) Genomic features of bacterial adaptation to plants. Nat Genet 50:138–150. https://doi.org/10.1038/s41588-017-0012-9

37) Lin GH, Chang CY, Lin HR (2015) Systematic profiling of indole-3-acetic acid biosynthesis in bacteria using LC–MS/MS. J Chromato B 988:53-58. https://doi.org/10.1016/j.jchromb.2015.02.025

38) Lindsey III BE, Rivero L, Calhoun CS, Grotewold E, Brkljacic J (2017) Standardized method for high-throughput sterilization of *Arabidopsis* seeds. JoVE 17:e56587. https://doi.org/10.3791/56587

39) Lundberg DS, Lebeis SL, Paredes SH, Yourstone S, Gehring J, Malfatti S, Tremblay J et al (2012) Defining the core *Arabidopsis thaliana* root microbiome. Nat 488:86-90. https://doi.org/10.1038/nature11237

40) Luo D, Langendries S, Garcia Mendez S, De Ryck J, Liu D, Beirinckx S, Willems A et al (2019) Plant growth promotion driven by a novel *Caulobacter* strain. Mol Plant-Microbe Interact 10:1162-1174. https://doi.org/10.1094/MPMI-12-18-0347-R

41) Mierziak J, Kostyn K, Kulma A (2014) Flavonoids as important molecules of plant interactions with the environment. Molecules 19:16240–16265. https://doi.org/10.3390/molecules191016240

42) Murashige T, Skoog F (1962) A revised medium for rapid growth and bio assays with tobacco tissue cultures. Physiologia plantarum 15:473-497. https://doi.org/10.1111/j.1399-3054.1962.tb08052.x

43) Najimi M, Lemos ML, Osorio CR (2008) Identification of siderophore biosynthesis genes essential for growth of *Aeromonas salmonicida* under iron limitation conditions. Appl Environ Microbiol 74:2341-2348. https://doi.org/10.1128/AEM.02728-07

44) Naveed M, Mitter B, Yousaf S, Pastar M, Afzal M, Sessitsch A (2014) The endophyte *Enterobacter* sp. FD17: a maize growth enhancer selected based on rigorous testing of plant beneficial traits and colonization characteristics. Biol and Fertility of Soils 50:249-262. https://doi.org/10.1007%2Fs00374-013-0854-y

45) Nierman WC, Feldblyum TV, Laub MT, Paulsen IT, Nelson KE, Eisen JA, Heidelberg JF et al. (2001) Complete genome sequence of *Caulobacter crescentus*. Proc Natl Acad Sci *USA* 98:4136-41. Doi: 10.1073/pnas.061029298

46) Patel S, Fletcher B, Scott DC, Ely B (2015) Genome sequence and phenotypic characterization of *Caulobacter segnis*. Curr Microbiol 70:355-363. https://doi.org/10.1007/s00284-014-0726-1

47) Patten CL, Glick BR (2002) Role of *Pseudomonas putida* indoleacetic acid in development of the host plant root system. Appl Environ Microbiol 68:3795–3801. https://doi.org/10.1128/AEM.68.8.3795-3801.2002

48) Penrose DM, Glick BR (2003) Methods for isolating and characterizing ACC deaminase-containing plant growth-promoting rhizobacteria. Physiologia plantarum 118:10-15. https://doi.org/10.1034/j.1399-3054.2003.00086.x

49) Pérez-Miranda S, Cabirol N, George-Téllez R, Zamudio-Rivera LS, Fernández FJ (2007) O-CAS, a fast and universal method for siderophore detection. J Microbiol Methods 70:127-131. https://doi.org/10.1016/j.mimet.2007.03.023

50) Poindexter JS (1964) Biological properties and classification of the *Caulobacter* group. Bacteriol Rev *28*:231

51) Polturak G, Aharoni A (2018) La Vie En Rose: Biosynthesis, sources, and applications of betalain pigments. Mol Plant 11:7-22. https://doi.org/10.1016/j.molp.2017.10.008

52) Saleemi M, Kiani MZ, Sultan T, Khalid A, Mahmood S (2017) Integrated effect of plant growth-promoting rhizobacteria and phosphate-solubilizing microorganisms on growth of wheat (*Triticum aestivum L*.) under rainfed condition. Agriculture & Food Security 6:46. https://doi.org/10.1186/s40066-017-0123-7

53) Schäfer M, Brütting C, Meza-Canales ID, Großkinsky DK, Vankova R, Baldwin IT, Meldau S (2015) The role of cis-zeatin-type cytokinins in plant growth regulation and mediating responses to environmental interactions. J Exp Bot 66:4873-4884. https://doi.org/10.1093/jxb/erv214

54) Scott D, Ely B (2015) Comparison of genome sequencing technology and assembly methods for the analysis of a GC-rich bacterial genome. Curr Microbiol 70:338-344. https://doi.org/10.1007/s00284-014-0721-6

55) Tamura K and Nei M (1993) Estimation of the number of nucleotide substitutions in the control region of mitochondrial DNA in humans and chimpanzees. Mol Biol and Evol 10:512-526

56) Tang Y, Horikoshi M, Li W (2016) ggfortify: Unified Interface to Visualize Statistical Result of Popular R Packages. The R J 8.2 478-489

57) Tatusova T, DiCuccio M, Badretdin A, Chetvernin V, Nawrocki EP, Zaslavsky L, Lomsadze A et al (2016) NCBI prokaryotic genome annotation pipeline. Nucl Ac Res 44:6614-6624. https://doi.org/10.1093/nar/gkw569

58) Taurian T, Anzuay MS, Angelini JG, Tonelli ML, Ludueña L, Pena D, Ibáñez F et al (2010) Phosphate-solubilizing peanut associated bacteria: screening for plant growth-promoting activities. Plant and Soil 329:421-431. https://doi.org/10.1007/s11104-009-0168-x

59) Verma SK, Kingsley K, Bergen M, English C, Elmore M, Kharwar RN, White JF (2018) Bacterial endophytes from rice cut grass (*Leersia oryzoides L*.) increase growth, promote root gravitropic response, stimulate root hair formation, and protect rice seedlings from disease. Plant and Soil 422:223-238. https://doi.org/10.1007/s11104-017-3339-1

60) Wattam AR, Davis JJ, Assaf R, Boisvert S, Brettin T, Bun C, Conrad N et al (2016) Improvements to PATRIC, the all-bacterial Bioinformatics

Database and Analysis Resource Center. Nucl Ac Res 45:D535-D542. https://doi.org/ 10.1093/nar/gkw1017

61) Wickham H (2016) ggplot2: Elegant Graphics for Data Analysis. In: J Stat Soft, 2nd edn. Springer-Verlag, New York, pp 260

62) Wilhelm RC (2018) Following the terrestrial tracks of *Caulobacter*-redefining the ecology of a reputed aquatic oligotroph. ISME J 12:3025-3037. https://doi.org/10.1038/s41396-018-0257-z

63) Yazaki K, Arimura GI, Ohnishi T (2017) 'Hidden' terpenoids in plants: their biosynthesis, localization and ecological roles. Plant and Cell Physiol 58:1615-1621. https://doi.org/10.1093/pcp/pcx123

64) Yan X, Wang Z, Mei Y, Wang X, Xu Q, Zhou Y, Wei C (2018) Isolation, Diversity, and Growth-Promoting Activities of Endophytic Bacteria From Tea Cultivars of Zijuan and Yunkang-10. Front Microbiol 9:1848. https://doi.org/10.3389/fmicb.2018.01848

65) Yang E, Sun L, Ding X, Sun D, Liu J, Wang W (2019) Complete genome sequence of *Caulobacter flavus* RHGG3 T, a type species of the genus *Caulobacter* with plant growth-promoting traits and heavy metal resistance. 3 Biotech 9:42. https://doi.org/ 10.1007/s13205-019-1569-z

66) Zhang X, Baars O, Morel FM (2019) Genetic, structural, and functional diversity of low and high-affinity siderophores in strains of nitrogen fixing *Azotobacter chroococcum*. Metallomics 11:201-212. https://doi.org/ 10.1039/c8mt00236c

CHAPTER 3

GENES RELATED TO REDOX AND CELL CURVATURE FACILITATE INTERACTIONS BETWEEN CAULOBACTER STRAINS AND ARABIDOPSIS[3]

[3]Berrios L, Ely B (2021) Genes related to redox and cell curvature facilitate interactions between *Caulobacter* strains and Arabidopsis. *PLOS ONE* 16(4): e0249227 doi: 10.1371/journal.pone.0249227

Abstract

Bacteria play an integral role in shaping plant growth and development. However, the genetic factors that facilitate plant-bacteria interactions remain largely unknown. Here, we demonstrated the importance of two bacterial genetic factors that facilitate the interactions between plant-growth-promoting (PGP) bacteria in the genus *Caulobacter* and the host plant *Arabidopsis*. Using homologous recombination, we disrupted the cytochrome ubiquinol oxidase (*cyo*) operon in both *C. vibrioides* CB13 and *C. segnis* TK0059 by knocking out the expression of *cyoB* (critical subunit of the *cyo* operon) and showed that the mutant strains were unable to enhance the growth of *Arabidopsis*. In addition, disruption of the *cyo* operon, metabolomic reconstructions, and pH measurements suggested that both elevated *cyoB* expression and acid production by strain CB13 contribute to the previously observed inhibition of *Arabidopsis* seed germination. We also showed that the crescent shape of the PGP bacterial strain *C. crescentus* CB15 contributes to its ability to enhance plant growth. Thus, we have identified specific genetic factors that explain how select *Caulobacter* strains interact with *Arabidopsis* plants.

Author summary

The bacterial genus *Caulobacter* possesses strains that naturally associate with various plant species, and some strains have been shown to enhance plant growth and development. However, the factors that enable these bacteria to enhance plant growth have yet to be established. To elucidate these factors, we disrupted the function of two bacterial genes that we hypothesized would be involved in *Caulobacter*-mediated plant growth enhancement and demonstrated that the

expression of these genes indeed facilitates *Caulobacter*-mediated plant growth enhancement. Specifically, our data suggest that *Caulobacter* strains may scavenge reactive oxygen species to aid plant growth and development, and the curvature of *Caulobacter* cells may enhance plant-bacteria interactions. In addition, we showed that acid production during bacterial growth contributes (in part) to the inhibition of seed germination. Collectively, our findings have begun to provide mechanistic insights into how common plant-associated bacteria can bolster plant growth.

Introduction

Terrestrial plants and microbes have been coevolving for over 100 million years [1], and their interactions contribute to global biogeochemical cycles and agricultural fecundity [2]. Recent advances in microbial ecology have facilitated taxonomical and functional classifications of plant-associated microbes (PAMs), and core plant microbiomes (conserved microbial taxa) have begun to be identified across various plant species and diverse geographic regions [3,4]. For instance, sequence-based approaches have highlighted the abundance of *Alphaproteobacteria* species in (endosphere) and around (rhizosphere) the roots of many plant genera such as *Arabidopsis*, *Glycine*, *Hordeum*, *Panicum*, *Sorghum, Triticum*, and *Zea mays* across diverse geographical regions [5-12]. Pioneering work borne out of the last decade has expedited our understanding of PAMs and has highlighted the prevalence of plant-growth-promoting bacteria (PGPB) [5,8,13,14]. The seminal works of Bulgarelli et al. (2015) and Lundberg et al. (2012) established that the core microbiome of *Arabidopsis* assembles based primarily on

the ability of its microbial members to metabolize root exudates (primarily carbon), and ‘hub strains’ tend to play integral roles in the assembly and maintenance of plant microbiomes. However, detailed functional roles for hub strains have yet to be established, and the degree to which they function as PGPB remains elusive.

Recent communications have commented on the prevalence of reductive and oxidative (redox) enzyme coding genes in the genomes of PAMs [15-18], and functional interactions between PAMs and their hosts have been further understood by implementing inoculum-based synthetic communities to explore and verify the requirement of select microbial genes for a given function (e.g., root colonization) [18,19]. Nonetheless, functional genetics approaches that seek to resolve the function of redox related activities in the context of PGPB assays have not been communicated and many reports consider only correlative data involving common PGP factors (1-aminocyclopropane deaminase (ACC deaminase), cytokinin biosynthesis, indole-3-acetic acid (IAA) production, nitrogen fixation, and phosphate solubilization) as proxies to assess the potential of a bacterial strain to enhance plant growth [20,21]. However, common PGP factors can also negatively correlate with plant fitness [22].

The genus *Caulobacter*, a member of the class *Alphaproteobacteria*, possesses many strains that have been isolated from the endosphere and rhizosphere of *Arabidopsis*, *Citrullus*, *Lavandula* and *Zea mays* [23-26], which in part implicates members of the *Caulobacter* genus as representative microbial hub species [27]. Moreover, select *Caulobacter* strains have been shown to increase plant biomass and alter root architecture relative to uninoculated conditions [22-

24]. Functional roles that explain *Caulobacter*-mediated plant growth enhancement, however, have not been reported [22-24]. A recent report from Luo et al. (2019) demonstrated that *Caulobacter* sp. RHG1 cells localize to regions of lateral root formation in *Arabidopsis* and increase root length and lateral root formation compared to the roots of uninoculated plants. Similarly, we previously identified six *Caulobacter* strains that could increase plant weight and root length relative to control conditions [22], and our results suggested that common PGP factors did not explain the plant growth enhancement that we observed in our system.

To identify presumptive genes that facilitate *Caulobacter*-mediated plant growth enhancement, we previously employed a genome-wide association study (GWAS) and observed that the genomes of PGP *Caulobacter* strains harbored ~2-fold more genes with predicted reactive oxygen species (ROS) scavenging functions compared to the genomes of non-PGP *Caulobacter* strains. Specifically, we observed an extra operon (*cyo*) that is predicted to code for the biosynthesis of gomphrenin-I, which is a betalain-type ROS scavenging molecule that has been shown previously to exhibit high ROS scavenging activity [28]. Since ROS act as intracellular signaling molecules and facilitate plant growth and development [29-32], we hypothesized that this additional ROS scavenging-related operon may play a role in *Caulobacter*-mediated plant growth enhancement.

Bacterial cell shape has previously been shown to facilitate adsorption and may be a prerequisite for select cellular functions (e.g., ROS scavenging for plant host). For example, Persat et al. (2014) demonstrated that the curvature of

Caulobacter cells enhances colonization in flow, albeit curvature diversity may be selected for based on the environmental context. Similarly, the spiral shape of the bacterium *Helicobacter pylori* remains a prerequisite for effective stomach colonization and subsequent pathogenesis [33]. Recent larger scale analyses have even demonstrated that spatiotemporal distributions (i.e., proximity to plant roots as a function of time) of bacterial species may be predicated on cell shape and structure [34]. However, cell curvature has yet to be examined in the context of PGP factors. Thus, we investigated *Caulobacter* cell shape in the context of plant-microbe interactions and hypothesized that the crescent shape of *C. crescentus* cells may contribute to the *Caulobacter*-mediated plant growth enhancement that we previously observed [22].

To test our hypotheses, we disrupted the cytochrome ubiquinol oxidase subunit 1 (EC 1.10.3-) (hereafter *cyoB*) gene in two different PGP *Caulobacter* species (*C. vibrioides* CB13 and *C. segnis* TK0059) and compared the impact that each mutant strain had on the growth of *Arabidopsis* relative to that provided by their parental strains (wild-type). To determine if cell curvature facilitates PGP factors, we compared the effect of a *creS* mutant (required for *Caulobacter* crescent cell shape) on plant growth relative to its PGP parental strain (*C. crescentus* CB15). In addition, ROS play critical roles during seed germination [32], and we observed previously that CB13 severely inhibits seed germination rates, but it still increases plant weight relative to that of uninoculated plants [22]. Therefore, we explored whether differential gene expression patterns of *cyoB* across PGP *Caulobacter* strains occurred. As such, we reasoned that since

elevated ROS levels are required for the seed-to-seedling transition in *Arabidopsis* [35-37], and previous reports have linked increased ROS scavenging activity to seed germination suppression [38,39], CB13 may exhibit elevated *cyoB* gene expression levels relative to other PGP strains, which would suggest that CB13 may dampen ROS levels in *Arabidopsis* seeds below the required oxidative window that drives seed germination [29]. Moreover, we determined that CB13 likely inhibits *Arabidopsis* seed germination (in part) by lowering proximal pH concentrations. Taken together, our results suggest functional roles for betalain-related gene products and cell curvature regarding *Caulobacter*-mediated plant growth enhancement and demonstrate that pH reducing metabolic factors may cause CB13 to inhibit seed germination.

Results

cyoB and *creS* contribute to *Caulobacter*-mediated plant growth enhancement

Since our previous analyses suggested that the expression of betalain synthesis related genes may contribute to the *Caulobacter*-mediated plant growth enhancement that we observed in our system [22], we knocked-out the expression of the *cyoB* gene (part of the *cyoA-D* operon*;* EC 1.10.3-) that is predicted to code for an enzyme that is involved in the biosynthesis of betalain. Using homologous recombination, we disrupted the function of the *cyoB* gene in two *Caulobacter* strains, *C. vibrioides* CB13 (CB13Δ*cyoB*) and *C. segnis* TK0059 (*C. segnis*Δ*cyoB*) to subsequently test our hypothesis that a functional *cyo* operon is a PGP factor for more than one *Caulobacter* species. Operationally defining plant growth

enhancement as increased plant weight (PW), we observed that both CB13Δ*cyoB* and *C. segnis*Δ*cyoB* were unable to significantly enhance plant growth relative to control conditions and their parental strains (**Figure 3.1A**).

To tease out differential effects on specific *Arabidopsis* anatomical features as a result of bacterial cell inoculation, we measured the basal rosette diameter (BRD), inflorescence height (IH), and silique quantity (SQ) and then analyzed these parameters among inoculum conditions. Consistent with our PW data, the mutant strains had little impact on BRD, IH, and SQ relative to the control plants (**Figure 3.1B-D**). The one exception was that seeds that were inoculated with CB13Δ*cyoB* cells were unable to increase BRD relative to control conditions, but seeds that were inoculated with *C. segnis*Δ*cyoB* cells were still able to enhance BRD relative to control conditions (**Figure 3.1B**). Although changes in SQ were observed between parental and mutant strains, none of the strains increased SQ relative to the control conditions (**Figure 3.1D**), which aligns with our previous analyses [22]. Prior to using the mutant constructs for plant bioassays (**Figure 3.1**), we ensured that neither mutant incurred obvious growth defects relative to their parental strains by measuring the growth rates of each assayed *Caulobacter* strain under low aeration conditions (**Figure 3.2A**) and moderate aeration conditions (growth on PYE agar plates at ambient O_2 concentrations). Since differences in growth rates (cell density in PYE broth and colony forming rates on PYE plates) were not observed between mutant strains and their corresponding parental strains, and our bacterial cell re-isolation assays suggested that the observed differences in growth stimulation were likely not related to differential bacterial cell

growth dynamics in the soil (**Figure 3.2B and Table A.7**), our data demonstrate the importance of a functional *cyoB* gene in the context of *Caulobacter*-mediated plant growth enhancement in two different *Caulobacter* species.

Since bacterial cell shape has been linked to colonization abilities [33,40], and *Caulobacter* cells can colonize plant roots both in artificial environments [23] and in natural environments [41], we tested whether the cell curvature of *Caulobacter* cells (i.e., using CB15 as a proxy for PGP *Caulobacter* strains since cell curvature is a conserved feature among the *Caulobacter* strains that we previously tested [22]) contributes to *Caulobacter*-mediated plant growth enhancement by conducting our plant bioassays with CB15Δ*creS* (rod shaped as opposed to the typical crescent shape of *C. crescentus* cells). We observed that plants grown to maturation in the presence of CB15Δ*creS* cells were significantly smaller (PW, BRD) than those grown in the presence of CB15 cells (**Figure 3.1A-C**). However, both the CB15 and CB15Δ*creS* strains caused a reduction in SQ (**Figure 3.1D**). Thus, these results suggest that cell curvature contributes to *C. crescentus*-mediated plant growth enhancement, albeit other *Caulobacter* species

that lack the *creS* gene (i.e., *C. flavus* RHGG3) have been shown to enhance plant growth [26].

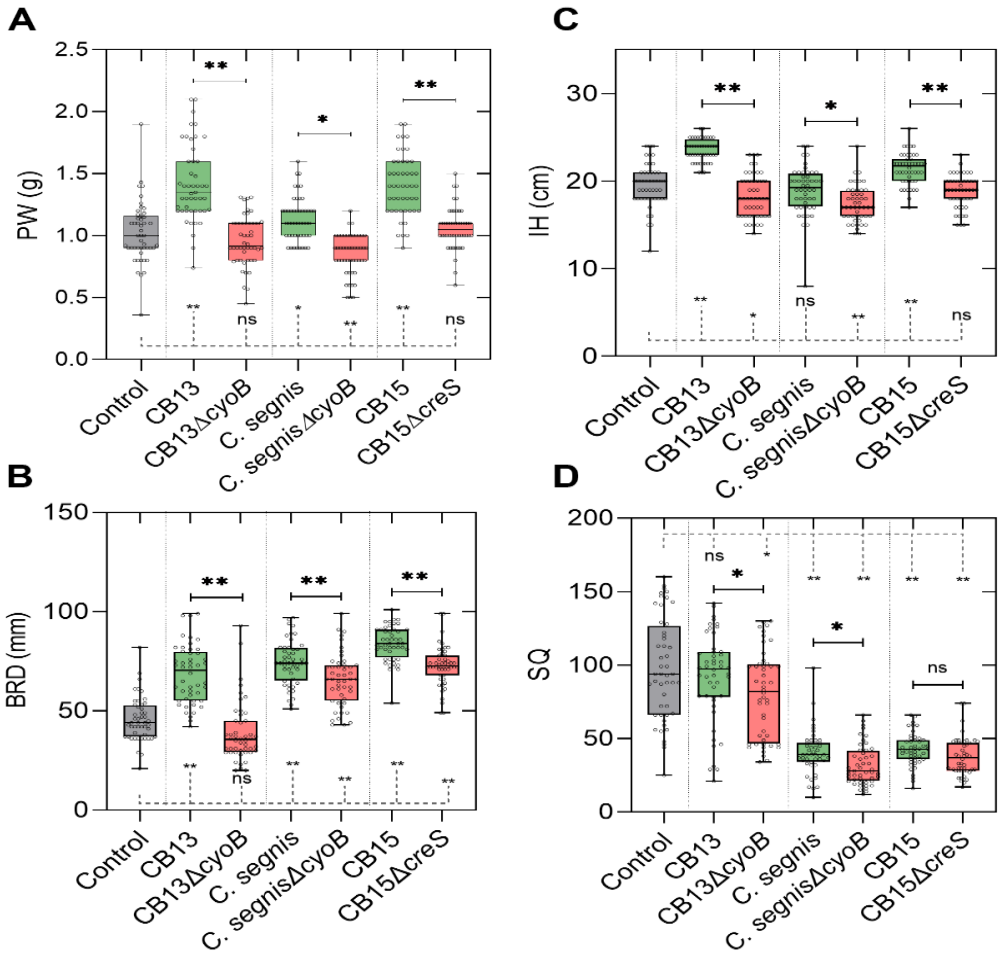

Figure 3.1. *cyoB* and *creS* contribute to *Caulobacter*-mediated plant growth enhancement. A) Box-and-whisker plot illustrating plant weight (PW) in grams (g), **B)** basal rosette diameter (BRD) in millimeters (mm), **C)** inflorescence height (IH) in centimeters (cm), and **D)** silique quantity (SQ) for each experimental condition. Seedlings and ungerminated seeds were transplanted from MS (Murashige and Skoog) plates to soil after 11 days. A total of 48 data points for each condition are displayed. Whiskers indicate maximum and minimum data points, and boxes span 25-75% quartiles with central bars representing the median values of the populations. A one-way ANOVA and pairwise Welch's t-tests were performed to derive p-values. * = $p < 0.01$; ** = $p < 0.001$; ns = $p > 0.01$. Pairwise significance values between control and experimental conditions are connected by dashed, gray lines..

Elevated *cyoB* gene expression and media composition explain CB13-mediated seed germination inhibition for *Arabidopsis* seeds

Previously, we demonstrated that CB13 inhibited *Arabidopsis* seed germination more than any other *Caulobacter* strain we assayed (PGP or non-PGP) but still significantly enhanced plant growth relative to control conditions [22]. Given that a critical oxidative window is necessary to induce *Arabidopsis* seed germination [29], we hypothesized that CB13 may exhibit increased *cyoB* (presumptive betalain biosynthesis function) gene expression relative to other PGP *Caulobacter* strains, which would suggest that CB13 may dampen the ROS levels below the optimal oxidative window [29]. Additionally, we hypothesized that CB13 seed germination inhibition may be media-specific and concentration dependent since bacterial end-products have been shown to affect seed germination [42].

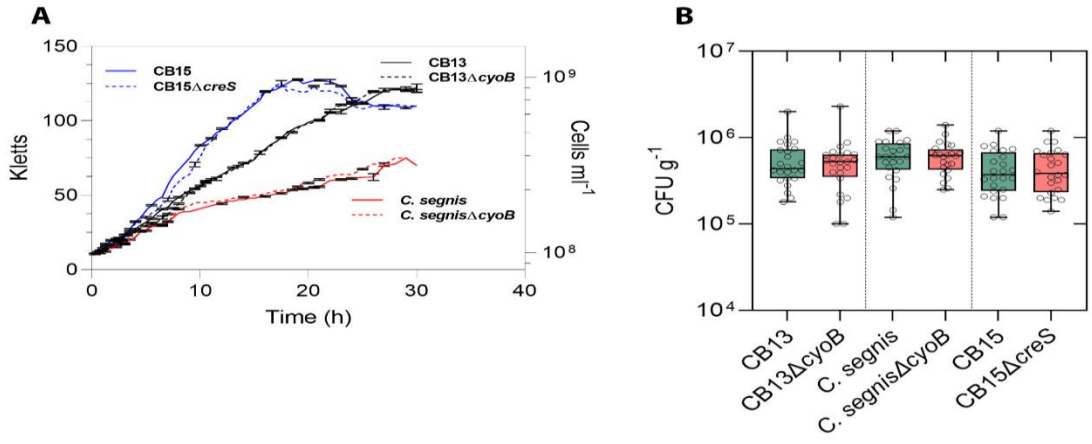

Figure 3.2. *Caulobacter* strain growth curve and re-isolation data. A) Replicate values (n=3) are displayed for each timepoint. **B)** Colony-forming units (CFUs) per gram of soil are displayed for each condition. Bacteria were recovered from 12 soil samples after plant growth across each condition for both independent experiments (n = 2). The box and whisker plots include all data points. Whiskers indicate maximum and minimum data points, and boxes span 25-75% quartiles with central bars representing the median values of the populations. The raw data are in **Table A.7** (ns = $p > 0.01$).

To test our first hypothesis, we performed RT-qPCR to determine the relative expression of two genes with predicted functions involved in betalain synthesis (*cyoB* and *cydA;* EC 1.10.3-) and found that the *cyoB* and *cydA* genes of CB13 were expressed at significantly higher levels than those of *C. segnis* (PGP *Caulobacter* strain that moderately decreases *Arabidopsis* germination rates but enhances plant growth) (**Figure 3.3A**). To address any species-specific differences regarding gene expression, we also quantified the relative gene expression of these genes in two additional PGP *Caulobacter* strains that enhanced seed germination rates (*C. crescentus* CB15 and *C. crescentus* CBR1), and we observed that CB13 also expressed the *cyoB* and *cydA* genes at higher levels than those observed in these strains (**Figure 3.3A and Table A.9**). Next, bacterial cultures were used to inoculate sterile *Arabidopsis* seeds and germination rates were measured 7 days post inoculation (DPI). We reasoned that since CB13 exhibits relatively high ROS scavenging related gene expression compared to other PGP strains, the *Arabidopsis* seeds that were inoculated with the knockout mutant cells (CB13Δ*cyoB*) would have increased germination rates relative to seeds inoculated with CB13 cells. Consistent with our hypothesis, we observed that seeds inoculated with CB13Δ*cyoB* cells germinated at a rate of ~5-fold greater than did those inoculated with CB13 cells (7 DPI), and lateral root formation was increased relative to those in the CB13 inoculum condition at 18 DPI (**Figure 3.3B-C**). In contrast, differences in germination rates between the *C. segnis* and *C. segnis*Δ*cyoB* inoculum conditions were not observed (**Table A.10**), which is consistent with the elevated expression of *cyoB* that we observed in CB13 cells.

Given that CB13 and CB13Δ*cyoB* cells appeared to grow similarly on MS plates with *Arabidopsis* seeds (**Figure B.3**), the increased *cyoB* gene expression that we observed in CB13 (relative to other conditions) may play a role in dampening the oxidative window below the optimal concentrations that drive *Arabidopsis* seed-to-seedling transitions.

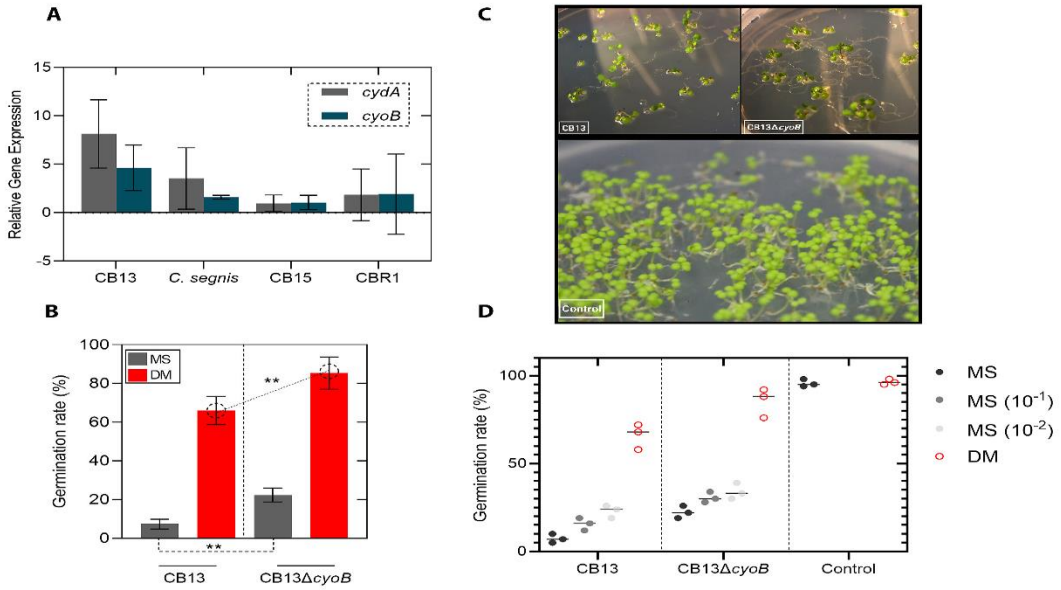

Figure 3.3. Effects of *cyoB* mutation and media composition on *Arabidopsis* seed germination. A) Relative gene expression of *cyoB* and *cydA* demonstrating the elevated expression of these genes by CB13 relative to other *Caulobacter* strains. Expression levels were determined using *rho* as the internal standard, and Δct values are displayed. Bars denote variance between independent replicates. **B)** Germination rate comparisons between experimental conditions are represented. Bars denote replication variances, and p-values were derived using a Welch's t-test (** = p ≤ 0.001). A total of 50 seeds per condition were used in each independent replicate (n=3). **C)** Seedlings grown in the presence of either sterile tap water (control), CB13 cells, or CB13Δ*cyoB* cells on defined media (DM; see Materials and Methods). Photos were captured at 18 days after seed plating (14 days after transfer to the environmental chamber). **D)** Germination rate comparisons (media composition and *cyoB* gene knockout effects) for CB13 and CB13Δ*cyoB* experimental conditions are displayed (MS = Murashige and Skoog; DM = defined media). Each dot corresponds to an independent experiment (**Table A.9**).

To test whether the growth medium impacted CB13-mediated seed germination, we first plated CB13 inoculated *Arabidopsis* seeds on standard MS plates (pH adjusted to 7.5) and defined media (DM) plates (0.5 mM $MgSO_4$ + 1 mM $CaCl_2$ + 1.5% Bacto agar) and calculated relative germination rates at 7 DPI. Our results suggested that the ability of CB13 cells to inhibit seed germination is media-specific since germination rates were increased when seeds were plated on DM compared to MS plates (**Figure 3.3C-D; Table A.9; and Figure B.4**). Importantly, the media composition (MS vs. DM) did not affect the germination rates of the uninoculated seeds (**Figure 3.3D and Figure B.3-B.4**). In addition, we reasoned that CB13-mediated seed germination inhibition (on MS plates) would be contingent on bacterial cell concentration. To address this idea, we inoculated *Arabidopsis* seeds with discrete concentrations of CB13 cells ($OD600_{nm}$= 1.0, 0.1, 0.01) and observed that a decrease in CB13 cell concentration led to an increase in *Arabidopsis* seed germination rates on MS plates. In contrast, differing CB13 cell concentrations did not appear to alter *Arabidopsis* seed germination rates when they were grown on DM plates (**Table A.9**). Moreover, seeds that were inoculated with CB13Δ*cyoB* cells showed increased germination rates and enhanced root growth on each media type (MS and DM) compared to seeds that were inoculated with CB13 cells (**Figure 3.3C-D and Table A.9**). To determine the degree to which these two variables (media composition and *cyoB* function) contribute to the CB13-mediated seed germination inhibition, we analyzed this dataset using a two-way ANOVA. Our results suggested that media-composition addressed ~80.0% of the germination inhibition, while 15.0% of the variation was

explained by the impact of the knockout mutation and the remaining ~2.0% (~3.0% uncertainty) was explained by interactions between the two variables (**Table A.10**). Thus, both elevated *cyoB* gene expression and the seed plating media composition contribute to the CB13-mediated seed germination inhibition that we previously observed [22].

CB13 may inhibit *Arabidopsis* seed germination by lowering local pH concentrations

Since our seed plating assay results indicated that CB13-mediated germination inhibition is significantly linked to the media-specific component, we leveraged the PATRIC 3.6.7 database to construct a flux balance analysis (FBA) metabolome model (ModelSEED) that predicts the relative H^+ ions exchanged (byproducts of nutrient cycling) in the environment (MS media) for each of the experimentally tested *Caulobacter* strains (**Figure 3.4A**). Our results suggested that CB13 harnesses the potential to yield more H^+ ions than any of the other *Caulobacter* strains that we analyzed (AP07, CB1, CB2, CB4, CB15, *C. segnis* TK0059, K31), and the increase of H^+ ion flux would likely not be buffered since phosphate fluxes were predicted to remain relatively constant (**Figure 3.4A and Table A.12**). In contrast, when we reconstructed the metabolomic potential for CB13 using DM + glucose as the substrate, the H^+ ion flux substantially decreased (**Table A.12**). Given that our FBA factored in substrate availability (MS and DM media) and reaction stoichiometry, it is likely that the results gained from our metabolic reconstruction analyses reflect those of our seed plating assays (**Figure 3.3D**). In addition, compared to the genomes of other *Caulobacter* strains, the CB13

genome harbors an additional predicted gene product that codes for an aldehyde dehydrogenase enzyme (2,5-dioxovalerate dehydrogenase; EC 1.2.1.26) (**Figure 3.4B**), which renders H+ ions as a result of its catalytic activity (carbohydrate metabolism). To test the results derived from our computational analyses, we measured the pH of bacterial cultures grown in MS media and DM media (+1% glucose to adjust for the carbon source that germinating seeds provide) at 11 DPI. Consistent with our FBA analyses, CB13 decreased the pH in the MS media below that of the other *Caulobacter* strains. In contrast, significant pH reductions in the DM media were not observed for any strain (**Figure 3.4C and Table A.12**). Further, when we tested the pH directly surrounding the developing seedlings on MS media (11 DPI), we observed that seedlings inoculated with CB13 and CB13Δ*cyoB* cells were surrounded by a pH of ~6, whereas all other conditions maintained a pH of ~7-8 (**Table A.12**). Moreover, when we artificially increased the local pH concentrations surrounding the developing seedlings (pH 7.5 to pH 10), we observed that both CB13 and CB13/CB13Δ*cyoB* inoculated seed conditions decreased the local pH concentrations (from pH 10 to 9), whereas the other conditions maintained a pH of 10 (**Table A.12**). As a result, CB13 and CB13Δ*cyoB* strains enhanced germination rates relative to neutral pH conditions and control conditions (**Fig. B.5**). Since low pH has been linked to reduced *Arabidopsis* seed germination rates [43-45], it is plausible that the additional 2,5-dioxovalerate

dehydrogenase encoding gene in the CB13 genome may (in part) contribute to CB13-mediated seed germination that we observed under neutral pH conditions.

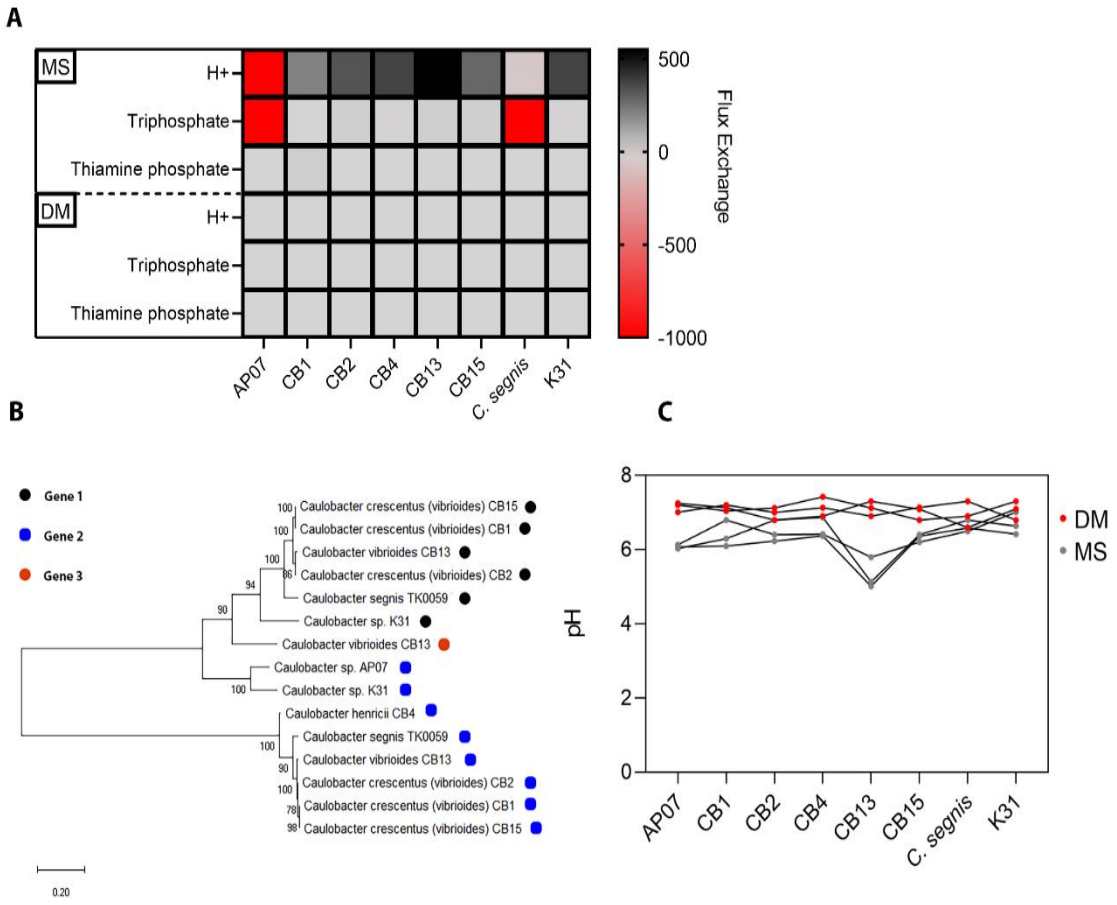

Figure 3.4. Genomic mining for metabolite associations. A) Heatmap of ModelSEED Flux balance analysis values depicting the unbuffered abundance of H^+ ions theoretically generated by CB13. **B)** Phylogenetic tree comparing the predicted amino acid homology of the multiple 2,5-dioxovalerate dehydrogenases (aldehyde dehydrogenase; EC 1.2.1.26) found in *Caulobacter* genomes. Amino acid sequences were aligned using CLUSTAL in MEGAX (Jones-Taylor-Thornton Model), and bootstrap values (1000X) are shown on branches. Branch lengths correspond to amino acid substitutions per site. **C)** Line plot of measured pH values derived from post-incubation cultures (11 DPI) of select *Caulobacter* strains grown in defined media (DM) and Murashige and Skoog (MS) media.

Discussion

The advent of large-scale omics projects has catapulted our understanding of which bacterial genera tend to associate with plants, and recent studies have begun to hone our knowledgebase regarding the functional prerequisites of these plant-bacteria interactions [22,46]. However, many outstanding questions remain concerning the functional factors that many plant-growth-promoting bacteria (PGPB) provide to their host(s). Here, we elucidate two underlying genetic factors (*cyoB* and *creS*) that contribute to *Caulobacter*-mediated plant growth enhancement (increased biomass) and provide computationally-derived factors that may explain the seed germination inhibition that we previously observed in our plant growth system [22].

Although the key molecular mechanisms that drive the interactions between PGP *Caulobacter* strains and *Arabidopsis* remain outstanding, our study demonstrates that a functional *cyo* operon is required for select PGP *Caulobacter* strains to enhance the growth of *Arabidopsis* plants. Moreover, given the predicted function(s) of the *cyo* operon our data suggest that ROS scavenging activities might impact positive interactions between PGP *Caulobacter* strains and *Arabidopsis*. However, the detailed mechanisms that govern the crosstalk between select PGP *Caulobacter* strains and *Arabidopsis* in the context of ROS scavenging abilities remain unknown. Therefore, future investigations will be aimed at understanding if and to what degree select PGP *Caulobacter* strains can regulate ROS levels in *Arabidopsis* plants to ultimately enhance plant growth. Nevertheless, it is well-established that in plants (as in other organisms) ROS develop as a result

of aerobic metabolism, and they can cause irreversible DNA damage leading to cell death or alternatively drive important signal cascades that subsequently regulate normal plant growth and development [47,48]. Thus, ROS molecules must be kept in balance to maintain plant biochemical and physiological states. Given that plants and microbes have coevolved for millions of years [1], orchestrated processes (between plant and microbe) that maintain the balance of ROS have likely undergone functional selection.

In a previous paper, we proposed that ROS scavenging might be a PGP factor that select *Caulobacter* strains employ to enhance plant growth since they contain an extra cytochrome ubiquinol oxidase operon and the proteins produced from both the *cyo* and *cyd* operons can contribute to ROS scavenging [22]. Previous studies linked gomphrenin-I—a type of betalain—to high ROS scavenging activity [28] and suggested that even under optimal plant growth conditions additional ROS scavenging activity supplied by the local microbiome could modulate plant growth through development stages [47,49,50]. Given that PGP *Caulobacter* strains harbor the genomic architecture (i.e., *cyo* and *cyd* operons) to potentially biosynthesize multiple betalain types (**Figure 3.5**) and do not depend on the functionality of the *cyo* operon for survival (**Figure 3.2**), the *cyo* operon may indeed confer PGP *Caulobacter* strains with fitness benefits that could be deemed advantageous in plant-microbe contexts. Consistent with these predictions, when we disrupted the cytochrome ubiquinol oxidase *cyoB* gene, the resultant strain had lost its ability to enhance the growth of *Arabidopsis* (**Figure 3.1**). We also predicted that disruption of the *cyo* operon would not impair the

function of the electron transport chain since some *Caulobacter* strains contain only the *cyd* operon [22]. Our bacterial cell growth assays (**Figure 3.2A**) and re-isolation data (**Figure 3.2B and Table A.7**) support this hypothesis since no differences were observed when the growth rates of the *cyo* knockouts were compared to those of their parent strains. However, we acknowledge that differences (e.g., plant root colonization ability) between parental and mutant strains could have persisted *in vivo* as a function of plant development, which our bacterial cell growth assays and re-isolation experiments would not have captured.

The *cyo* operon predicted protein sequences (*cyoA-D*) in the genomes of both CB13 and *C. segnis* TK0059 share significant amino acid homology (>60%) with those of various bacterial genera, and a few of the strains within these genera have been isolated from plant microbiomes (**Table A.13**). The *cyo* operon also includes three additional genes, one annotated as a SURF1 family gene that would assist in cytochrome oxidase complex assembly and two genes that code for a sensor histidine kinase and its corresponding receptor. This gene arrangement is a conserved feature of the *cyo* operons found in PGP *Caulobacter* strains whose genomes represent all three branches of the *Caulobacter* phylogenetic tree (**Figure 3.5**). Since the sensor histidine kinase and receptor genes are distal to the *cyoB* gene, the disruption of the operon in our constructs may have eliminated the expression of these downstream genes. Therefore, the loss of sensor histidine kinase expression in the *cyoB* mutants could contribute to the inability to enhance plant growth. Moreover, we did not investigate the functional consequence(s) of direct mutations to the *cyoA,C,D* gene(s), nor did we employ mutant phenotype

rescue experiments (i.e., complementation); therefore, further investigations should be targeted toward understanding the functional role(s) of each gene in the *cyo* operon in the context *Caulobacter*-mediated plant growth enhancement. Nevertheless, these experiments indicate that a functional *cyoB* gene is required for both *C. vibrioides* CB13 and *C. segnis* TK0059 to enhance the growth of *Arabidopsis*.

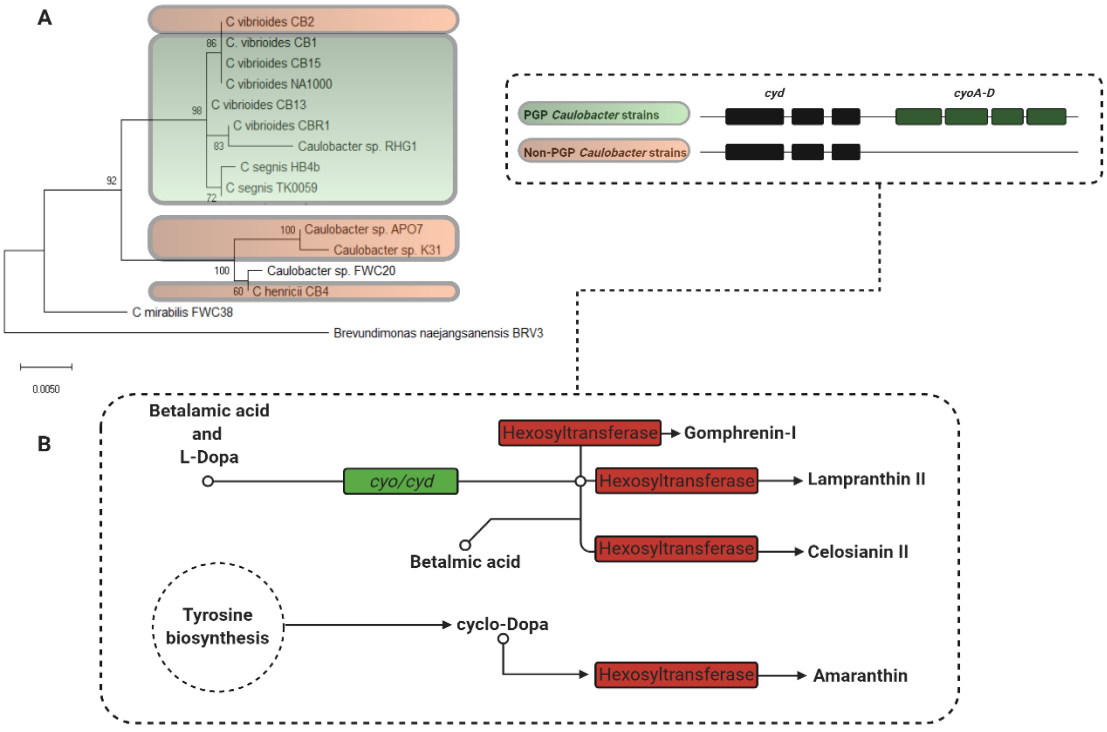

Figure 3.5. Simplified cartoon of betalain biosynthesis **A)** Phylogeny of various *Caulobacter* strains based on 16S rDNA sequences. Strains harboring both the *cyo* and *cyd* operons are highlighted in green (PGP strains), whereas strains with only the *cyd* operon are highlighted in red (Non-PGP strains). Nucleotide sequences were aligned using CLUSTAL in MEGAX (Tamura-Nei Model), and bootstrap values (1000X) are shown on branches. Branch lengths correspond to nucleotide substitutions per site. **B)** Gomphrenin-I, lampranthin II, and celosianin II function as betalains, while amaranthin functions as a lectin with betacyanin properties. *Cyo* (EC 1.10.3-) corresponds to the operon (*cyoA-D*) that is unique to PGP *Caulobacter* strain genomes, and *cyd* (EC 1.10.3-) corresponds to the *cyd* operon that is conserved among the *Caulobacter* strains we previously analyzed [22]. Hexosyltransferase facilitates the conversion of several betalains and the lectin, amaranthin.

Our previous observations [22] suggested that the interactions between developing *Arabidopsis* seedlings and CB13 cells were complex since CB13 cells significantly decreased seed germination but subsequently enhanced plant biomass (data collected roughly six weeks post germination). And, given the high degree of genomic synteny among the PGP *Caulobacter* strains we analyzed [22], we reasoned that variations in redox related gene expression among the strains may provide insight regarding these complex interactions since ROS are critical during seedling development [29,35-39]. To test our hypothesis that expression of the *cyo* operon might explain the severe decrease in seed germination that we observed for CB13 inoculated seeds, we plated *Arabidopsis* seeds with either CB13 cells or CB13Δ*cyoB* cells and calculated germination rates. Consistent with our hypothesis, the *cyoB* loss-of-function mutation facilitated an increased germination rate for *Arabidopsis* seeds (**Figure 3.3B and Figure B.3-B.4**), and the resultant seedlings developed slightly longer roots and more root hairs relative to those inoculated with CB13 cells (**Figure 3.3C**), which is in agreement with previous reports that showed that increased ROS concentrations can increase root length and root hair formation [32,51].

Although a functional *cyoB* gene partially explained the CB13-mediated seed germination inhibition that we observed, germination rates still appeared diminished compared to those in control conditions and other PGP *Caulobacter* strain conditions (**Table A.10**). To establish a theoretical framework for CB13-mediated inhibition of seed germination, we performed a metabolomic reconstruction analysis of the CB13 genome and determined that growth of CB13

might lower the pH of the surrounding microenvironment. When we measured the pH of cultures and the proximal zones surrounding developing seedlings (11 DPI), we found that, as predicted, CB13 produced more acid than any other strain, which lowered the pH in the surrounding environment (**Figure 3.4C and Table A.13A**). After artificially increasing the pH surrounding the developing seedlings (from 7.5 to 10), we also observed that both the CB13 and CB13Δ*cyoB* inoculated seeds germinated at faster rates than they did under neutral pH conditions (**Figure B.5**). The pH concentrations surrounding the seedlings also dropped to ~9 in both the CB13 and CB13Δ*cyoB* inoculated conditions, whereas each of the other conditions remained at a pH 10 (**Table A.12**), which suggests that the expression of the *cyoB* gene does not impact acid production, and CB13 inhibits *Arabidopsis* seed germination (in part) by lowering the surrounding pH. Next, we plated *Arabidopsis* seeds on defined media (DM) plates where only limited growth could occur (**Figure B.3-B.4**) and observed that seed germination in the presence of CB13 was greatly improved (**Figure 3.3D**). However, abundant bacterial growth alone likely does not explain germination rate inhibition by CB13 since seeds inoculated with varying concentrations of CB13 cells did not appear to impact seed germination on DM plates (**Table A.9**), and seeds inoculated with *C. segnis* cells germinated efficiently despite developing in the presence of abundant bacterial growth (**Figure B.3**). Taken together, our observations are consistent with several reports that link low pH to decreased germination rates [43-45]. However, other reports [52,53] have linked low external pH to faster germination rates, and external pH changes have also been shown to modulate IAA production, pectinase activity, and iron uptake

gene expression [52,53,55]. Therefore, the interplay between pH and several signaling pathways probably impacts seed germination in variable and complex ways.

Another functional insight that we gleaned from our experiments was the impact that cell curvature had on PGP ability (**Figure 3.1**). Using a mutant strain unable to form curved or 'crescent' shaped cells [40], we demonstrated that the loss of cell curvature reduced the ability of *C. crescentus* CB15 to enhance plant growth (**Figure 3.1**). It is highly unlikely that cell curvature alone is the causal factor for *Caulobacter*-mediated plant growth enhancement since some PGP *Caulobacter* strains lack the *creS* gene [26]. A functional *creS* gene may, however, facilitate the presumed proximity-dependent requirement for PGP factors (i.e., a functional *cyoB* gene) if bacterial cell attachment to root structures is a prerequisite for *Caulobacter*-mediated plant growth enhancement [23], but these microscale interactions (e.g., endosphere vs. rhizosphere colonization dynamics) remain to be tested. Nevertheless, recent evidence suggests that cell curvature may provide a selective advantage for niche adaptation in select contexts [40]. Additional findings have also demonstrated that cell shape, cell wall composition, and motility factors may function as valuable proxies for estimating species abundance across environmental gradients [34], albeit the exact mechanistic factors governing these host-microbe interactions have been relatively unexplored. Nonetheless, the cell curvature of CB15 cells appears to facilitate their ability to enhance plant growth, but cell shape is not a sole determinant of *Caulobacter*-mediated plant growth

enhancement since our previous analyses demonstrated that plant growth enhancement is not a conserved feature among *C. crescentus* strains [22].

Taken together, these results suggest that PGP bacteria have a complex relationship with their plant hosts and the elucidation of these relationships requires careful experimentation under controlled conditions.

Materials and Methods

Bacterial growth conditions

Overnight cultures were grown in peptone yeast extract (PYE) [56] and were derived from frozen stocks. Each culture was viewed with a phase-contrast microscope to check for contamination prior to experimentation. For low aeration growth curve assays, cells were cultured overnight, and cell cultures (mid-log phase) were then diluted 100-fold to a final volume of 10 mL with a surface area to volume ratio of 0.1:1.0. Subsequent cultures were placed in an orbital incubator shaker set to 100-150 rpm. Optical densities were collected using a Klett-Summerson photoelectric colorimeter. Growth curve assays were performed three times independently, and values are reported as Klett and cells per milliliter. In addition, overnight cultures were also streaked on PYE plates, and subsequent colony growth was observed at 24- and 48-hours post-incubation. To determine pH concentrations of the assayed cultures, bacterial cultures were grown in Murashige and Skoog (MS) [57] and defined media (DM) (1 mM $MgSO_4$ + 0.5 mM $CaCl_2$) supplemented with 1% glucose for 11 days and pH values were determined using a pH probe (**Table A.12**).

Plasmid construction and bacterial mutant generation

The plasmid used to generate *cyoB* mutants was commercially constructed (GeneScript), and it was used to generate gene knockouts via homologous recombination. Briefly, ~250 bp of the *cyoB* flanking regions were cloned into the vector pUC57-Kan at *Pfo*I and *Nde*I (left flanking region) and *Bsa*XI and *Pfl*III (right flanking region) sites. Electrocompetent cells were prepared as previously described by Gilchrist and Smit (1991), and the pUC57-Kan-cyoB vector was electroporated into either *C. vibrioides* CB13 or *C. segnis* TK0059 cells using a Bio-Rad Gene Pulser (2.5 kV, 25 µF, 400 Ω). Subsequently, 1 mL of PYE was added to each electroporated strain, and the resultant cell suspensions were grown for three hours at 30°C with aeration. Afterwards, cell cultures were plated on PYE+ kanamycin (50 mg/L) agar plates and incubated at 30°C for 48-72 hours. Single colonies were aseptically streaked onto PYE + kanamycin plates, and a single colony from each plate was grown in PYE broth to generate pure cultures for DNA extraction (Dneasy Blood and Tissue Kit). To confirm that the anticipated homologous recombination events occurred without a tandem insertion of exogenous DNA (i.e., the mutant strain constructs did not harbor the wildtype allele) in the *Caulobacter* strain genomes, mutant strain DNA was subjected to PCR using the following primer pairs: *cyoBFWD* (5'-TTTGAATTCCCTGTTCTTCGCCTGGAAGT-3'), *cyoBREV* (5'-TTTTTTCTCGAGACCAGAGCGATGAAGCTCAA-3'), 16sFWD (5'-GGTTACCTTGTTACGACTT-3′), and 16sREV (5'-GTGCCAGCMGCCGCGGTAA-3′), and subsequent Sanger sequencing was

employed to validate the sequences (both the 16s rDNA and the *cyoB*-Kan insert). The cell curvature mutant (CB15Δ*creS*) was obtained from Zemer Gitai's laboratory at Princeton University.

Plant growth experiments

All plant growth assays were conducted as previously described by Berrios and Ely (2020). Briefly, bacterial cultures were grown overnight and were then pelleted and rinsed (3X) with sterile tap water to remove residual metabolites. Culture concentrations were adjusted to an $OD600_{nm}$ = 1.0, and sterilized *Arabidopsis* seeds (Ler-O) were inoculated with 500 µL of the bacterial culture (depending on the condition). Control seeds were inoculated with 500 µL of sterile tap water. Seed mixtures were incubated at room temperature for 30-45 minutes and were plated on either Murashige and Skoog (MS) or defined media (DM: 1 mM $MgSO_4$ + 0.5 mM $CaCl_2$ + 1.5% Bacto agar) with pH conditions adjusted to 7.5. The plated seeds were stratified for 4 days at 4°C and were transferred to an environmental chamber (16:8 light/dark photoperiod) under a light intensity of ~150 µM/m2/s. Germination rates were calculated (total number of germinated seeds divided by the total number of plated seeds; n=50) at 7 DPI, and the pH concentrations surrounding developing seedlings were derived using ADVANTEC® Whole Range pH test strips (TOYO ROSHI KAISHA, LTD.) at 11 DPI. Seedlings along with any ungerminated seeds were transferred aseptically from MS plates to sterilized soil in pre-washed plastic trays (3 X 4 grid), and plastic domes were placed over each tray to increase humidity for the first week and then the domes were removed thereafter. The plants were bottom watered as needed (1-2 times per week) with sterile tap water for 5-

6 weeks. Each experiment was conducted twice (24 plants per condition), which yielded a final dataset of 48 plants per condition. Fresh plant weight (PW), inflorescence height (IH), basal rosette diameter (BRD), silique quantity (SQ) data, root architecture, and bacterial cell re-isolation data were collected for each sample as previously described [22]. One-way ANOVAs and Welch's t-tests were performed to determine significant differences within and between conditions.

RNA extraction and RT-qPCR

Bacterial cultures were grown in PYE to mid-log phase (rotational incubator at 30°C). RNA was extracted using a Qiagen Rneasy kit according to the manufacturer's protocols. The forward and reverse primers that were used to measure *cyoB* gene expression in both wildtype and mutant constructs were 5'-CAACTGGCTGTTCACGATGTA-3' and 5'-GATCACGAAGGTGACCATGAA-3', respectively, and the forward and reverse primers that were used to measure *cydA* gene expression were 5'-TGGTCATCATGGAGAGCATCTA-3' and 5'-ACGAAGTTGATGCCGAACAG-3', respectively. The *rho* gene was used as an internal control, and the corresponding forward and reverse primers used for amplification were 5'-GCACGGTGAAGGGCGAGG-3' and 5'-GAGTCC AGCAGGATGACGA-3', respectively. Each assay was performed twice in triplicate, and relative expression (Δct) values (internal control (*rho*) compared to the target gene) are reported.

Comparative genomics

Metabolomic reconstruction analyses of the genomes of *Caulobacter* strains were conducted in PATRIC 3.6.7 and analyzed in ModelSEED [58]. Homology-based calculations were derived from BLASTn or BLASTp for nucleotide and amino acid sequence comparisons, respectively [59]. Quantitative gene binning was performed in PATRIC 3.6.7 using subsystem and pathway functions. Gene and protein sequences were deemed homologous using E-value cutoffs of 10^{-5}, query coverages of >60%, and identities of >70%.

Phylogenetic analyses were performed using CLUSTAL in MEGAX (Jones-Taylor-Thornton Model or Tamura-Nei Model). Each alignment was bootstrapped (1000X), and branch lengths depict the degree of amino acid or nucleotide substitutions among sequences. A complete list of each of the strains used in these analyses and their corresponding accession numbers can be found in **Table A.11**.

Acknowledgements

We thank Taylor Carter for his assistance with RNA extractions and RT-qPCR assays. We also thank Zemer Gitai, Benjamin Bratton, and Joseph Sheehan for providing us with the CB15Δ*creS* mutant.

References

1) Lutzoni F, Nowak MD, Alfaro ME, Reeb V, Miadlikowska J, Krug M, Arnold AE et al. Contemporaneous radiations of fungi and plants linked to symbiosis. Nature Communications. 2018 Dec 21;9(1):1-1. Doi: 10.1038/s41467-018-07849-9.
2) Talbot JM, Bruns TD, Taylor JW, Smith DP, Branco S, Glassman SI et al. Endemism and functional convergence across the North American soil mycobiome. Proc Nat Acad Sci USA. 2014 Apr 29;111(17):6341-6. Doi: 10.1073/pnas.1402584111.
3) Levy A, Conway JM, Dangl JL, Woyke T. Elucidating bacterial gene functions in the plant microbiome. Cell Host & Microbe. 2018 Oct 10;24(4):475-85. Doi: 10.1016/j.chom.2018.09.005.
4) Ramirez-Villacis DX, Finkel OM, Salas-González I, Fitzpatrick CR, Dangl JL, Jones CD et al. Root microbiome modulates plant growth promotion induced by low doses of glyphosate. Msphere. 2020 Aug 26;5(4). Doi: 10.1128/mSphere.00484-20.
5) Bulgarelli D, Garrido-Oter R, Münch PC, Weiman A, Dröge J, Pan Y et al. Structure and function of the bacterial root microbiota in wild and domesticated barley. Cell host & Microbe. 2015 Mar 11;17(3):392-403. Doi: 10.1016/j.chom.2015.01.011.

6) Dominguez JJ, Bacosa HP, Chien MF, Inoue C. Enhanced degradation of polycyclic aromatic hydrocarbons (PAHs) in the rhizosphere of sudangrass (*Sorghum*× *drummondii*). Chemosphere. 2019 Nov 1;234:789-95. Doi: 10.1016/j.chemosphere.2019.05.290

7) Hu W, Strom NB, Haarith D, Bushley K, Chen S. Seasonal variation and crop sequences shape the structure of bacterial communities in cysts of soybean cyst nematode. Frontiers Microbiol. 2019;10:2671. Doi: 10.3389/fmicb.2019.02671.

8) Lundberg DS, Lebeis SL, Paredes SH, Yourstone S, Gehring J, Malfatti S et al. Defining the core *Arabidopsis thaliana* root microbiome. Nature. 2012 Aug;488(7409):86-90. Doi: 10.1038/nature11237.

9) Mashiane RA, Ezeokoli OT, Adeleke RA, Bezuidenhout CC. Metagenomic analyses of bacterial endophytes associated with the phyllosphere of a Bt maize cultivar and its isogenic parental line from South Africa. World J Microbiol and Biotechnol. 2017 Apr 1;33(4):80. Doi: 10.1007/s11274-017-2249-y.

10) Ramírez-Vega H, Arteaga-Garibay RI, Maya-Lucas O, Gómez-Rodríguez VM, Chávez-Díaz IF et al. The bacterial community associated with the Amarillo Zamorano maize (*Zea mays*) landrace silage process. Microorganisms. 2020 Oct;8(10):1503. Doi:10.3390/microorganisms8101503.

11) Singer E, Bonnette J, Woyke T, Juenger T. Conservation of the endophyte microbiome structure across two Panicum grass species. Frontiers Microbiol. 2019;10:2181. Doi: 10.3389/fmicb.2019.02181.

12) Wyszkowska J, Borowik A, Olszewski J, Kucharski J. Soil bacterial community and soil enzyme activity depending on the cultivation of *Triticum aestivum*, *Brassica napus*, and *Pisum sativum ssp. Arvense*. Diversity. 2019 Dec;11(12):246. Doi: 10.3390/d11120246.

13) Blaser MJ, Cardon ZG, Cho MK, Dangl JL, Donohue TJ, Green JL et al. Toward a predictive understanding of Earth's microbiomes to address 21st century challenges. mBio. Doi: 10.1128/mBio.00714-16.

14) Hacquard S, Garrido-Oter R, González A, Spaepen S, Ackermann G, Lebeis S et al. Microbiota and host nutrition across plant and animal kingdoms. Cell Host & Microbe. 2015 May 13;17(5):603-16. Doi: 10.1016/j.chom.2015.04.009.

15) Garcia-Lemos AM, Großkinsky DK, Stokholm MS, Lund OS, Nicolaisen MH, Roitsch T et al. Root-associated microbial communities of *Abies nordmanniana*: insights into interactions of microbial communities with antioxidative enzymes and plant growth. Frontiers Microbiol. 2019;10:1937. Doi: 10.3389/fmicb.2019.01937.

16) Gray MW. Mitochondrial evolution. Cold Spring Harb Perspect Biol. 2012; 4 (9): a011403. Epub 2012/09/07. doi: 10.1101/cshperspect. A011403 PMID: 22952398.

17) Tiepo AN, Constantino LV, Madeira TB, Gonçalves LS, Pimenta JA, Bianchini E et al. Plant growth-promoting bacteria improve leaf antioxidant metabolism of drought-stressed neotropical trees. Planta. 2020 Apr;251(4):1-1. Doi: 10.1007/s00425-020-03373-7.

18) Voges MJ, Bai Y, Schulze-Lefert P, Sattely ES. Plant-derived coumarins shape the composition of an *Arabidopsis* synthetic root microbiome. Proc Nat Acad Sci USA. 2019 Jun 18;116(25):12558-65. Doi: 10.1073/pnas.1820691116.

19) Cole BJ, Feltcher ME, Waters RJ, Wetmore KM, Mucyn TS, Ryan EM et al. Genome-wide identification of bacterial plant colonization genes. PloS Biol. 2017 Sep 22;15(9):e2002860. Doi: 10.1371/journal.pbio.2002860.

20) Taurian T, Anzuay MS, Angelini JG, Tonelli ML, Ludueña L, Pena D et al. Phosphate-solubilizing peanut associated bacteria: screening for plant growth-promoting activities. Plant Soil 2010 329:421-431. Doi: 10.1007/s11104-009-0168-x.

21) Yan X, Wang Z, Mei Y, Wang X, Xu Q, Zhou Y et al. Isolation, diversity, and growth-promoting activities of endophytic bacteria from tea cultivars of Zijuan and Yunkang-10. Front Microbiol 2018; 9:1848. Doi: 10.3389/fmicb.2018.01848.

22) Berrios L, Ely B. Plant growth enhancement is not a conserved feature in the *Caulobacter* genus. Plant and Soil. 2020 Mar 2:1-5. Doi: 10.1007/s11104-020-04472-w.

23) Luo D, Langendries S, Mendez SG, De Ryck J, Liu D, Beirinckx S et al. Plant growth promotion driven by a novel *Caulobacter* strain. Mol Plant-Microbe Int. 2019 Sep 14;32(9):1162-74. Doi: 10.1094/MPMI-12-18-0347-R.

24) Naveed M, Mitter B, Yousaf S, Pastar M, Afzal M, Sessitsch A (2014) The endophyte Enterobacter sp. FD17: a maize growth enhancer selected based on rigorous testing of plant beneficial traits and colonization characteristics. Biol Fertil Soils 50:249-262. Doi: 10.1007/s00374-013-0854-y.

25) Pereira SI, Monteiro C, Vega AL, Castro PM. Endophytic culturable bacteria colonizing *Lavandula dentata L.* plants: isolation, characterization and evaluation of their plant growth-promoting activities. Ecol Eng. 2016 Feb 1;87:91-7. Doi: 10.1016/j.ecoleng.2015.11.033.

26) Yang E, Sun L, Ding X, Sun D, Liu J, Wang W. Complete genome sequence of *Caulobacter flavus* RHGG3 T, a type species of the genus *Caulobacter* with plant growth-promoting traits and heavy metal resistance. 3 Biotech. 2019 Feb 1;9(2):42. Doi: 10.1007/s13205-019-1569-z.

27) Agler MT, Ruhe J, Kroll S, Morhenn C, Kim ST, Weigel D et al. Microbial hub taxa link host and abiotic factors to plant microbiome variation. PloS Biol. 2016 14:e1002352. Doi: 10.1371/journal.pbio.1002352.

28) Cai Y, Sun M, Corke H. Antioxidant activity of betalains from plants of the Amaranthaceae. J Agric Food Chem. 2003 51:2288-2294. Doi: 10.1021/jf030045u.

29) Bailly C, El-Maarouf-Bouteau H, Corbineau F. From intracellular signaling networks to cell death: the dual role of reactive oxygen species in seed physiology. Comptes rendus biologies. 2008 Oct 1;331(10):806-14. Doi: 10.1016/j.crvi.2008.07.022.

30) Schippers JH, Foyer CH, van Dongen JT. Redox regulation in shoot growth, SAM maintenance and flowering. Current Opinion Plant Biol. 2016 Feb 1;29:121-8. Doi: 10.1016/j.pbi.2015.11.009.

31) Singh R, Singh S, Parihar P, Mishra RK, Tripathi DK, Singh VP et al. Reactive oxygen species (ROS): beneficial companions of plants' developmental processes. Frontiers Plant Sci. 2016 Sep 27;7:1299. Doi: 10.3389/fpls.2016.01299.

32) Su C, Liu L, Liu H, Ferguson BJ, Zou Y, Zhao Y et al. H2O2 regulates root system architecture by modulating the polar transport and redistribution of auxin. J Plant Biol. 2016 Jun 1;59(3):260-70. Doi: 10.1007/s12374-016-0052-1.

33) Yang DC, Blair KM, Taylor JA, Petersen TW, Sessler T, Tull CM et al. A genome-wide *Helicobacter pylori* morphology screen uncovers a membrane-spanning helical cell shape complex. J Bacteriol. 2019 Jul 15;201(14):e00724-18. Doi: 10.1128/JB.00724-18.

34) Willing CE, Pierroz G, Coleman-Derr D, Dawson TE. The generalizability of water-deficit on bacterial community composition; Site-specific water-availability predicts the bacterial community associated with coast redwood roots. Mol Ecol. 2020 Oct 1. Doi: 10.1111/mec.15666.

35) Bi C, Ma Y, Wu Z, Yu YT, Liang S, Lu K, Wang XF. *Arabidopsis* ABI5 plays a role in regulating ROS homeostasis by activating CATALASE 1 transcription in seed germination. Plant Mol Biol. 2017 May 1;94(1-2):197-213. Doi: 10.1007/s11103-017-0603-y.

36) Leymarie J, Vitkauskaité G, Hoang HH, Gendreau E, Chazoule V, Meimoun P, Corbineau F, El-Maarouf-Bouteau H, Bailly C. Role of reactive oxygen species in the regulation of *Arabidopsis* seed dormancy. Plant Cell Physiol. 2012 Jan 1;53(1):96-106. Doi: 10.1093/pcp/pcr129.

37) Ye N, Zhu G, Liu Y, Zhang A, Li Y, Liu R, Shi L, Jia L, Zhang J. Ascorbic acid and reactive oxygen species are involved in the inhibition of seed germination by abscisic acid in rice seeds. J Exp Botany. 2012 Mar 1;63(5):1809-22. Doi: 10.1093/jxb/err336.

38) Baek D, Cha JY, Kang S, Park B, Lee HJ, Hong H et al. The *Arabidopsis* a zinc finger domain protein ARS1 is essential for seed germination and ROS homeostasis in response to ABA and oxidative stress. Frontiers Plant Sci. 2015 Nov 4;6:963. Doi: 10.3389/fpls.2015.00963.

39) El-Maarouf-Bouteau H, Bailly C. Oxidative signaling in seed germination and dormancy. Plant Signal Behav. 2008;3(3):175-182. Doi:10.4161/psb.3.3.5539.

40) Persat A, Stone HA, Gitai Z. The curved shape of *Caulobacter crescentus* enhances surface colonization in flow. Nature Communications. 2014 May 8;5(1):1-9. Doi: 10.1038/ncomms4824.

41) Berrios L, Ely B. The isolation and characterization of Kronos, a novel *Caulobacter* rhizosphere phage that is similar to lambdoid phages. Current Microbiol. 2019 May 15;76(5):558-65. Doi: 10.1007/s00284-019-01656-1.

42) Chahtane H, Nogueira Füller T, Allard PM, Marcourt L, Ferreira Queiroz E, Shanmugabalaji V et al. The plant pathogen *Pseudomonas aeruginosa* triggers a DELLA-dependent seed germination arrest in *Arabidopsis*. Elife. 2018 Aug 28;7:e37082. Doi: 10.7554/eLife.37082.

43) Koger CH, Reddy KN, Poston DH. Factors affecting seed germination, seedling emergence, and survival of texasweed (*Caperonia palustris*). Weed Sci. 2004 Nov;52(6):989-95. Doi: 10.1614/WS-03-139R2.

44) Lin PC, Hwang SG, Endo A, Okamoto M, Koshiba T, Cheng WH. Ectopic expression of ABSCISIC ACID 2/GLUCOSE INSENSITIVE 1 in *Arabidopsis* promotes seed dormancy and stress tolerance. Plant Physiol. 2007 Feb 1;143(2):745-58. Doi: 10.1104/pp.106.084103.

45) Müller K, Levesque-Tremblay G, Bartels S, Weitbrecht K, Wormit A, Usadel B et al. Demethylesterification of cell wall pectins in *Arabidopsis* plays a role in seed germination. Plant Physiol. 2013 Jan 1;161(1):305-16. Doi: 10.1104/pp.112.205724.

46) Finkel OM, Salas-González I, Castrillo G, Conway JM, Law TF, Teixeira PJ et al. A single bacterial genus maintains root growth in a complex microbiome. Nature. 2020 Sep 30:1-6. Doi: 10.1038/s41586-020-2778-7.

47) Foyer CH, Noctor G. Redox regulation in photosynthetic organisms: signaling, acclimation, and practical implications. Antioxidants & Redox Signaling. 2009 Apr 1;11(4):861-905. Doi: 10.1089/ars.2008.2177.

48) Zeng J, Dong Z, Wu H, Tian Z, Zhao Z. Redox regulation of plant stem cell fate. EMBO J. 2017 Oct 2;36(19):2844-55. Doi: 10.15252/embj.201695955.

49) Huang H, Ullah F, Zhou DX, Yi M, Zhao Y. Mechanisms of ROS regulation of plant development and stress responses. Frontiers Plant Sci. 2019;10. Doi: 10.3389/fpls.2019.00800.

50) Miller GA, Suzuki N, Ciftci-Yilmaz SU, Mittler RO. Reactive oxygen species homeostasis and signalling during drought and salinity stresses. Plant, Cell & Environment. 2010 Apr;33(4):453-67. Doi: 10.1111/j.1365-3040.2009.02041.x.

51) Achard P, Renou JP, Berthomé R, Harberd NP, Genschik P. Plant DELLAs restrain growth and promote survival of adversity by reducing the levels of reactive oxygen species. Current Biol. 2008 May 6;18(9):656-60. Doi: 10.1016/j.cub.2008.04.034.

52) Lager ID, Andréasson O, Dunbar TL, Andreasson E, Escobar MA, Rasmusson AG. Changes in external pH rapidly alter plant gene expression and modulate auxin and elicitor responses. Plant, Cell & Environment. 2010 Sep;33(9):1513-28. Doi: 10.1111/j.1365-3040.2010.02161.x.

53) Phyo P, Gu Y, Hong M. Impact of acidic pH on plant cell wall polysaccharide structure and dynamics: insights into the mechanism of acid growth in plants

from solid-state NMR. Cellulose. 2019 Jan 15;26(1):291-304. Doi: 10.1007/s10570-018-2094-7.

54) Zhao T, Ling HQ. Effects of pH and nitrogen forms on expression profiles of genes involved in iron homeostasis in tomato. Plant, Cell & Environment. 2007 Apr;30(4):518-27. Doi: 10.1111/j.1365-3040.2007.01638.x.

55) Escobar MA, Geisler DA, Rasmusson AG. Reorganization of the alternative pathways of the *Arabidopsis* respiratory chain by nitrogen supply: opposing effects of ammonium and nitrate. The Plant J. 2006 Mar;45(5):775-88. Doi: 10.1111/j.1365-313X.2005.02640.x.

56) Johnson RC, Ely B. Isolation of spontaneously derived mutants of *Caulobacter crescentus*. Genetics. 1977 May 1;86(1):25-32.

57) Murashige T, Skoog F. A revised medium for rapid growth and bio assays with tobacco tissue cultures. Physiologia plantarum. 1962 Jul;15(3):473-97.

58) Henry CS, DeJongh M, Best AA, Frybarger PM, Linsay B, Stevens RL. High-throughput generation, optimization and analysis of genome-scale metabolic models. Nature Biotechnol. 2010 Sep;28(9):977-82. Doi: 10.1038/nbt.1672.

59) Altschul S, Madden TL, Schäffer AA, Zhang J, Zhang Z, Miller W et al. Gapped BLAST and PSI-BLAST: a new generation of protein database search programs. Nuc Ac Res. 1997 25:3389-3402. Doi: 10.1093/nar/25.17.3389.

CHAPTER 4

CONCLUSIONS

Plant microbiomes possess an immense degree of diversity and complexity. From interactions that span the three domains of life to anthropogenic impacts, the factors that shape plant development in natural environments certainly remain in flux. Undoubtedly, untangling these complex plant-microbe relationships will benefit from technological advances. In the meantime, however, reductionist approaches that leverage established databases to understand how select microbes (i.e., strains within a single bacterial genus) interact with plants can offer a piecemeal design that can hone the yet-to-be understood (stochastic) mechanistic interactions between microbes and their plant host.

Leveraging the established genetic framework for *Caulobacter* species and prior knowledge that select strains naturally associate with plant roots, I developed a tractable system to assess how *Caulobacter* strains interact with plants (i.e., *Arabidopsis*). In doing so, I demonstrated that not all *Caulobacter-Arabidopsis* interactions are equal: some are beneficial (increase plant biomass), whereas others are neutral (no observable impact) or negative (decrease plant biomass). Some strains enhance germination rates (CB1, CB2, CB15, CBR1, HB4b), and some strains deter germination rates (AP07, CB13, *C. segnis* TK0059, FWC20, K31). Moreover, I also demonstrated that CB13 (a PGP strain) decreased germination rates by lowering local pH concentrations (in part) and by growing to levels beyond what is tolerable for efficient seed germination. Of 11 *Caulobacter* strains assessed for their impacts on the growth and development of *Arabidopsis*, six strains (CB1, CB13, CB15, CBR1, *C. segnis* TK0059, HB4b) were able to enhance plant fitness (i.e., plant biomass), two strains (K31, FWC20) exhibited no

observable effect on plant fitness, and three strains (AP07, CB2, CB4) had a negative effect on plant fitness. Importantly, species-specific plant interactions were not clearly delineated since select *C. vibrioides* strains (CB1, CB13, CB15) were able to enhance plant growth, whereas *C. vibrioides* CB2 negatively impact plant fitness. In contrast, each of the *C. segnis* strains (CBR1, HB4b, TK0059) positively impacted plant growth. The remaining strains (AP07, CB4, FWC20, K31) fall outside of the *vibrioides* and *segnis* species, but aside from CB4 (which is a *henricii* species) they (AP07, FWC20, K31) have yet to receive species designations.

To investigate causal factors that explain how select *Caulobacter* strains enhance plant growth, I began by assaying the above 11 strains for common plant growth-promoting (PGP) factors (ACC deaminase, IAA production, phosphate solubilization, siderophore biosynthesis). Interestingly, none of these common PGP factors appeared to contribute to positively impacting plant growth. For instance, none of the strains were observed to solubilize phosphate or biosynthesize siderophores, and ACC deaminase activity appeared to relatively consistent among each of the assayed strains. Moreover, IAA production appeared to negatively correlate with plant fitness (i.e., strains producing higher levels (>20 µg/mL) tended to negatively impact plant growth). However, select PGP strains (TK0059, HB4b) did produce IAA at relatively low levels (<10 µg/mL). Thus, although IAA production and ACC deaminase activity likely do not constitute the primary PGP factors for these strains, they may provide some benefit for these strains in the context of plant interactions. Nevertheless, these findings indicate

that strain specific *Caulobacter-Arabidopsis* interactions exist, and common PGP factors are insufficient to assess the mechanisms governing these interactions.

Building on data derived from the biochemical experiments and plant bioassays, I next sought to analyze the genomes of select PGP strains with the aim of identifying regions of homology that may explain the positive plant interactions that were observed. Factoring out homologous regions shared among each of the *Caulobacter* genomes (i.e., PGP vs. non-PGP), I located an operon (*cyo*) that was specific to the PGP strain genomes. Given that this operon harnessed predicted functions related to oxidative stress (e.g., reactive oxygen scavenging), and recent studies have commented on the abundance of reductive-oxidative stress related genes in the genomes of plant-associated bacteria (relative to non-plant-associated bacteria), I sought to determine if the *cyo* operon was necessary for select PGP strains to enhance plant growth (i.e., biomass). After knocking out the expression of one subunit within the cyo operon (*cyoB*) in the genomes of two *Caulobacter* species (*C*. *vibrioides* CB13 and *C*. *segnis* TK0059) and subjecting the resulting mutant strains to plant bioassays, I determined that indeed a functional *cyo* is necessary for plant growth enhancement. For CB13, elevated expression of *cyoB* also contributed to its inhibitory effects on seed germination (above), which suggests complex molecular mechanisms are involved. In addition, I demonstrated that cell curvature also mediates positive interactions between *Caulobacter* and their host—a hypothesis derived from several sources that alluded to cell shape as a fitness factor for bacteria. As a

result, this is the first report to detail the genetic underpinnings that mediate positive *Caulobacter-Arabidopsis* interactions.

Despite the advances that I have communicated regarding the interactions between *Caulobacter* strains and plants, many outstanding questions remain. For example, although I have established a genetic framework for *Caulobacter-Arabidopsis* interactions, many molecular mechanisms remain unresolved. To this end, further research should seek to resolve if and to what degree select *Caulobacter* strains can dampen or regulate plant derived reactive oxygen species. Moreover, determining whether root tip colonization functions as a prerequisite to PGP factors (and what role cell curvature plays in plant structure localization) or if root tip colonization is a conserved feature among *Caulobacter* strains (despite PGP ability) holds merit to produce mechanistic models. Moving forward, employing a reductionist approach to uncovering the varied and complex interactions of *Caulobacter* strains and plants offers many advantages (e.g., causal linkages with reduced complexity). However, plants naturally develop in a microbial milieu with varying degrees of abiotic fluctuations. Therefore, piecemeal introductions of complexity (e.g., addition of other microbial taxa, temperature and pH fluctuations) could increase the level of realism that presently exists in this system.

REFERENCES

1) Abraham WR, Strömpl C, Meyer H, Lindholst S, Moore ER, Christ R, Vancanneyt M et al. (1999) Phylogeny and polyphasic taxonomy of *Caulobacter* species. Proposal of *Maricaulis* gen. nov. with *Maricaulis maris* (Poindexter) comb. nov. as the type species, and emended description of the genera *Brevundimonas* and *Caulobacter*. Int J Systematic and Evol Microbiol. 49:1053-1073. https://doi.org/10.1099/00207713-49-3-1053
2) Achard P, Renou JP, Berthomé R, Harberd NP, Genschik P. Plant DELLAs restrain growth and promote survival of adversity by reducing the levels of reactive oxygen species. Current Biol. 2008 May 6;18(9):656-60. doi: 10.1016/j.cub.2008.04.034.
3) Agler MT, Ruhe J, Kroll S, Morhenn C, Kim ST, Weigel D, Kemen EM (2016) Microbial hub taxa link host and abiotic factors to plant microbiome variation. PLoS Biol 14:e1002352. https://doi.org/10.1371/journal.pbio.1002352
4) Agrawal T, Zaidi NW, Singh US (2018) Host Specific Plant Growth Promoting Activity of IAA Producing and Phosphate Solubilizing Fluorescent *Pseudomonas*. Int J Curr Microbiol App Sci 7:3511-3532. https://doi.org/10.20546/ijcmas.2018.702.418

5) Altschul S, Madden TL, Schäffer AA, Zhang J, Zhang Z, Miller W et al. Gapped BLAST and PSI-BLAST: a new generation of protein database search programs. Nuc Ac Res. 1997 25:3389-3402. doi: 10.1093/nar/25.17.3389.

6) Ash K, Brown T, Watford T, Scott LE, Stephens C and Ely B (2014) A comparison of the *Caulobacter* NA1000 and K31 genomes reveals extensive genome rearrangements and differences in metabolic potential. Open Biol 4:140128. https://doi.org/10.1098/rsob.140128

7) Aziz RK, Bartels D, Best AA, DeJongh M, Disz T, Edwards RA, Formsma K et al (2008) The RAST Server: rapid annotations using subsystems technology. BMC Genomics 9:75. https://doi:10.1186/1471-2164-9-75

8) Backer R, Rokem J, Ilangumaran G, Lamont J, Praslickova D, Ricci E, Subramanian S et al (2018) Plant growth-promoting rhizobacteria: context, mechanisms of action, and roadmap to commercialization of biostimulants for sustainable agriculture. Front in Plant Sci 9:1473. https://doi.org/10.3389/fpls.2018.01473

9) Baek D, Cha JY, Kang S, Park B, Lee HJ, Hong H et al. The *Arabidopsis* a zinc finger domain protein ARS1 is essential for seed germination and ROS homeostasis in response to ABA and oxidative stress. Frontiers Plant Sci. 2015 Nov 4;6:963. doi: 10.3389/fpls.2015.00963.

10) Bailly C, El-Maarouf-Bouteau H, Corbineau F. From intracellular signaling networks to cell death: the dual role of reactive oxygen species in seed

physiology. Comptes rendus biologies. 2008 Oct 1;331(10):806-14. doi: 10.1016/j.crvi.2008.07.022.

11) Bailly C, El-Maarouf-Bouteau H, Corbineau F. From intracellular signaling networks to cell death: the dual role of reactive oxygen species in seed physiology. Comptes rendus biologies. 2008 Oct 1;331(10):806-14. doi: 10.1016/j.crvi.2008.07.022.

12) Baykov AA, Evtushenko OA, Avaeva SM (1988) A malachite green procedure for orthophosphate determination and its use in alkaline phosphatase-based enzyme immunoassay. Anal Biochem 171:266-270. https://doi.org/10.1016/0003-2697(88)90484-8

13) Berrios L, Ely B (2018) Achieving accurate sequence and annotation data for *Caulobacter vibrioides* CB13. Curr Microbiol 75:1642-1648. https://doi.org/10.1007/s00284-018-1572-3

14) Berrios L, Ely B. Plant growth enhancement is not a conserved feature in the *Caulobacter* genus. Plant and Soil. 2020 Mar 2:1-5. doi: 10.1007/s11104-020-04472-w.

15) Berrios L, Ely B. The isolation and characterization of Kronos, a novel *Caulobacter* rhizosphere phage that is similar to lambdoid phages. Current Microbiol. 2019 May 15;76(5):558-65. doi: 10.1007/s00284-019-01656-1.

16) Bhattacharyya PN, Jha DK (2012) Plant growth-promoting rhizobacteria (PGPR): emergence in agriculture. World J of Microbiol and Biotechnol 28:1327-1350. https://doi.org/10.1007%2Fs11274-011-0979-9

17) Bi C, Ma Y, Wu Z, Yu YT, Liang S, Lu K, Wang XF. *Arabidopsis* ABI5 plays a role in regulating ROS homeostasis by activating CATALASE 1 transcription in seed germination. Plant Mol Biol. 2017 May 1;94(1-2):197-213. doi: 10.1007/s11103-017-0603-y.

18) Blaser MJ, Cardon ZG, Cho MK, Dangl JL, Donohue TJ, Green JL et al. Toward a predictive understanding of Earth's microbiomes to address 21st century challenges. mBio. doi: 10.1128/mBio.00714-16.

19) Blaser MJ, Cardon ZG, Cho MK, Dangl JL, Donohue TJ, Green JL et al. Toward a predictive understanding of Earth's microbiomes to address 21st century challenges. mBio. doi: 10.1128/mBio.00714-16.

20) Brown SD, Utturkar SM, Klingeman DM, Johnson CM, Martin SL, Land ML, Lu TY et al. (2012) Twenty-one genome sequences from *Pseudomonas* species and 19 genome sequences from diverse bacteria isolated from the rhizosphere and endosphere of *Populus deltoides*. *J Bacteriol* 194:5991-5993. https://doi.org/10.1128/JB.01243-12

21) Buell CR, Joardar V, Lindeberg M, Selengut J, Paulsen IT, Gwinn ML, Dodson RJ et al. (2003) The complete genome sequence of the *Arabidopsis* and tomato pathogen *Pseudomonas syringae* pv. tomato DC3000. Proc Natl Acad Sci USA 100:10181-10186. https://doi.org/10.1073/pnas.1731982100

22) Bulgarelli D, Garrido-Oter R, Münch PC, Weiman A, Dröge J, Pan Y et al. Structure and function of the bacterial root microbiota in wild and

domesticated barley. Cell host & Microbe. 2015 Mar 11;17(3):392-403. doi: 10.1016/j.chom.2015.01.011.

23) Bulgarelli D, Schlaeppi K, Spaepen S, Van Themaat EV, Schulze-Lefert P (2013) Structure and functions of the bacterial microbiota of plants. Annual Review of Plant Biol 64:807-838. https://doi.org/10.1146/annurev-arplant-050312-120106

24) Cai Y, Sun M, Corke H (2003) Antioxidant activity of betalains from plants of the Amaranthaceae. Journal of Agricultural and Food Chem 51:2288-2294. https://doi.org/10.1021/jf030045u

25) Chahtane H, Nogueira Füller T, Allard PM, Marcourt L, Ferreira Queiroz E, Shanmugabalaji V et al. The plant pathogen *Pseudomonas aeruginosa* triggers a DELLA-dependent seed germination arrest in *Arabidopsis*. elife. 2018 Aug 28;7:e37082. doi: 10.7554/eLife.37082.

26) Chaiharn M, Lumyong S (2011) Screening and optimization of indole-3-acetic acid production and phosphate solubilization from rhizobacteria aimed at improving plant growth. Curr Microbiol 62:173-181. https://doi.org/ 10.1007%2Fs00284-010-9674-6

27) Cole BJ, Feltcher ME, Waters RJ, Wetmore KM, Mucyn TS, Ryan EM, Wang G et al (2017) Genome-wide identification of bacterial plant colonization genes. PLoS Biol 15:e2002860. https://doi.org/10.1371/journal.pbio.2002860

28) de Jesus Suarez-Moo P, Vovides AP, Griffith MP, Barona-Gomez F, Cibrian-Jaramillo A (2019) Unlocking a high bacterial diversity in the

coralloid root microbiome from the cycad genus *Dioon*. PloS One 14:e0211271. https://doi.org/10.1371/journal.pone.0211271

29) de Souza RSC, Armanhi JS, Damasceno ND, Imperial J, Arruda P (2019) Genome sequences of a plant beneficial synthetic bacterial community reveal genetic features for successful plant colonization. Frontiers in Microbiol 10:1779. https://doi.org/10.3389/fmicb.2019.01779

30) Dominguez JJ, Bacosa HP, Chien MF, Inoue C. Enhanced degradation of polycyclic aromatic hydrocarbons (PAHs) in the rhizosphere of sudangrass (*Sorghum*× *drummondii*). Chemosphere. 2019 Nov 1;234:789-95. doi: 10.1016/j.chemosphere.2019.05.290

31) 31 El-Maarouf-Bouteau H, Bailly C. Oxidative signaling in seed germination and dormancy. Plant Signal Behav. 2008;3(3):175-182. doi:10.4161/psb.3.3.5539.

32) Ely B (1991) Genetics of *Caulobacter crescentus*. In: Methods in Enzymology (Vol. 204, pp. 372-384). Academic Press. https://doi.org/10.1016/0076-6879(91)04019-K

33) Ely B, Wilson K, Ross K, Ingram D, Lewter T, Herring J, Duncan D et al (2019) Genome comparisons of wild isolates of *Caulobacter crescentus* reveal rates of inversion and horizontal gene transfer. Curr Microbiol 76:159-167. https://doi.org/10.1007/s00284-018-1606-x

34) Escobar MA, Geisler DA, Rasmusson AG. Reorganization of the alternative pathways of the *Arabidopsis* respiratory chain by nitrogen

supply: opposing effects of ammonium and nitrate. The Plant J. 2006 Mar;45(5):775-88. doi: 10.1111/j.1365-313X.2005.02640.x.

35) Etesami H, Alikhani HA, Hosseini HM (2015) Indole-3-acetic acid (IAA) production trait, a useful screening to select endophytic and rhizosphere competent bacteria for rice growth promoting agents. MethodsX 2:72-78. https://doi.org/10.1016/j.mex.2015.02.008

36) Felsenstein J. (1985) Confidence limits on phylogenies: An approach using the bootstrap. Evol 39:783-791

37) Finkel OM, Salas-González I, Castrillo G, Conway JM, Law TF, Teixeira PJ et al. A single bacterial genus maintains root growth in a complex microbiome. Nature. 2020 Sep 30:1-6. doi: 10.1038/s41586-020-2778-7.

38) Foyer CH, Noctor G. Redox regulation in photosynthetic organisms: signaling, acclimation, and practical implications. Antioxidants & Redox Signaling. 2009 Apr 1;11(4):861-905. doi: 10.1089/ars.2008.2177.

39) Garcia-Lemos AM, Großkinsky DK, Stokholm MS, Lund OS, Nicolaisen MH, Roitsch T et al. Root-associated microbial communities of *Abies nordmanniana*: insights into interactions of microbial communities with antioxidative enzymes and plant growth. Frontiers Microbiol. 2019;10:1937. doi: 10.3389/fmicb.2019.01937.

40) Glick BR (2005) Modulation of plant ethylene levels by the bacterial enzyme ACC deaminase. FEMS Microbiol Lett 251:1-7. https://doi.org/10.1016/j.femsle.2005.07.030

41) Glick BR (2014) Bacteria with ACC deaminase can promote plant growth and help to feed the world. Microbiol Res 169:30-39. https://doi.org/10.1016/j.micres.2013.09.009

42) Gordon SA, Weber RP (1951) Colormetric estimation of indoleacetic acid. Plant Physiol 26:192–195. https://doi.org/10.1104/pp.26.1.192

43) Gray MW. Mitochondrial evolution. Cold Spring Harb Perspect Biol. 2012; 4 (9): a011403. Epub 2012/09/07. doi: 10.1101/cshperspect. a011403 PMID: 22952398.

44) Gurdeep KA, Reddy MS (2015) Effects of phosphate-solubilizing bacteria, rock phosphate and chemical fertilizers on maize-wheat cropping cycle and economics. Pedosphere 25:428-437. https://doi.org/10.1016/S1002-0160(15)30010-2

45) Hacquard S, Garrido-Oter R, González A, Spaepen S, Ackermann G, Lebeis S et al. Microbiota and host nutrition across plant and animal kingdoms. Cell Host & Microbe. 2015 May 13;17(5):603-16. doi: 10.1016/j.chom.2015.04.009.

46) Hammer Ø, Harper DA, Ryan PD (2001) PAST: Paleontological statistics software package for education and data analysis. Palaeontologia electronica 4:9

47) Henrici AT, Johnson DE (1935) Studies of freshwater bacteria: II. stalked bacteria, a new order of schizomycetes. J Bacteriol 30:61-93

48) Henry CS, DeJongh M, Best AA, Frybarger PM, Linsay B, Stevens RL. High-throughput generation, optimization and analysis of genome-scale

metabolic models. Nature Biotechnol. 2010 Sep;28(9):977-82. doi: 10.1038/nbt.1672.

49) Hu W, Strom NB, Haarith D, Bushley K, Chen S. Seasonal variation and crop sequences shape the structure of bacterial communities in cysts of soybean cyst nematode. Frontiers Microbiol. 2019;10:2671. doi: 10.3389/fmicb.2019.02671.

50) Huang H, Ullah F, Zhou DX, Yi M, Zhao Y. Mechanisms of ROS regulation of plant development and stress responses. Frontiers Plant Sci. 2019;10. doi: 10.3389/fpls.2019.00800.

51) Janssen J, Weyens N, Croes S, Beckers B, Meiresonne L, Van Peteghem P, Carleer R et al (2015) Phytoremediation of metal contaminated soil using willow: exploiting plant-associated bacteria to improve biomass production and metal uptake. Int J of Phytorem 17:1123-1136. https:// doi.org/10.1080/15226514.2015.1045129

52) Jenal U, Stephens C, Shapiro L (1995) Regulation of asymmetry and polarity during the *Caulobacter* cell cycle. Adv Enzymol Relat Areas Mol Biol 71:1–39

53) Johnson RC, Ely B. Isolation of spontaneously derived mutants of Caulobacter crescentus. Genetics. 1977 May 1;86(1):25-32.

54) Khan N, Bano A, Babar MA (2019) Metabolic and physiological changes induced by plant growth regulators and plant growth promoting rhizobacteria and their impact on drought tolerance in *Cicer arietinum L*. PloS One 14:e0213040. https://doi.org/10.1371/journal.pone.0213040

55) Koger CH, Reddy KN, Poston DH. Factors affecting seed germination, seedling emergence, and survival of texasweed (*Caperonia palustris*). Weed Sci. 2004 Nov;52(6):989-95. doi: 10.1614/WS-03-139R2.

56) Kumar S, Stecher G, Li M, Knyaz C, Tamura K (2018). MEGA X: Molecular Evolutionary Genetics Analysis across computing platforms. Mol Biol and Evol 35:1547-1549

57) Lager ID, Andréasson O, Dunbar TL, Andreasson E, Escobar MA, Rasmusson AG. Changes in external pH rapidly alter plant gene expression and modulate auxin and elicitor responses. Plant, Cell & Environment. 2010 Sep;33(9):1513-28. doi: 10.1111/j.1365-3040.2010.02161.x.

58) Laub MT, McAdams HH, Feldblyum T, Fraser CM, Shapiro L (2000) Global analysis of the genetic network controlling a bacterial cell cycle. Sci 290:2144-2148. https://doi.org/10.1126/science.290.5499.2144

59) Laub MT, Shapiro L, McAdams HH (2007) Systems biology of *Caulobacter*. Annu Rev Genet 41:429-441

60) Lemanceau P, Blouin M, Muller D, Moënne-Loccoz Y (2017) Let the core microbiota be functional. Trends in Plant Sci 22:583-595. https://doi.org/10.1016/j.tplants.2017.04.008

61) Levy A, Conway JM, Dangl JL, Woyke T. Elucidating bacterial gene functions in the plant microbiome. Cell Host & Microbe. 2018 Oct 10;24(4):475-85. doi: 10.1016/j.chom.2018.09.005.

62) Levy A, Salas Gonzalez I, Mittelviefhaus M, Clingenpeel S, Paredes SH, Miao J, Wang K et al (2017) Genomic features of bacterial adaptation to plants. Nat Genet 50:138–150. https://doi.org/10.1038/s41588-017-0012-9

63) Leymarie J, Vitkauskaité G, Hoang HH, Gendreau E, Chazoule V, Meimoun P, Corbineau F, El-Maarouf-Bouteau H, Bailly C. Role of reactive oxygen species in the regulation of *Arabidopsis* seed dormancy. Plant Cell Physiol. 2012 Jan 1;53(1):96-106. doi: 10.1093/pcp/pcr129.

64) Lin GH, Chang CY, Lin HR (2015) Systematic profiling of indole-3-acetic acid biosynthesis in bacteria using LC–MS/MS. J Chromato B 988:53-58. https://doi.org/10.1016/j.jchromb.2015.02.025

65) Lin PC, Hwang SG, Endo A, Okamoto M, Koshiba T, Cheng WH. Ectopic expression of ABSCISIC ACID 2/GLUCOSE INSENSITIVE 1 in *Arabidopsis* promotes seed dormancy and stress tolerance. Plant Physiol. 2007 Feb 1;143(2):745-58. doi: 10.1104/pp.106.084103.

66) Lindsey III BE, Rivero L, Calhoun CS, Grotewold E, Brkljacic J (2017) Standardized method for high-throughput sterilization of *Arabidopsis* seeds. JoVE 17:e56587. https://doi.org/10.3791/56587

67) Lundberg DS, Lebeis SL, Paredes SH, Yourstone S, Gehring J, Malfatti S, Tremblay J et al (2012) Defining the core *Arabidopsis thaliana* root microbiome. Nat 488:86-90. https://doi.org/10.1038/nature11237

68) Luo D, Langendries S, Mendez SG, De Ryck J, Liu D, Beirinckx S et al. Plant growth promotion driven by a novel Caulobacter strain. Mol Plant-

Microbe Int. 2019 Sep 14;32(9):1162-74. doi: 10.1094/MPMI-12-18-0347-R.

69) Lutzoni F, Nowak MD, Alfaro ME, Reeb V, Miadlikowska J, Krug M, Arnold AE et al. Contemporaneous radiations of fungi and plants linked to symbiosis. Nature Communications. 2018 Dec 21;9(1):1-1. doi: 10.1038/s41467-018-07849-9.

70) Mashiane RA, Ezeokoli OT, Adeleke RA, Bezuidenhout CC. Metagenomic analyses of bacterial endophytes associated with the phyllosphere of a Bt maize cultivar and its isogenic parental line from South Africa. World J Microbiol and Biotechnol. 2017 Apr 1;33(4):80. doi: 10.1007/s11274-017-2249-y.

71) Mierziak J, Kostyn K, Kulma A (2014) Flavonoids as important molecules of plant interactions with the environment. Molecules 19:16240–16265. https://doi.org/10.3390/molecules191016240

72) Miller GA, Suzuki N, Ciftci-Yilmaz SU, Mittler RO. Reactive oxygen species homeostasis and signalling during drought and salinity stresses. Plant, Cell & Environment. 2010 Apr;33(4):453-67. doi: 10.1111/j.1365-3040.2009.02041.x.

73) Müller K, Levesque-Tremblay G, Bartels S, Weitbrecht K, Wormit A, Usadel B et al. Demethylesterification of cell wall pectins in *Arabidopsis* plays a role in seed germination. Plant Physiol. 2013 Jan 1;161(1):305-16. doi: 10.1104/pp.112.205724.

74) Murashige T, Skoog F (1962) A revised medium for rapid growth and bio assays with tobacco tissue cultures. Physiologia plantarum 15:473-497. https://doi.org/10.1111/j.1399-3054.1962.tb08052.x

75) Najimi M, Lemos ML, Osorio CR (2008) Identification of siderophore biosynthesis genes essential for growth of *Aeromonas salmonicida* under iron limitation conditions. Appl Environ Microbiol 74:2341-2348. https://doi.org/10.1128/AEM.02728-07

76) Naveed M, Mitter B, Yousaf S, Pastar M, Afzal M, Sessitsch A (2014) The endophyte Enterobacter sp. FD17: a maize growth enhancer selected based on rigorous testing of plant beneficial traits and colonization characteristics. Biol Fertil Soils 50:249-262. doi: 10.1007/s00374-013-0854-y.

77) Nierman WC, Feldblyum TV, Laub MT, Paulsen IT, Nelson KE, Eisen JA, Heidelberg JF et al. (2001) Complete genome sequence of *Caulobacter crescentus*. Proc Natl Acad Sci *USA* 98:4136-41. doi: 10.1073/pnas.061029298

78) Patel S, Fletcher B, Scott DC, Ely B (2015) Genome sequence and phenotypic characterization of *Caulobacter segnis*. Curr Microbiol 70:355-363. https://doi.org/10.1007/s00284-014-0726-1

79) Patten CL, Glick BR (2002) Role of *Pseudomonas putida* indoleacetic acid in development of the host plant root system. Appl Environ Microbiol 68:3795–3801. https://doi.org/10.1128/AEM.68.8.3795-3801.2002

80) Penrose DM, Glick BR (2003) Methods for isolating and characterizing ACC deaminase-containing plant growth-promoting rhizobacteria. Physiologia plantarum 118:10-15. https://doi.org/10.1034/j.1399-3054.2003.00086.x

81) Pereira SI, Monteiro C, Vega AL, Castro PM. Endophytic culturable bacteria colonizing Lavandula dentata L. plants: isolation, characterization and evaluation of their plant growth-promoting activities. Ecol Eng. 2016 Feb 1;87:91-7. doi: 10.1016/j.ecoleng.2015.11.033.

82) Pérez-Miranda S, Cabirol N, George-Téllez R, Zamudio-Rivera LS, Fernández FJ (2007) O-CAS, a fast and universal method for siderophore detection. J Microbiol Methods 70:127-131. https://doi.org/10.1016/j.mimet.2007.03.023

83) Persat A, Stone HA, Gitai Z. The curved shape of Caulobacter crescentus enhances surface colonization in flow. Nature Communications. 2014 May 8;5(1):1-9. doi: 10.1038/ncomms4824.

84) Phyo P, Gu Y, Hong M. Impact of acidic pH on plant cell wall polysaccharide structure and dynamics: insights into the mechanism of acid growth in plants from solid-state NMR. Cellulose. 2019 Jan 15;26(1):291-304. doi: 10.1007/s10570-018-2094-7.

85) Poindexter JS (1964) Biological properties and classification of the *Caulobacter* group. Bacteriol Rev *28*:231

86) Polturak G, Aharoni A (2018) La Vie En Rose: Biosynthesis, sources, and applications of betalain pigments. Mol Plant 11:7-22. https://doi.org/10.1016/j.molp.2017.10.008

87) Ramírez-Vega H, Arteaga-Garibay RI, Maya-Lucas O, Gómez-Rodríguez VM, Chávez-Díaz IF et al. The bacterial community associated with the Amarillo Zamorano maize (*Zea mays*) landrace silage process. Microorganisms. 2020 Oct;8(10):1503. doi:10.3390/microorganisms8101503.

88) Ramirez-Villacis DX, Finkel OM, Salas-González I, Fitzpatrick CR, Dangl JL, Jones CD et al. Root microbiome modulates plant growth promotion induced by low doses of glyphosate. Msphere. 2020 Aug 26;5(4). doi: 10.1128/mSphere.00484-20.

89) Saleemi M, Kiani MZ, Sultan T, Khalid A, Mahmood S (2017) Integrated effect of plant growth-promoting rhizobacteria and phosphate-solubilizing microorganisms on growth of wheat (*Triticum aestivum L*.) under rainfed condition. Agriculture & Food Security 6:46. https://doi.org/10.1186/s40066-017-0123-7

90) Schäfer M, Brütting C, Meza-Canales ID, Großkinsky DK, Vankova R, Baldwin IT, Meldau S (2015) The role of cis-zeatin-type cytokinins in plant growth regulation and mediating responses to environmental interactions. J Exp Bot 66:4873-4884. https://doi.org/10.1093/jxb/erv214

91) Schippers JH, Foyer CH, van Dongen JT. Redox regulation in shoot growth, SAM maintenance and flowering. Current Opinion Plant Biol. 2016 Feb 1;29:121-8. doi: 10.1016/j.pbi.2015.11.009.

92) Scott D, Ely B (2015) Comparison of genome sequencing technology and assembly methods for the analysis of a GC-rich bacterial genome. Curr Microbiol 70:338-344. https://doi.org/10.1007/s00284-014-0721-6

93) Singer E, Bonnette J, Woyke T, Juenger T. Conservation of the endophyte microbiome structure across two Panicum grass species. Frontiers Microbiol. 2019;10:2181. doi: 10.3389/fmicb.2019.02181.

94) Singh R, Singh S, Parihar P, Mishra RK, Tripathi DK, Singh VP et al. Reactive oxygen species (ROS): beneficial companions of plants' developmental processes. Frontiers Plant Sci. 2016 Sep 27;7:1299. doi: 10.3389/fpls.2016.01299.

95) Su C, Liu L, Liu H, Ferguson BJ, Zou Y, Zhao Y et al. H2O2 regulates root system architecture by modulating the polar transport and redistribution of auxin. J Plant Biol. 2016 Jun 1;59(3):260-70. doi: 10.1007/s12374-016-0052-1.

96) Talbot JM, Bruns TD, Taylor JW, Smith DP, Branco S, Glassman SI et al. Endemism and functional convergence across the North American soil mycobiome. Proc Nat Acad Sci USA. 2014 Apr 29;111(17):6341-6. doi: 10.1073/pnas.1402584111.

97) Tamura K and Nei M (1993) Estimation of the number of nucleotide substitutions in the control region of mitochondrial DNA in humans and chimpanzees. Mol Biol and Evol 10:512-526

98) Tang Y, Horikoshi M, Li W (2016) ggfortify: Unified Interface to Visualize Statistical Result of Popular R Packages. The R J 8.2 478-489

99) Tatusova T, DiCuccio M, Badretdin A, Chetvernin V, Nawrocki EP, Zaslavsky L, Lomsadze A et al (2016) NCBI prokaryotic genome annotation pipeline. Nucl Ac Res 44:6614-6624. https://doi.org/10.1093/nar/gkw569

100) Taurian T, Anzuay MS, Angelini JG, Tonelli ML, Ludueña L, Pena D et al. Phosphate-solubilizing peanut associated bacteria: screening for plant growth-promoting activities. Plant Soil 2010 329:421-431. doi: 10.1007/s11104-009-0168-x.

101) Tiepo AN, Constantino LV, Madeira TB, Gonçalves LS, Pimenta JA, Bianchini E et al. Plant growth-promoting bacteria improve leaf antioxidant metabolism of drought-stressed neotropical trees. Planta. 2020 Apr;251(4):1-1. doi: 10.1007/s00425-020-03373-7.

102) Verma SK, Kingsley K, Bergen M, English C, Elmore M, Kharwar RN, White JF (2018) Bacterial endophytes from rice cut grass (*Leersia oryzoides L*.) increase growth, promote root gravitropic response, stimulate root hair formation, and protect rice seedlings from disease. Plant and Soil 422:223-238. https://doi.org/10.1007/s11104-017-3339-1

103) Voges MJ, Bai Y, Schulze-Lefert P, Sattely ES. Plant-derived coumarins shape the composition of an *Arabidopsis* synthetic root microbiome. Proc Nat Acad Sci USA. 2019 Jun 18;116(25):12558-65. doi: 10.1073/pnas.1820691116.

104) Wattam AR, Davis JJ, Assaf R, Boisvert S, Brettin T, Bun C, Conrad N et al (2016) Improvements to PATRIC, the all-bacterial Bioinformatics Database and Analysis Resource Center. Nucl Ac Res 45:D535-D542. https://doi.org/ 10.1093/nar/gkw1017

105) Wickham H (2016) ggplot2: Elegant Graphics for Data Analysis. In: J Stat Soft, 2nd edn. Springer-Verlag, New York, pp 260

106) Wilhelm RC (2018) Following the terrestrial tracks of *Caulobacter*-redefining the ecology of a reputed aquatic oligotroph. ISME J 12:3025-3037. https://doi.org/10.1038/s41396-018-0257-z

107) Willing CE, Pierroz G, Coleman-Derr D, Dawson TE. The generalizability of water-deficit on bacterial community composition; Site-specific water-availability predicts the bacterial community associated with coast redwood roots. Mol Ecol. 2020 Oct 1. doi: 10.1111/mec.15666.

108) Wyszkowska J, Borowik A, Olszewski J, Kucharski J. Soil bacterial community and soil enzyme activity depending on the cultivation of *Triticum aestivum*, *Brassica napus*, and *Pisum sativum ssp. arvense*. Diversity. 2019 Dec;11(12):246. doi: 10.3390/d11120246.

109) Yan X, Wang Z, Mei Y, Wang X, Xu Q, Zhou Y et al. Isolation, diversity, and growth-promoting activities of endophytic bacteria from tea

cultivars of Zijuan and Yunkang-10. Front Microbiol 2018; 9:1848. doi: 10.3389/fmicb.2018.01848.

110) Yan X, Wang Z, Mei Y, Wang X, Xu Q, Zhou Y, Wei C (2018) Isolation, Diversity, and Growth-Promoting Activities of Endophytic Bacteria From Tea Cultivars of Zijuan and Yunkang-10. Front Microbiol 9:1848. https://doi.org/10.3389/fmicb.2018.01848

111) Yang DC, Blair KM, Taylor JA, Petersen TW, Sessler T, Tull CM et al. A genome-wide Helicobacter pylori morphology screen uncovers a membrane-spanning helical cell shape complex. J Bacteriol. 2019 Jul 15;201(14):e00724-18. doi: 10.1128/JB.00724-18.

112) Yang E, Sun L, Ding X, Sun D, Liu J, Wang W. Complete genome sequence of Caulobacter flavus RHGG3 T, a type species of the genus Caulobacter with plant growth-promoting traits and heavy metal resistance. 3 Biotech. 2019 Feb 1;9(2):42. doi: 10.1007/s13205-019-1569-z.

113) Yazaki K, Arimura GI, Ohnishi T (2017) 'Hidden' terpenoids in plants: their biosynthesis, localization and ecological roles. Plant and Cell Physiol 58:1615-1621. https://doi.org/10.1093/pcp/pcx123

114) Ye N, Zhu G, Liu Y, Zhang A, Li Y, Liu R, Shi L, Jia L, Zhang J. Ascorbic acid and reactive oxygen species are involved in the inhibition of seed germination by abscisic acid in rice seeds. J Exp Botany. 2012 Mar 1;63(5):1809-22. doi: 10.1093/jxb/err336.

115) Zeng J, Dong Z, Wu H, Tian Z, Zhao Z. Redox regulation of plant stem cell fate. EMBO J. 2017 Oct 2;36(19):2844-55. doi: 10.15252/embj.201695955.

116) Zhang X, Baars O, Morel FM (2019) Genetic, structural, and functional diversity of low and high-affinity siderophores in strains of nitrogen fixing *Azotobacter chroococcum*. Metallomics 11:201-212. https://doi.org/ 10.1039/c8mt00236c

117) Zhao T, Ling HQ. Effects of pH and nitrogen forms on expression profiles of genes involved in iron homeostasis in tomato. Plant, Cell & Environment. 2007 Apr;30(4):518-27. doi: 10.1111/j.1365-3040.2007.01638.x.

APPENDIX A

SUPPLEMENTARY TABLES

Table A.1. Whole genome sequence GenBank Accession Numbers. Accession numbers are only listed for strains subjected to whole-genome analyses. *Caulobacter* strains were selected based on isolation source (aquatically-sourced vs. soil-derived) and based on genetic relatedness. A gradient of genetic relatedness was exploited in an attempt to narrow the genetic underpinnings of PGP traits.

Strain	GenBank Accession Number	Isolation source	Reference
Caulobacter crescentus CB1	CP023314.2	Tap water	Ely et al. (2019)
Caulobacter crescentus CB2	CP023313.2	Tap water	Ely et al. (2019)
Caulobacter crescenuts CB4	CP013002.1	Aquatic	Scott et al. (2016)
Caulobacter crescentus CB13	CP023315.3	Pond water	Ely et al. (2019)
Caulobacter crescentus CB15	NC_002696.2	Pond water	Nierman et al. (2001)
Caulobacter sp. CBR1	N/A	Soil/rhizosphere	Berrios and Ely (2019)
Caulobacter sp. *HB4b*	N/A	Soil/rhizosphere	This paper
C. segnis TK0059	NZ_CP027850.1	Soil	Patel et al. (2015)
Caulobacter sp. FWC20	N/A	Sludge	Abraham et al. (1999)
Caulobacter sp. K31	CP000927.1	Groundwater	Ash et al. (2014)
Caulobacter sp. AP07	AKKF00000000.1	Soil/rhizosphere	Brown et al. (2012)
Pseudomonas sp. HB2a	N/A	Soil/rhizosphere	This paper

Pseudomonas syringae pv. tomato DC3000	N/A	Soil/rhizosphere	Buell et al. (2003)

Table A.2. *Caulobacter* CFU $g^{-1}ml^{-1}$ soil versus total plant weight (fresh)

CB1		**CB2**		**CB4**		**CB13**	**CB15**		
PW/g	CFU*g	PW/g	CFU*g	PW/g	CFU*g	PW/g	CFU*g	PW (g)	CFU*g
1.01	22000000	0.735	2200000	0	400000	2.387	6000000	1.064	3400000
1.17	32000000	1.237	2200000	0.283	34000	1.417	40000	0.970	600000
0.71	14000000	0.05	6000000	0.608	2600	1.772	430000	1.972	30000000
CBR1		***C. segnis***		**HB4b**		**K31**		**AP07**	
1.005	60000000	1.34	800000	1.220	2100000	0.841	2400000	0.15	4000000
1.483	22000000	1.32	200000	1.333	2400000	0.330	2600000	1.00	200000
2.100	60000000	0.98	100000	1.199	2000000	1.298	3800000	0	1800000
FWC20		***Sphingomonas***		***DC3000***		***HB2a***		**Control**	
1.130	40000	0.94	340000	0	200000	0.345	550000	0.73	150
0.649	40000	0.68	300000	1.060	15000	0.638	31000	1.44	124

0.722	9200000	1.32	380000	0.623	27000	0.972	3800	1.18	220

Table A.3. Extended *Caulobacter* CFU $g^{-1}ml^{-1}$ soil versus total plant weight

CB1		CB2		CB4		CB13		CB15	
PW (g)	CFU $g^{-1}ml^{-1}$	PW (g)	CFU $g^{-1}ml^{-1}$	PW (g)	CFU $g^{-1}ml^{-1}$	PW (g)	CFU $g^{-1}ml^{-1}$	PW (g)	CFU $g^{-1}ml^{-1}$
2.3	4800000	1.52	420000	1.7	145000	1.89	130000	3.1	770000
2.2	4550000	1.85	380000	1.5	130000	2.08	430000	2	280000
2	4000000	1.77	320000	1.5	120000	2.18	670000	2	300000
2	4200000	1.65	350000	0.7	330000	2.16	530000	2	330000
2.2	4500000	0.96	520000	1.3	190000	2.01	290000	2.5	670000
2.3	4300000	1.75	300000	1.8	290000	2.36	570000	1.8	320000
2.1	4200000	0.34	570000	0	600000	2.13	530000	2	480000
1.9	4100000	1.64	530000	0.2	320000	2.45	970000	0.9	150000
1.8	3700000	1.93	380000	1.6	290000	2.13	600000	2.5	590000
2.4	5100000	1.27	520000	0.9	520000	2.18	270000	2	300000

3	5200000	2.07	330000	0.2	620000	2.11	410000	2.4	570000
0.8	3500000	0.86	520000	1.1	440000	2.3	630000	2	270000
CBR1		***C. segnis***		**HB4b**		**K31**		**AP07**	
PW (g)	CFUg^{-1}ml^{-1}	PW (g)	CFUg^{-1}ml^{-1}	PW (g)	CFUg^{-1}ml^{-1}	PW (g)	CFUg^{-1}ml^{-1}	PW (g)	CFUg^{-1}ml^{-1}
2.4	7600000	1.83	370000	2	300000	1.5	410000	0	400000
2.1	5200000	1.94	530000	2.4	630000	2	220000	0	430000
2.2	6300000	2.12	600000	2.2	450000	0.9	380000	1.5	100000
2.3	6800000	2.46	770000	1.9	280000	2.2	190000	1.6	140000
2.1	5000000	2.38	630000	2.5	770000	1.2	510000	1.8	130000
2.4	7300000	2.25	670000	1.9	330000	2	340000	1.5	180000
2.5	7700000	2.1	620000	2.4	350000	1.8	260000	1.8	100000
2.5	7500000	2.23	630000	2.4	420000	1.8	300000	1.6	210000
2.5	7200000	2.38	700000	1.6	230000	1.8	600000	1.4	200000
2.6	7300000	2.3	430000	2.5	670000	2.1	210000	1.3	290000
2.2	6400000	2.07	530000	2.1	420000	2.1	200000	1.4	200000

2.3	6800000	1.9	400000	2.2	500000	1.6	100000	1.3	280000
FWC20		***Sphingomonas* sp.**		***P. syringae* pv tomato DC3000**		***Pseudomonas* sp. HB2a**		**Control**	
PW (g)	CFUg^{-1}ml^{-1}	PW (g)	CFU g^{-1}ml^{-1}	PW (g)	CFU g^{-1}ml^{-1}	PW (g)	CFUg^{-1}ml^{-1}	PW (g)	CFU g^{-1}ml^{-1}
0.84	3200000	1.3	300000	0.5	410000	1.13	410000	2.1	4000
1.83	2200000	1.7	610000	0.2	530000	0.07	690000	1.5	6300
1.67	5800000	2.1	360000	1.1	190000	0	670000	1.5	2900
2.09	2900000	2	260000	0.5	415000	1.59	380000	1	6400
0.95	4700000	2.1	200000	0.7	300000	0	630000	1.7	2900
1.7	6300000	1.1	220000	0	630000	1.78	330000	1.7	3500
0.96	6000000	2.1	660000	0	660000	0	650000	1.8	670
1.9	4000000	1	160000	0.9	520000	0	630000	1	6100
1.76	6700000	2.1	230000	1.1	210000	1.59	270000	1.5	740
1.97	6600000	1.6	400000	0.6	500000	1.61	250000	1.3	390
0.14	3000000	2.2	300000	0.4	260000	0	530000	1.9	5200

1.09	2500000	1.6	760000	0	620000	0	570000	1.5	430

Table A.4. *C. crescentus* CB1 and CB2 Protein families (PFs)

Protein families unique to CB1

Family ID	Proteins	Description
PGF_00919165	1	3-oxoadipyl-CoA thiolase (EC 2.3.1.174)
PGF_01196329	1	ADP-ribosylglycohydrolase
PGF_09945671	1	Acetate kinase (EC 2.7.2.1)
PGF_02160099	1	Aminoglycoside N(6')-acetyltransferase (EC 2.3.1.82) => AAC(6')-Ic,f,g,h,j,k,l,r-z
PGF_10372736	1	Antirestriction protein
PGF_04883561	1	Assimilatory nitrate reductase large subunit (EC 1.7.99.4)
PGF_03226153	1	Bacteriophage protein gp37
PGF_02969155	1	CAAX amino terminal protease family protein
PGF_12700504	1	Capsular polysaccharide biosynthesis protein
PGF_00419496	1	CopG domain-containing protein
PGF_08301315	1	Cytochrome O ubiquinol oxidase subunit I (EC 1.10.3.-)
PGF_05122891	1	Cytochrome O ubiquinol oxidase subunit II (EC 1.10.3.-)
PGF_00420155	1	Cytochrome O ubiquinol oxidase subunit III (EC 1.10.3.-)
PGF_04012930	1	Cytochrome O ubiquinol oxidase subunit IV (EC 1.10.3.-)
PGF_06943909	1	Cytochrome b
PGF_00422465	1	DUF1801 domain-containing protein
PGF_00422625	1	Death on curing protein, Doc toxin
PGF_01197732	1	Death on curing protein, Doc toxin
PGF_04579393	1	Death on curing protein, Doc toxin
PGF_05893169	1	Death on curing protein, Doc toxin
PGF_01197731	1	EF hand domain protein
PGF_00689884	1	Efflux transport system, outer membrane factor (OMF) lipoprotein XCC0419
PGF_10551113	1	FIG140336: TPR domain protein
PGF_00003770	1	FMN oxidoreductase
PGF_00011472	1	Hemolysin activation/secretion protein
PGF_00013631	1	IS1111A/IS1328/IS1533 family transposase
PGF_10387734	1	IncF plasmid conjugative transfer DNA-nicking and unwinding protein TraI

PGF_12770209	5	Insertion element ISR1 (Rhizobium class IV strains) transposase
PGF_01195717	1	Lactoylglutathione lyase and related lyases
PGF_01197664	1	Large exoproteins involved in heme utilization or adhesion
PGF_08231425	1	Lasso peptide maturation, ATP-dependent lactam synthetase McjC family
PGF_02960449	1	Lasso peptide maturation, cysteine protease McjB family
PGF_01197667	1	Mobile element protein
PGF_12872216	5	Mobile element protein
PGF_00023758	1	N-acetylglucosamine kinase bacterial type predicted (EC 2.7.1.59) / Transcriptional regulator
PGF_05671503	1	NAD(P)H dehydrogenase (quinone) family protein
PGF_00025686	1	Nitrate ABC transporter, ATP-binding protein
PGF_03882257	1	Nitrate ABC transporter, permease protein
PGF_03039710	2	Nitrate ABC transporter, substrate-binding protein
PGF_06014884	1	Nitrate transporter NasA
PGF_09358806	1	Nitrite reductase [NAD(P)H] large subunit (EC 1.7.1.4)
PGF_03879367	1	Nitrite reductase [NAD(P)H] small subunit (EC 1.7.1.4)
PGF_01195882	1	OmpA-related protein
PGF_02345287	1	Oxidoreductase
PGF_00029992	1	ParD protein (antitoxin to ParE)
PGF_03984798	1	ParD protein (antitoxin to ParE)
PGF_01650262	1	ParE toxin protein
PGF_00849350	1	Peptidase, S41 family
PGF_00032576	1	Phage protein
PGF_00033197	1	Phosphate acetyltransferase (EC 2.3.1.8)
PGF_00036609	1	Prevent host death protein, Phd antitoxin
PGF_01196074	1	Protein of unknown function DUF86, BT0167 group
PGF_00038982	1	Purine nucleoside permease
PGF_02905816	1	Putative peptidase
PGF_01395856	1	RND efflux system, inner membrane transporter KPN_02144
PGF_00394669	1	RND efflux system, membrane fusion protein KPN_02145
PGF_00047903	1	Response regulator NasT
PGF_00048788	1	Ribose-phosphate pyrophosphokinase, possible alternative form 2
PGF_00473519	1	Superoxide dismutase [Mn] (EC 1.15.1.1)
PGF_00055894	1	TRAP-type C4-dicarboxylate transport system, small permease component

PGF_07980447	1	Threonine dehydrogenase and related Zn-dependent dehydrogenases
PGF_00056876	1	Thymidine phosphorylase (EC 2.4.2.4)
PGF_00745988	1	Transcriptional regulator KPN_02146, AcrR family
PGF_12786021	1	Transcriptional regulator, AcrR family
PGF_10505351	1	Transcriptional regulator, AraC family
PGF_00059115	1	Transcriptional regulator, Xre family
PGF_01195891	1	Transcriptional regulator, Xre family
PGF_09978608	5	Transposase
PGF_10312056	1	Type II restriction enzyme, methylase subunits
PGF_00064046	1	UDP-galactopyranose mutase (EC 5.4.99.9)
PGF_00067129	1	Xylulose-5-phosphate phosphoketolase (EC 4.1.2.9) @ Fructose-6-phosphate phosphoketolase (EC 4.1.2.22)
PGF_04843875	1	cytochrome b561 family protein
PGF_00163311	198	hypothetical protein
PGF_00402639	1	peptidoglycan binding domain protein
PGF_01195873	1	putative TonB-dependent receptor
PGF_00410366	1	putative restriction endonuclease
PGF_01197729	1	putative subtilisin proteinase-like protein

Protein families unique to CB2

Family ID	Proteins	Description
PGF_00025679	1	thiolase (EC 2.3.1.174)
PGF_09969323	1	CopG protein
PGF_00419566	1	Copper resistance protein CopD
PGF_07032168	1	Copper/silver efflux RND transporter, membrane fusion protein CusB
PGF_03376178	1	Copper/silver efflux RND transporter, outer membrane protein CusC
PGF_10279967	1	Copper/silver efflux RND transporter, transmembrane protein CusA
PGF_10489706	1	Cu(I)-responsive transcriptional regulator
PGF_00420329	1	Cytochrome c family protein
PGF_03139272	1	Dienelactone hydrolase and related enzymes
PGF_01767794	1	Excinuclease ABC, C subunit-like
PGF_09675703	1	FIG001353: Acetyltransferase
PGF_00426263	1	FIG00481833: hypothetical protein
PGF_12928762	1	Flp pilus assembly protein, pilin Flp
PGF_10474812	1	High-affinity Fe2+/Pb2+ permease precursor
PGF_06724323	1	O-acetyl-ADP-ribose deacetylase
PGF_08560330	1	Oar protein
PGF_03962887	1	Phage antirepressor protein
PGF_08770713	1	Phage head, portal protein B

PGF_00072235	1	Phage head, terminase DNA packaging protein A
PGF_02895979	1	Phage major capsid protein
PGF_12797415	1	Phage major head subunit Mup34, T
PGF_01675198	1	Phage portal protein
PGF_00045602	1	Putative type II restriction enzyme NmeDIP (EC 3.1.21.4) (Endonuclease NmeDIP) (R.NmeDIP)
PGF_10625559	1	Pyridoxal-dependent decarboxylase family protein
PGF_00046482	1	RNA polymerase ECF-type sigma factor
PGF_01641254	1	Ribonucleotide reductase of class III (anaerobic), activating protein (EC 1.97.1.4)
PGF_01724713	1	Ribose-5-phosphate isomerase B (EC 5.3.1.6)
PGF_00039335	1	Serine recombinase, PinQ/PinR-type
PGF_00052858	2	Site-specific DNA methylase
PGF_00053808	1	SpoVT/AbrB-like
PGF_04692091	1	Toxin HigB
PGF_06031744	1	Transcriptional regulator, AcrR family
PGF_00069882	1	Zinc-binding GTPase YciC
PGF_00080246	277	hypothetical protein
PGF_07726695	1	phage terminase GpA

Table A.5. *Caulobacter* strains containing a gene required for phosphate solubilization

Strain	**PATRIC Database Genome ID**
Caulobacter flavus CGMCC1 15093	1679497.5
Caulobacter flavus RHGG3	1679497.6
Caulobacter mirabilis FWC 38	69666.3
Caulobacter sp. 410	2055137.3
Caulobacter sp. 695	2172650.3
Caulobacter sp. 736	2172651.3
Caulobacter sp. 774	2172652.3
Caulobacter sp. D4A	2204171.3
Caulobacter sp. D5	357400.3
Caulobacter vibrioides T5M6	155892.3

Table A.6. *Caulobacter* strains harboring a duplicated BGC operon in their genome. Strains used in our experiments are bolded.

Strain	Accession number
Caulobacter crescentus OR37	APMP01000001
Caulobacter vibrioides strain UBA2596	DDKO01000023
Caulobacter vibrioides strain CB2A	CP034122
Caulobacter vibrioides strain T5M6	LNIY01000101
***Caulobacter vibrioides* strain CB13b1a**	**CP023315**
***Caulobacter vibrioides* strain CB1**	**CP023314**
uncultured *Caulobacter sp*. strain MGYG-HGUT-01261	CABKLV010000126
Caulobacter flavus strain CGMCC1 15093	PJRQ01000021
Caulobacter flavus strain RHGG3	CP026100
***Caulobacter crescentus* CB15**	**NC_002696**
Caulobacter sp. BP25	PEGH01000008
Caulobacter sp. X	PEGF01000001
Caulobacter sp. 410	PJRS01000012
Caulobacter sp. 695	QDKO01000043
Caulobacter sp. 736	QDKP01000011
Caulobacter sp. 774	QDKQ01000023
Caulobacter sp. D4A	QHJZ01000434
Caulobacter sp. D5	QHJY01000033
Caulobacter segnis ATCC 21756	NC_014100
Caulobacter crescentus NA1000	NC_011916
Caulobacter mirabilis strain FWC 38	CP024201
***Caulobacter segnis* strain TK0059**	**CP027850**
Caulobacter segnis strain S2_003_000_R2_4	QFQZ01000031

Table A.7. Bacterial cell re-isolation dataset

EXP-1		CB 13	CB 13cyoB	C. segnis	C. segniscyoB	CB 15	CB 15creS					
	CFU/mL	5.00E+05	4.00E+05	3.50E+05	6.30E+05	5.30E+05	1.90E+05					
	CFU/mL	2.00E+06	5.30E+05	6.00E+05	3.00E+05	7.00E+05	3.70E+05					
	CFU/mL	9.00E+05	1.00E+05	9.00E+05	9.00E+05	2.80E+05	9.00E+05					
	CFU/mL	5.10E+05	6.40E+05	1.20E+05	1.40E+06	3.40E+05	7.20E+05					
	CFU/mL	4.20E+05	6.90E+05	5.20E+05	8.40E+05	1.20E+05	4.00E+05					
	CFU/mL	4.00E+05	2.30E+06	1.45E+05	6.40E+05	4.90E+05	6.40E+05					
	CFU/mL	7.40E+05	4.50E+05	6.00E+05	2.50E+05	3.40E+05	3.70E+05					
	CFU/mL	6.00E+05	2.00E+05	7.00E+05	6.00E+05	2.00E+05	2.00E+05					
	CFU/mL	4.00E+05	1.00E+05	8.00E+05	3.40E+05	8.30E+05	6.30E+05					
	CFU/mL	2.00E+05	5.20E+05	9.00E+05	6.50E+05	4.10E+05	1.40E+05					

	CFU/mL	3.40E+05	3.90E+05	1.20E+06	3.80E+05	7.20E+05	1.90E+05					
	CFU/mL	1.80E+05	2.20E+05	5.20E+05	5.00E+05	2.10E+05	3.50E+05					
AVGs		**5.99E+05**	**5.45E+05**	**6.13E+05**	**6.19E+05**	**4.31E+05**	**4.25E+05**					
EXP-2	**CFU/mL**	**CB13**	**CB13coyoB**	**C.segnis**	**C.segniscyoB**	**CB15**	**CB15creS**					
	CFU/mL	4.20E+05	6.34E+05	1.20E+06	2.60E+05	6.00E+05	5.70E+05					
	CFU/mL	6.90E+05	8.80E+05	2.60E+05	8.20E+05	7.40E+05	6.70E+05					
	CFU/mL	9.00E+05	3.40E+05	8.80E+05	6.60E+05	2.50E+05	2.30E+05					
	CFU/mL	3.40E+05	7.90E+05	9.40E+05	4.50E+05	4.10E+05	4.80E+05					
	CFU/mL	2.80E+05	6.70E+05	5.30E+05	1.10E+06	3.30E+05	9.00E+05					
	CFU/mL	4.60E+05	5.40E+05	7.50E+05	7.50E+05	2.40E+05	2.50E+05					
	CFU/mL	8.40E+05	6.30E+05	6.00E+05	6.30E+05	1.20E+06	3.20E+05					

	CFU/mL	2.30E+05	5.00E+05	4.20E+05	4.90E+05	2.00E+05	7.00E+05					
	CFU/mL	1.00E+06	5.80E+05	7.20E+05	6.80E+05	8.00E+05	2.00E+05					
	CFU/mL	7.20E+05	4.50E+05	3.30E+05	4.20E+05	1.20E+05	3.00E+05					
	CFU/mL	4.20E+05	1.80E+05	4.50E+05	5.20E+05	4.20E+05	1.20E+06		**T-test p-values**			
	CFU/mL	3.20E+05	5.50E+05	6.00E+05	6.10E+05	3.40E+05	5.10E+05					
AVGs		**5.52E+05**	**5.62E+05**	**6.40E+05**	**6.16E+05**	**4.71E+05**	**5.28E+05**		**CB13 v CB13cyoB**	**C. segnis v C. segniscyoB**	**CB15 v creS**	
									0.85	0.91	0.75	

Table A.8. RT-qPCR dataset

CB13		**rho (ct) 1**	**rho (ct) 2**			**cyoB (ct) 1**	**cyoB (ct) 2**			**cydA (ct) 1**	**cydA (ct) 2**		**cyoB (Δct) 1**	**cyoB (Δct) 2**		**cydA (Δct) 1**	**cydA (Δct) 2**
		33.96	39.46			28.02	38.38			24.21	33.84		**6.30**	**2.96**		**10.63**	**5.64**
		35.90	39.88			28.01	35.46			24.24	33.90						
		33.72	39.03			28.64	35.65			23.23	33.72						
	Avg.	34.53	39.46			28.22	36.50			23.89	33.82						

C. segnis		rho (ct) 1	rho (ct) 2			cyoB (ct) 1	cyoB (ct) 2			cydA (ct) 1	cydA (ct) 2		cyoB (ΔΔct) 1	cyoB (ΔΔct) 2		cydA (ΔΔct) 1	cydA (ΔΔct) 2
		28.65	30.14			26.76	26.03			23.01	26.36		**1.73**	**1.45**		**5.78**	**1.29**
		28.53	27.93			27.01	27.79			22.91	24.97						
		28.67	26.14			26.89	26.05			22.59	29.02						
	Avg.	28.62	28.07			26.89	26.62			22.84	26.78						
CB 15		**rho (ct) 1**	**rho (ct) 2**			**cyoB (ct) 1**	**cyoB (ct) 2**			**cydA (ct) 1**	**cydA (ct) 2**		**cyoB (ΔΔct) 1**	**cyoB (ΔΔct) 2**		**cydA (ΔΔct) 1**	**cydA (ΔΔct) 2**
		34.69	35.12			33.80	36.24			35.22	34.34		**0.52**	**1.57**		**0.37**	**1.57**
		35.81	38.74			35.12	34.02			34.77	35.69						
		35.00	34.33			35.00	33.21			34.40	34.23						
	Avg.	35.16	36.06			34.64	34.49			34.79	34.75						
CBR1		**rho (ct) 1**	**rho (ct) 2**			**cyoB (ct) 1**	**cyoB (ct) 2**			**cydA (ct) 1**	**cydA (ct) 2**		**cyoB (ΔΔct) 1**	**cyoB (ΔΔct) 2**		**cydA (ΔΔct) 1**	**cydA (ΔΔct) 2**
		35.22	32.15			29.75	34.03			31.172	34.03		**4.85**	**-1.01**		**3.72**	**-0.06**
		38.01	33.72			30.87	35.19			31.874	32.08						
		32.60	31.04			30.68	30.70			31.64	30.98						
	Avg.	35.28	32.30			30.43	33.31			31.56	32.36						

Table A.9. Germination rate data. Rates were recorded at seven DPI.

Condion	DM			DM (10^{-1})			DM (10^{-2})			MS			MS (10^{-1})			MS (10^{-2})		
CB13	58	68	72	72	68	60	72	66	62	6	8	10	12	16	20	24	26	20
CB13Δ*cyoB*	88	92	76	92	88	86	92	80	88	22	20	26	28	30	34	30	40	34
C. segnis	84	90	90	92	90	88	96	86	90	92	86	82	96	88	82	90	96	88
CB15	92	92	94	N/A	N/A	N/A	N/A	N/A	N/A	92	94	90	N/A	N/A	N/A	N/A	N/A	N/A
CB15Δcres	96	94	92	N/A	N/A	N/A	N/A	N/A	N/A	90	92	90	N/A	N/A	N/A	N/A	N/A	N/A
C. segnis*Δ*cyoB	90	84	88	94	90	90	94	90	94	90	84	94	92	88	92	88	84	96
Control	94	96	98	N/A	N/A	N/A	N/A	N/A	N/A	96	98	94	N/A	N/A	N/A	N/A	N/A	N/A

Table A.10. Two-way ANOVA: Media composition and *cyoB* mutation

Two-way ANOVA	Ordinary				
Alpha	0.05				
Source of Variation	% of total variation	P value	P value summary	Significant?	
Interaction	2.057	0.0155	*	Yes	
Row Factor	14.97	<0.0001	****	Yes	
Column Factor	80.18	<0.0001	****	Yes	
ANOVA table	SS	DF	MS	F (DFn, DFd)	P value
Interaction	498	5	99.5	F (5, 24) = 3.536	P=0.0155
Row Factor	3620	1	3620	F (1, 24) = 128.6	P<0.0001
Column Factor	19392	5	3878	F (5, 24) = 137.8	P<0.0001

Table A.11. Flux Balance Analysis (FBA)

		MS MEDIA			DM MEDIA + glucose		
Strain	**GenBank Accession Number**	**H+ Flux**	**Triphosphate**	**Thiamine phosphate**	**H+ Flux**	**Triphosphate**	**Thiamine phosphate**
CB13	**CP023315.3**	551.14	11.92	0.50	0	0	0
CB15	**NC_002696.2**	281.93	12.62	0.00	0	0	0
CB1	**CP023314.2**	213.13	0.00	14.37	0	0	0
CB2	**CP023313.2**	330.73	12.67	0.00	0	0	0
CB4	**CP013002.1**	374.00	-6.37	0.00	0	0	0
C. segnis	**NZ_CP027850.1**	-59.57	-1000.00	0.00	0	0	0
AP07	**AKKF00000000.1**	-1000.00	-1000.00	0.00	0	0	0
K31	**CP000927.1**	373.72	-6.37	0.00	0	0	0

Table A.12. *Caulobacter* strains grown in defined media (DM) and Murashige and Skoog (MS) media.

	AP07	**CB1**	**CB2**	**CB4**	**CB13/CB13cyoB**	**CB15**	***C. segnis***	**K31**
MS	6.07	6.1	6.23	6.37	5.01/5.5	6.36	6.58	6.42
MS	6.03	6.3	6.8	6.87	5.13/5.2	6.4	6.8	6.64
MS	6.13	6.8	6.4	6.42	5.8/5.4	6.2	6.5	7.01
DM	7.01	7.2	7	7.13	6.9/7.5	7.14	7.3	6.8
DM	7.2	7.04	7.12	7.42	7.12/7.2	6.8	6.9	7.3
DM	7.25	7.13	6.8	6.9	7.3/7.0	7.09	6.6	7.1

Table A.13. *cyoA-D* predicted protein sequence homologies to those of non-*Caulobacter* genera (top BLASTp match)

	cyoA		***cyoB***		***cyoC***		***cyoD***	
	NCHM	**AA % ID**	**NCHM**	**AA % ID**	**NCHM**	**AA % ID**	**NCHM**	**AA % ID**
CB13	*Kaistia soli* DSM 19436	68	*Thalassospira xianhensis* MCCC 1A02616 **(#)**	84.11	*Hansschlegelia beijingensis* PG04 **(*)**	81.73	*Ancylobacter pratisalsi* **(*)**	68.5
***C. segnis* TK0059**	*Sphingobium algorifontocola*	63.56	*Bordetella* sp. AU14267	83.64	*Polaromonas jejuensis* NBRC 106434	79.31	*Novosphingobium malaysiense* 273 **(*)**	62.88

APPENDIX B

SUPPLEMENTARY FIGURES

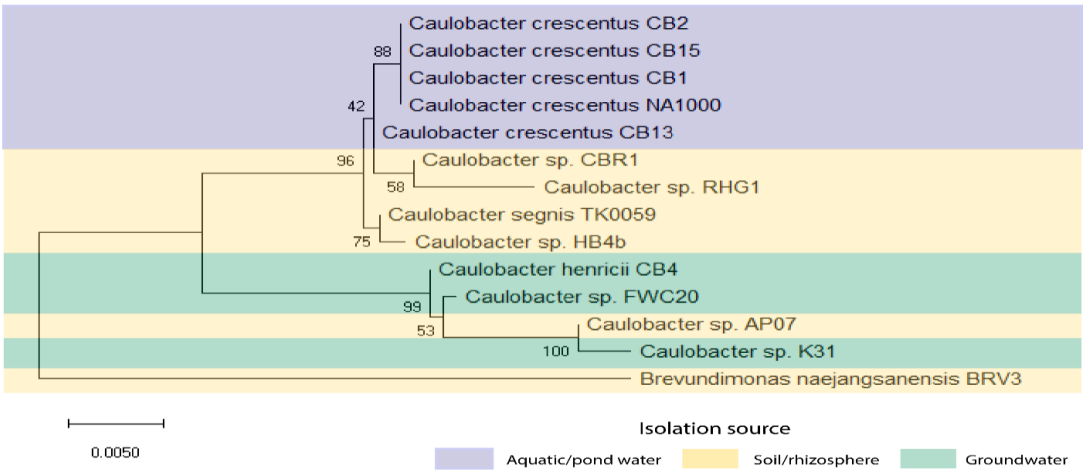

Figure B.1. Genomic comparisons of *Caulobacter* strains. A 16S rDNA phylogenic tree depicting the genetic relationships between the strains used in the plant growth assays. Caulobacter sp. RHG1 has recently been established as a PGP *Caulobacter* strain (Luo et al. 2019). *Brevundimonas naejangsanensis* BRV3 functions as an outgroup for this analysis (Berrios and Ely, accession number CP032707.1) The evolutionary history was inferred by using the Maximum Likelihood method and Tamura-Nei model (Tamura and Nei 1993). The bootstrap consensus tree inferred from 1000 replicates (Felsenstein 1985) is taken to represent the evolutionary history of the taxa analyzed (Felsenstein 1985). Branches corresponding to partitions reproduced in less than 50% bootstrap replicates are collapsed. The percentage of replicate trees in which the associated taxa clustered together in the bootstrap test (1000 replicates) are shown next to the branches (Felsenstein 1985). Initial tree(s) for the heuristic search were obtained automatically by applying Neighbor-Join and BioNJ algorithms to a matrix of pairwise distances estimated using the Maximum Composite Likelihood (MCL) approach and then selecting the topology with superior log likelihood value. This analysis involved 14 nucleotide sequences. All positions containing gaps and missing data were eliminated (complete deletion option). There were a total of 1412 positions in the final dataset. Evolutionary analyses were conducted in MEGA X (Kumar et al. 2018).

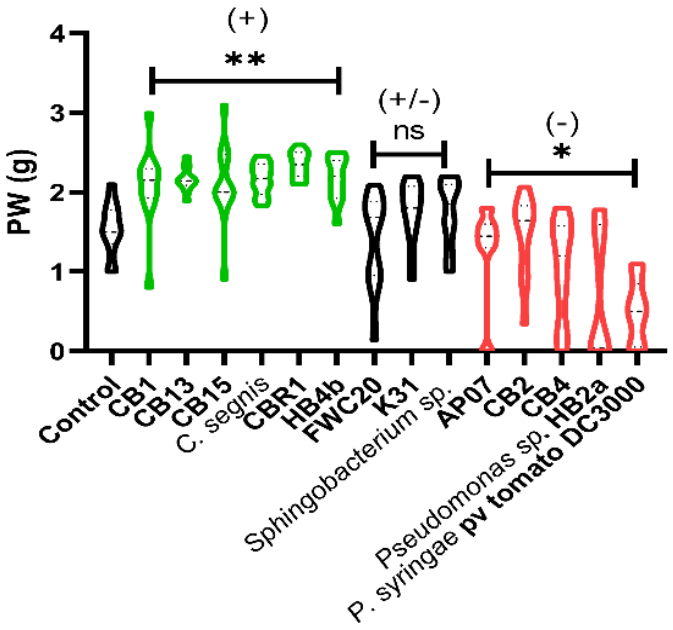

Figure B.2. Replicated plant weight (PW) data. Violin plot depicting the impact of a given bacterial strain on *A. thaliana* plant weight (PW) in grams (g). Samples (n) per condition (n=12). A one-way ANOVA was performed in R, and p-values were adjusted by the Benjamini-Hochberg method using the ggplot2 package. * ≤ 0.05; ** ≤ 0.001; ns = not significant relative to control plant weight (average).

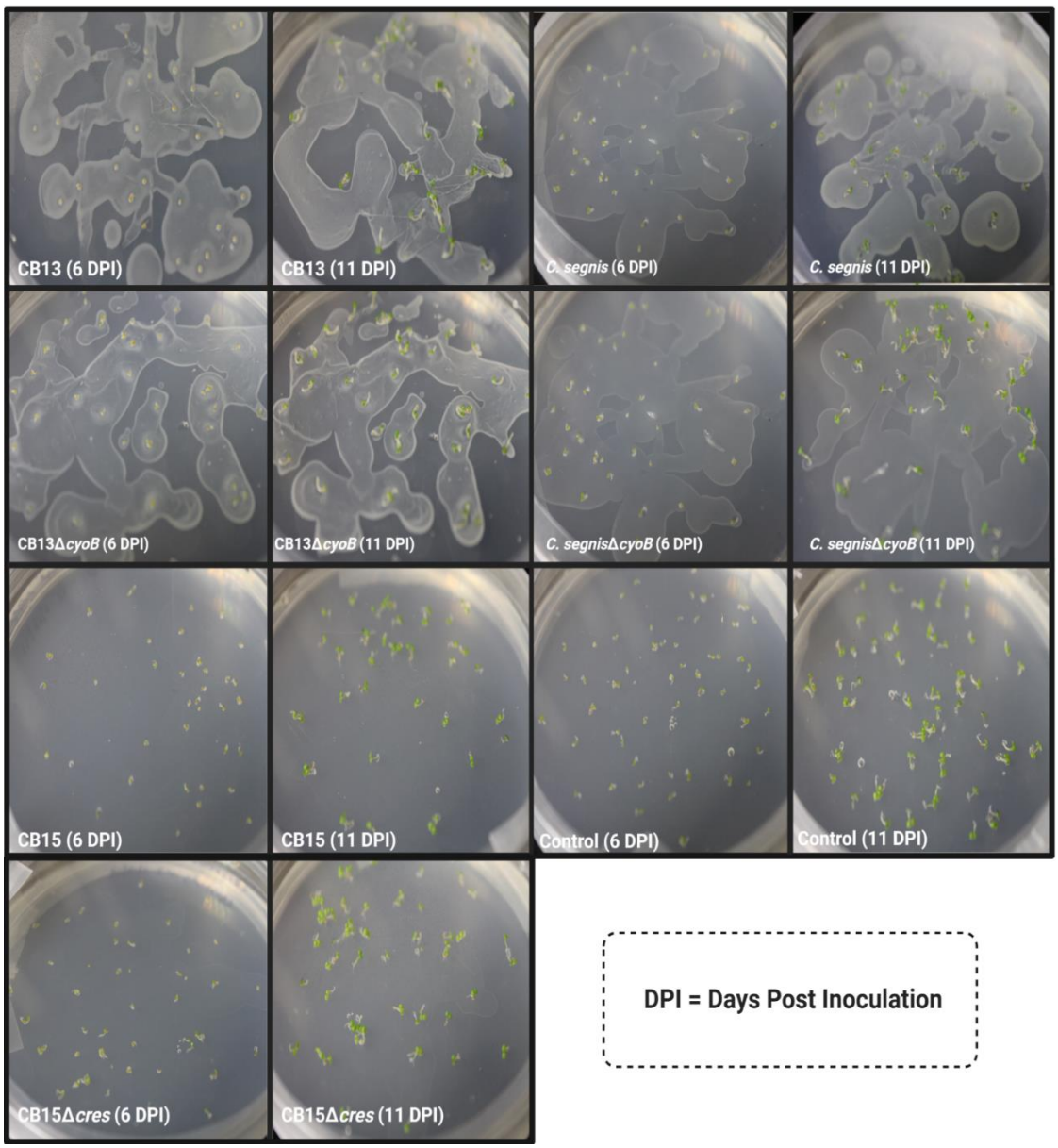

Figure B.3. Germination assays on Murashige and Skoog (MS) agar plates.

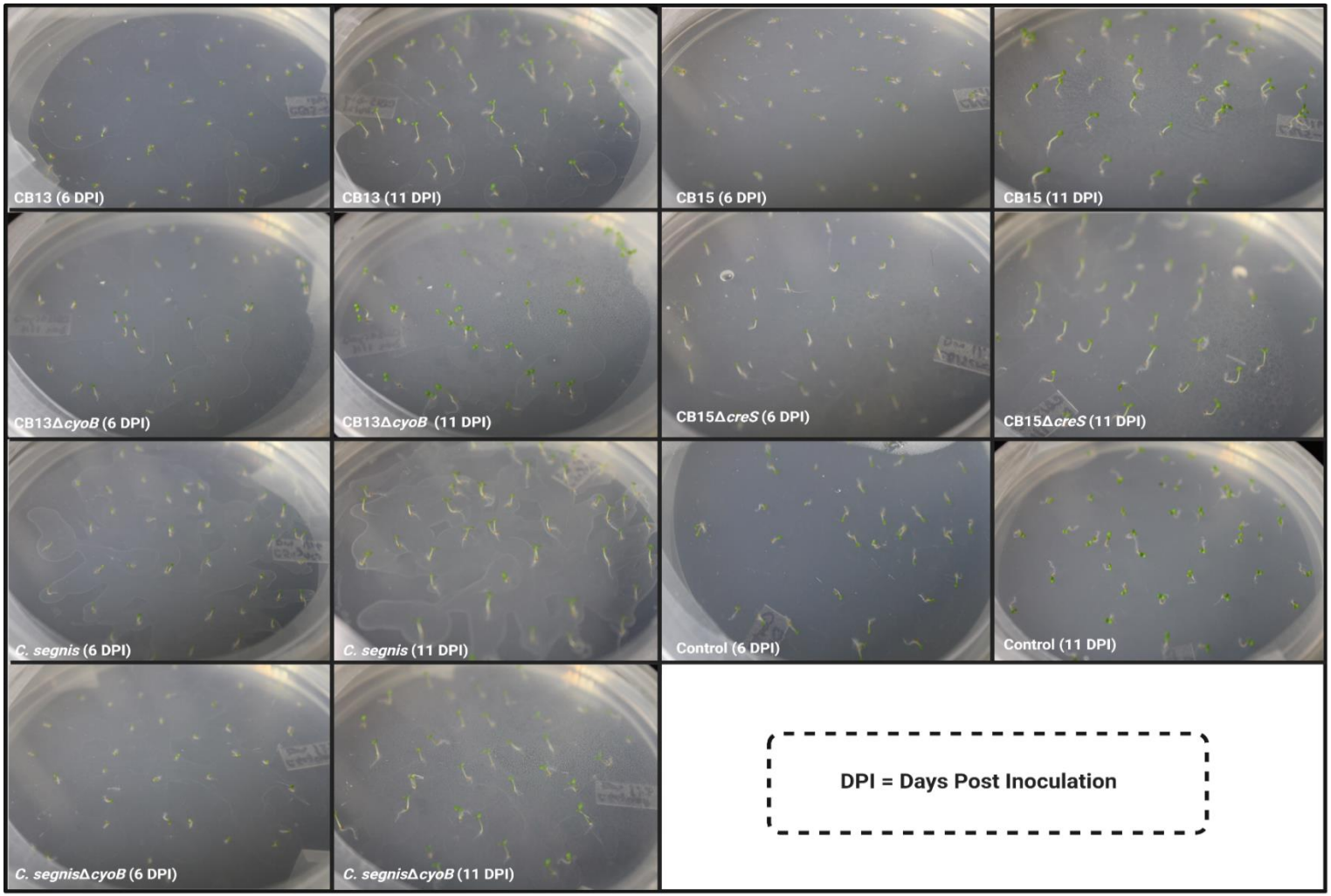

Figure B.4. Germination assays on Defined Media (DM) agar plates.

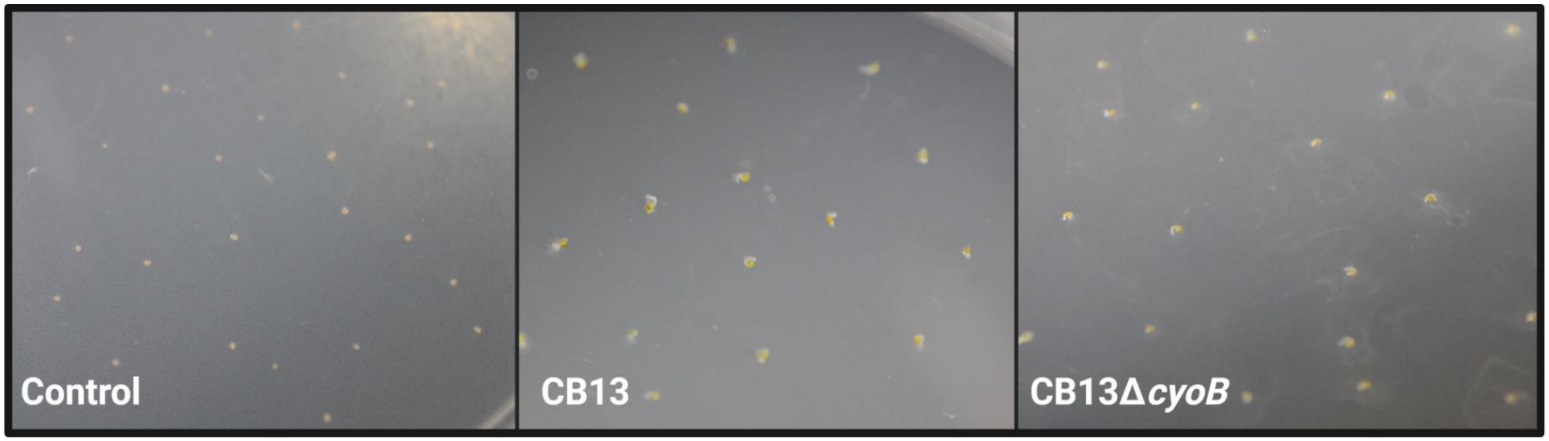

Figure B.5. Germination assays on Murashige and Skoog (MS) agar plates with pH adjusted to 10. Photographs were captured when noticeable radicle protrusion was observed (~ 6 days post inoculation/plating).

APPENDIX C

PERMISSIONS TO REPRINT

Confirmation of your Copyright Transfer

Dear Author,

Please note: This e-mail is a confirmation of your copyright transfer and was sent to you only for your own records.

1. Publication
The copyright to this article, (including any supplementary information and graphic elements therein (e.g. illustrations, charts, moving images) (the 'Article'), is hereby assigned for good and valuable consideration to Springer Nature Switzerland AG (the 'Assignee'). Headings are for convenience only.

2. Grant of Rights
In consideration of the Assignee evaluating the Article for publication, the Author(s) grant the Assignee without limitation the exclusive (except as set out in clauses 3, 4 and 5 a) iv), assignable and sub-licensable right, unlimited in time and territory, to copy-edit, reproduce, publish, distribute, transmit, make available and store the Article, including abstracts thereof, in all forms of media of expression now known or developed in the future, including pre- and reprints, translations, photographic reproductions and extensions. Furthermore, to enable additional publishing services, such as promotion of the Article, the Author(s) grant the Assignee the right to use the Article (including the use of any graphic elements on a stand-alone basis) in whole or in part in electronic form, such as for display in databases or data networks (e.g. the Internet), or for print or download to stationary or portable devices. This includes interactive and multimedia use as well as posting the Article in full or in part or its abstract on social media, and the right to alter the Article to the extent necessary for such use. The Assignee may also let third parties share the Article in full or in part or its abstract on social media and may in this context sub-license the Article and its abstract to social media users. Author(s) grant to Assignee the right to re-license Article metadata without restriction (including but not limited to author name, title, abstract, citation, references, keywords and any additional information as determined by Assignee).

3. Self-Archiving
Author(s) are permitted to self-archive a pre-print and an author's accepted manuscript version of their Article.

a. A pre-print is the author's version of the Article before peer-review has taken place ("Pre-Print"). Prior to acceptance for publication, Author(s) retain the right to make a Pre-Print of their Article available on any of the following: their own personal, self-maintained website; a legally compliant, non-commercial pre-print server such as but not limited to arXiv and bioRxiv. Once the Article has been

published, the Author(s) should update the acknowledgement and provide a link to the definitive version on the publisher's website: "This is a pre-print of an article published in [insert journal title]. The final authenticated version is available online at: https://doi.org/[insert DOI]".

b. An Author's Accepted Manuscript (AAM) is the version accepted for publication in a journal following peer review but prior to copyediting and typesetting that can be made available under the following conditions:
    a. Author(s) retain the right to make an AAM of their Article available on their own personal, self-maintained website immediately on acceptance,
    b. Author(s) retain the right to make an AAM of their Article available for public release on any of the following 12 months after first publication ("Embargo Period"): their employer's internal website; their institutional and/or funder repositories. AAMs may also be deposited in such repositories immediately on acceptance, provided that they are not made publicly available until after the Embargo Period.

An acknowledgement in the following form should be included, together with a link to the published version on the publisher's website: "This is a post-peer-review, pre-copyedit version of an article published in [insert journal title]. The final authenticated version is available online at: http://dx.doi.org/[insert DOI]".

4. Authors' Retained Rights

Author(s) retain the following non-exclusive rights for the published version provided that, when reproducing the Article or extracts from it, the Author(s) acknowledge and reference first publication in the Journal:

a. to reuse graphic elements created by the Author(s) and contained in the Article, in presentations and other works created by them;
b. they and any academic institution where they work at the time may reproduce the Article for the purpose of course teaching (but not for inclusion in course pack material for onward sale by libraries and institutions); and
c. to reproduce, or to allow a third party Assignee to reproduce the Article in whole or in part in any printed volume (book or thesis) written by the Author(s).

5. Warranties

The Author(s) warrant and represent that:

a. (i) the Author(s) are the sole copyright owners or have been authorised by any additional copyright owner(s) to assign the rights defined in clause 2, (ii) the Article does not infringe any intellectual property rights (including without limitation copyright, database rights or trade mark rights) or other third party rights and no licence from or payments to a third party are required to publish the Article, (iii) the Article has not been previously published or licensed, (iv) if the Article contains material from other sources (e.g. illustrations, tables, text quotations), Author(s) have obtained written permissions to the extent necessary from the copyright holder(s), to license to the Assignee the same rights as set out in Clause 2 but on a non-exclusive basis and without the right to use any graphic elements on a stand-alone basis and have cited any such material correctly;
b. all of the facts contained in the Article are according to the current body of science true and accurate;
c. nothing in the Article is obscene, defamatory, violates any right of privacy or publicity, infringes any other human, personal or other rights of any person or entity or is otherwise unlawful and that informed consent to publish has been obtained for all research participants;

d. nothing in the Article infringes any duty of confidentiality which any of the Author(s) might owe to anyone else or violates any contract, express or implied, of any of the Author(s). All of the institutions in which work recorded in the Article was created or carried out have authorised and approved such research and publication; and
e. the signatory (the Author or the employer) who has signed this agreement has full right, power and authority to enter into this agreement on behalf of all of the Author(s).

6. Cooperation
The Author(s) shall cooperate fully with the Assignee in relation to any legal action that might arise from the publication of the Article, and the Author(s) shall give the Assignee access at reasonable times to any relevant accounts, documents and records within the power or control of the Author(s). The Author(s) agree that the distributing entity is intended to have the benefit of and shall have the right to enforce the terms of this agreement.

7. Author List
After signing, changes of authorship or the order of the authors listed will not be accepted unless formally approved in writing by the Assignee.

8. Edits & Corrections
The Author(s) agree(s) that the Assignee may retract the Article or publish a correction or other notice in relation to the Article if the Assignee considers in its reasonable opinion that such actions are appropriate from a legal, editorial or research integrity perspective.

This is an automated e-mail; please do not reply to this account. If you have any questions, please go to our help pages.

Thank you very much.

Kind regards,

Springer Author Services

Article Details

Journal title	Article title
Plant and Soil	Plant growth enhancement is not a conserved feature in the Caulobacter genus
DOI	**Corresponding Author**
10.1007/s11104-020-04472-w	Louis Berrios
Copyright transferred to	**Transferred on**
Springer Nature Switzerland AG	Thu Feb 20 14:58:43 CET 2020

Service Contacts

Springer Nature Customer Service Center

Tiergartenstr. 15-17
69121 Heidelberg
Germany
phone: +49 6221 345 0
fax: +49 6221 345 4229
customerservice@springernature.com

Springer New York, LCC

233 Spring Street
New York, NY 10013
USA
phone: +1 212 460 1500 or 800-SPRINGER
(Weekdays 8:30am - 5:30pm ET)
fax: +1 212-460-1700

You do not have to comply with the license for elements of the material in the public domain or where your use is permitted by an applicable exception or limitation.

No warranties are given. The license may not give you all of the permissions necessary for your intended use. For example, other rights such as publicity, privacy, or moral rights may limit how you use the material.